



Facoltà di Scienze Matematiche, Fisiche e Naturali  
Dipartimento di Biologia  
Scuola Dottorale in Biologia

**Sezione di Biologia Applicata alla Salute dell’Uomo (BASU)  
– XXIV ciclo –**

**“STUDY OF THE ROLE OF PRODUCTS AND  
ENZYMES OF CHOLESTEROL BIOSYNTHETIC  
PATHWAY IN MUSCLE TISSUES”**

**“STUDIO DEL RUOLO DEI PRODOTTI E DEGLI  
ENZIMI DELLA VIA BIOSINTETICA DEL  
COLESTEROLO NEI TESSUTI MUSCOLARI”**

Ph.D. Student: Dr. Laura Trapani

Supervisor: Prof. Valentina Pallottini

Coordinator of Biology Applied to Human Health section: Prof. Paolo Visca

A.A. 2010/2011

*To my own grandmother  
who meant the world  
to me*

## INDEX

<b>ABSTRACT.....</b>	<b>1</b>
<b>RIASSUNTO.....</b>	<b>2</b>
<b>INTRODUCTION.....</b>	<b>12</b>
<b>1. Mevalonate pathway.....</b>	<b>12</b>
<b>2. 3<math>\beta</math>-hydroxy 3<math>\beta</math>-methylglutharyl coenzyme A reductase .....</b>	<b>14</b>
2.1 HMGR regulation.....	16
<b>3. Mevalonate pathway's main end-products.....</b>	<b>18</b>
3.1.1. Cholesterol.....	18
3.1.2. Cholesterol functions in vertebrates.....	20
3.2. Ubiquinone .....	21
3.3. Dolichol.....	23
3.4. Prenylated proteins.....	24
<b>4. Muscle tissue.....</b>	<b>26</b>
4.1. Skeletal muscle development.....	28
4.2. Skeletal muscle regeneration.....	29
<b>5. HMGR inhibition: the statins.....</b>	<b>31</b>
<b>AIM.....</b>	<b>40</b>
<b>PAPERS CONCERNING PhD PROJECT</b>	
<b>3-Hydroxy 3-Methylglutaryl Coenzyme A Reductase Increase Is         Essential for Rat Muscle Differentiation (Paper 1)</b>	
<b>Mechanism Underlying Long-Term Regulation of 3-Hydroxy-3-         Methylglutaryl Coenzyme A Reductase During L6 Myoblast         Differentiation (Paper 2)</b>	
<b>3-Hydroxy 3-Methylglutaryl Coenzyme A Reductase inhibition impairs         muscle regeneration (Paper 3)</b>	
<b>Effects of myosin heavy chain (MHC) plasticity induced by HMG CoA-         reductase inhibition on skeletal muscle functions (Paper 4)</b>	
<b>HMG CoA reductase inhibition gets rat <math>\beta</math>-Myosin Heavy Chain         disappeared: a statin paradox (Paper 5)</b>	
<b>GENERAL CONCLUSIONS.....</b>	<b>I</b>

## ABSTRACT

The mevalonate pathway is an important metabolic pathway providing cells with vital bioactive compounds such as cholesterol, prenyls, ubiquinone and dolichol. All of them play pivotal roles in muscle structure and functions being involved in ATP production, contractile regulation and myoblast fusion into multinucleated syncytia. The key and rate limiting step of the pathway is the reduction of 3-hydroxy-3-methylglutaryl Coenzyme A in mevalonate, reaction catalized by the enzyme 3-hydroxy-3-methylglutaryl Coenzyme A reductase (HMGR) that, as a central modulator of cholesterol homeostasis, is highly regulated. Statins, drugs widely used in ipocholesterolemic therapies, competitively inhibit HMGR: besides the well known lipid lowering properties they can also exert muscle side effects with symptoms ranging from weakness and pain to symptoms associated with rhabdomyolysis, a life threatening condition. Statin-induced muscle adverse effects suggest that HMGR could play a central role in muscle physiological processes. The majority of the studies so far are limited to the definition of statin-induced myotoxicity without investigating whether and how HMGR inhibition can affect muscle physiology. Thus the PhD project was aimed at providing a comprehensive analysis of the role played by HMGR and its main end-products in skeletal muscle development, repair and functionality and in cardiac muscle structure and metabolism.

The thesis provides evidence that HMGR inhibition negatively affects myoblast differentiation and fusion, delays muscle regeneration, impairs the mechanical and functional features of glycolytic fibers, leads to changes in cardiac fiber phenotype, highlighting the crucial role exerted by this enzyme and its end-products in muscle tissues.

Thus, statin users might not only suffer from myopathy but also might not be able to repair any muscle damage. Furthermore, even though statins are supposed to reduce the risk of cardiovascular disease, they can also affect energy-dependent myocardial functions.

In conclusion the results suggest that more efforts should be spent to find alternative pharmacological approaches to statin treatment, able to block cholesterol biosynthetic pathway downstream to HMGR, the inhibition of which can affect body health at multiple levels.

## RIASSUNTO

### Introduzione

Il pathway biosintetico del mevalonato è deputato alla produzione di isoprenoidi sterolici e non sterolici di primaria importanza nella fisiologia cellulare. Tra i prodotti finali del pathway si annoverano il **colesterolo**, precursore degli ormoni steroidei e degli acidi biliari nonché entità strutturale delle membrane plasmatiche e del sistema dei tubuli T nelle cellule muscolari, l'**ubichinone**, trasportatore di elettroni nella catena respiratoria mitocondriale, il **dolicolo**, intermedio della glicosilazione in N di proteine, alcune delle quali responsabili della fusione dei mioblasti in sincizi multinucleati durante lo sviluppo embrionale del muscolo scheletrico, i **prenili** fondamentali per la modificazione post-traduzionale di proteine, quali RhoA, coinvolta nel differenziamento dei mioblasti e nella regolazione della contrazione del muscolo liscio.

La tappa velocità limitante la sintesi del mevalonato è la deacilazione del 3-idrossi-3-metilglutaril coenzima A (HMG CoA) in mevalonato, reazione catalizzata dall'enzima 3-idrossi-3-metilglutaril coenzima A reduttasi (HMGR) che, come regolatore centrale dell'omeostasi del colesterolo, è finemente modulato da meccanismi quali:

- una regolazione a breve termine che agisce sull'attività enzimatica della proteina mediante reazioni di fosforilazione e defosforilazione;
- una regolazione a lungo termine che ne modula i livelli intervenendo sulla trascrizione e sulla degradazione dell'enzima in dipendenza del contenuto di steroli presenti nella cellula.
- una regolazione ormonale che influenza ambedue le modulazioni descritte.

Il tessuto muscolare, parenchima costitutivo di tutti i tipi di muscolo (liscio, scheletrico e striato cardiaco) e responsabile, insieme allo scheletro, della locomozione e del movimento del corpo, svolge le sue funzioni estrinsecando capacità contrattile: la trasformazione di energia chimica in energia meccanica -per scissione enzimatica di molecole di ATP- consente lo scorrimento di filamenti di dimensioni ultrastrutturali in cui si organizzano miosina, actina e proteine regolatorie. La miosina, in particolare, è una proteina esamerica costituita da quattro catene leggere (MLC) e due catene pesanti (MHC) ad attività ATPasica le cui diverse isoforme sono responsabili della velocità di contrazione delle fibre muscolari e della forza sviluppata durante il processo contrattile.

Le prevalenti isoforme di MHC e il metabolismo cellulare delle fibre muscolari scheletriche ne consentono la classificazione in:

- fibre lente ossidative (esprimenti MHC I)
- fibre rapide ossidative (esperimenti MHCIIa/x)
- fibre rapide glicolitiche (esprimenti MHCIIb)

Nel muscolo cardiaco MHC  $\alpha$  e  $\beta$  generano, nei ventricoli, tre differenti isoforme della miosina definite:

- V1, omodimero  $\alpha\alpha$
- V2, eterodimero  $\alpha\beta$
- V3, omodimero  $\beta\beta$ .

Gli atri contengono una quarta isoforma definita Va, un omodimero  $\alpha\alpha$  con un differente *set* di catene leggere rispetto all'isoforma ventricolare V1.

L'embriogenesi del muscolo scheletrico è un processo attraverso cui le fibre muscolari sono generate da mioblasti mononucleati che, in seguito all'arresto dell'attività proliferativa differenziano in miociti capaci di fondere in sincizi multinucleati.

La riparazione del muscolo segue processi che ricapitolano solo in parte l'quelli dell'embriogenesi. Infatti, poiché i nuclei presenti nelle fibre muscolari sono incapaci di replicare essendo irreversibilmente fuoriusciti dal ciclo cellulare e trovandosi pertanto in uno stato postmitotico permanente, la fibra di per sé non è in grado di riparare eventuali perdite di tessuto dovute a traumi o miopatie degenerative, non potendo ripristinare l'attività mitotica dei suoi nuclei. La riparazione avviene mediante la capacità di peculiari cellule staminali definite "satelliti" di ricostituire il tessuto: queste sono elementi mononucleati, normalmente quiescenti situati tra il plasmalemma e la lamina basale. In seguito ad eventuali lesioni, le cellule satelliti sono stimolate a proliferare, generando una popolazione cellulare che mantiene uno stato quiescente ed elementi che dopo un certo numero di mitosi, si fondono tra loro formando strutture sinciziali capaci di esprimere i prodotti differenziati propri delle fibre e di ricostituire quindi l'integrità del tessuto.

L'HMGCR è un target terapeutico appetibile per la cura farmacologica dell'ipercolesterolemia: l'inibizione intracellulare della sintesi del colesterolo induce una risposta omeostatica che determina l'incremento dell'esposizione di recettori superficiali di membrana in grado di mediare l'assunzione cellulare delle lipoproteine aterogeniche quali le LDL (Low Density Lipoprotein) e le VLDL (Very Low Density Lipoprotein).

Evidenze sperimentali e cliniche tuttavia dimostrano che il trattamento con le statine, potenti inibitori dell'HMGCR largamente impiegati nella terapie ipocolesterolemizzanti, provocano effetti collaterali quali mialgia, miosite e

rabdomiolisi e l'insorgenza di malattie clinicamente silenti quali la distrofia miotonica o la malattia di Kennedy e di McArdle. Ne consegue che l'interesse principale della comunità scientifica nel campo sia stato quello di definire i meccanismi alla base della miotossicità provocata dalle statine piuttosto che di comprendere la funzione dell'HMGR nella fisiologia del muscolo scheletrico e cardiaco.

Pertanto, obiettivo del progetto di dottorato, è stato l'analisi del ruolo dell'HMGR e dei suoi prodotti finali nello sviluppo, nella rigenerazione e funzionalità del muscolo scheletrico, così come nella struttura e nel metabolismo del muscolo cardiaco.

## **Risultati**

### **HMGR e suoi prodotti finali nello sviluppo del muscolo scheletrico**

*(3-Hydroxy 3-Methylglutaryl Coenzyme A Reductase Increase Is Essential for Rat Muscle Differentiation. J Cell Physiol. 2009 Aug;220(2):524-30) Paper 1*

Per comprendere il ruolo dell'HMGR e dei suoi prodotti finali nello sviluppo del muscolo scheletrico, come modello sperimentale sono stati impiegati mioblasti fetali di ratto L6, il cui differenziamento è stato indotto mediante insulina. Per valutare se l'HMGR fosse soggetto a modulazione durante il processo miogenico, i livelli proteici dell'enzima e dei suoi prodotti finali quali colesterolo, proteine prenilate e tra queste RhoA, sono stati monitorati in un time course di 72h. L'iniziale incremento dell'enzima è seguito da un decremento nelle fasi terminali del processo differenziativo: l'andamento di colesterolo, proteine prenilate e RhoA è simile a quello dell'HMGR (CFR fig. 2 *paper 1*).

Il ruolo dell'enzima nello sviluppo del muscolo scheletrico è stato indagato valutando i livelli proteici dei marker precoci e tardivi del differenziamento muscolare (miogenina e MHC embrionale) a 16 e a 24h dalla stimolazione con insulina, gli indici di fusione e differenziamento dei mioblasti a 72h dall'induzione della miogenesi, in presenza di 25OH colesterolo o mevinolina in grado, rispettivamente, di stimolare la degradazione e inibire l'attività dell'enzima. In ambedue le condizioni sperimentali i livelli dei marker del differenziamento e gli indici di fusione e differenziamento delle cellule manifestano una significativa riduzione rispetto ai controlli suggerendo che l'inibizione dell'HMGR possa rallentare il processo miogenico (CFR fig. 3, 4 *paper 1*).

Per comprendere quali proteine potessero essere coinvolte nella modulazione dell'HMGR durante il differenziamento dei mioblasti indotto da insulina, è stato inizialmente valutato lo stato di attivazione di una proteina di segnale, p38, in grado di indurre p21waf che, favorendo la fuoriuscita dal ciclo cellulare dei mioblasti in fase G1 ne consente il differenziamento. Accertato l'incremento della fosforilazione di p38 in seguito a stimolazione con insulina (CFR fig. 5 *paper 1*), è stato indagato il cross-talk tra p38, HMGR, p21waf e RhoA inibendo alternativamente p38 e HMGR e analizzando i livelli delle proteine precedentemente menzionate. L'inibizione di p38 determina la riduzione dei livelli proteici dell'HMGR, p21waf e RhoA; l'inibizione e la *down-regolazione* dell'HMGR riduce i livelli di p21waf e RhoA (CFR fig. 7, 8 *paper 1*).

I risultati ottenuti suggeriscono pertanto che l'insulina incrementa la fosforilazione e attivazione di p38 coinvolta nell'*up-regolazione* dell'HMGR a sua volta responsabile dell'aumento dei livelli di RhoA e di p21waf, eventi che, nelle fasi iniziali, favoriscono l'evolversi del processo miogenico.

*(Mechanism Underlying Long-Term Regulation of 3-Hydroxy-3-Methylglutaryl Coenzyme A Reductase During L6 Myoblast Differentiation. J Cell Biochem. 2010 May 15;110(2):392-8) Paper 2*

Per comprendere pienamente i meccanismi alla base della modulazione dell'HMGR nel differenziamento dei mioblasti fetali di ratto sono stati analizzati il pattern d'espressione dell'enzima e delle proteine coinvolte nella sua regolazione a lungo termine nonché il tasso di degradazione enzimatica. L'analisi condotta dimostra come l'enzima sia regolato da meccanismi differenti durante le varie fasi del processo miogenico. A tempi precoci del differenziamento, l'incremento dei livelli dell'mRNA e proteici dell'HMGR è imputabile all'induzione trascrizionale e al rallentamento della velocità di degradazione dell'enzima: il ridotto contenuto cellulare di Insig-1 (CFR fig. 2 *paper 2*) infatti consente la migrazione del complesso SREBP-Scap dal reticolo endoplasmatico all'Apparato di Golgi e il conseguente rilascio di nSREBP, fattore trascrizionale del gene codificante l'HMGR; i ridotti livelli di Insig-1 inoltre provocano il decremento del tasso di ubiquitinazione e degradazione proteosomale dell'enzima. La successiva riduzione dei livelli proteici dell'HMGR sembrerebbe essere dovuta all'aumentata velocità di degradazione dell'enzima, come giustificato dall'incremento del contenuto cellulare di Insig-1 e dal decremento dei livelli di nSREBP (CFR fig. 2, 3, 5



*.paper 2*). Negli stadi tardivi del differenziamento la riduzione dei livelli di mRNA e proteici dell'HMGR è imputabile ad un diminuito tasso trascrizionale: infatti, Insig-1, il cui contenuto cellulare si mantiene elevato nelle fasi terminali del processo miogenico,, trattenendo il complesso SREBP-Scap nel reticolo endoplasmatico impedisce il rilascio di nSREBP e la conseguente trascrizione del gene codificante l'HMGR, senza influenzare la velocità di degradazione dell'enzima (CFR fig. 2, 3, 5 *paper 2* )

### HMGR e suoi prodotti finali nella rigenerazione del muscolo scheletrico

*(3-Hydroxy 3-Methylglutaryl Coenzyme A Reductase inhibition impairs muscle regeneration. Pending editorial decision: Journal of Cellular Physiology) Paper 3*

Poiché la rigenerazione muscolare è un processo che ricapitola gli eventi principali che si succedono durante la miogenesi, è stato ipotizzato, sulla base dei risultati ottenuti sui mioblasti fetali di ratto, che l'HMGR potesse svolgere un ruolo chiave nel differenziamento delle cellule responsabili della riparazione del tessuto muscolare.

Pertanto nei mioblasti derivati da cellule satelliti murine (SCDM) (gentile concessione del Dottor Marco Crescenzi, Istituto Superiore di Sanità) è stato indotto il differenziamento mediante cambiamento di terreno e riduzione di siero, e sono stati monitorati i livelli proteici dell' HMGR e delle differenti isoforme di MHC in un *time course* di 72h.

I risultati ottenuti indicano che i livelli proteici dell'enzima e di MHC embrionale raggiungono il massimo incremento 6 ore dopo l'induzione del differenziamento e si riducono più tardivamente; l'aumento delle isoforme adulte di MHC (rapide e lente) si osserva 24 ore dopo il cambiamento del terreno e la riduzione del siero (CFR fig. 1 *paper 3*).

La simile modulazione dei livelli proteici dell'HMGR durante le prime fasi del differenziamento osservata nei mioblasti fetali di ratto (*paper 1*) e nelle SCDM murine (CFR fig. 1 *paper 3*) suggerisce che l'enzima possa svolgere un ruolo determinante anche nel differenziamento delle cellule responsabili della rigenerazione muscolare.

Le SCDM pertanto sono state trattate per 72h con simvastatina ad una dose paragonabile a quella dosata nel plasma di pazienti sottoposti a trattamento cronico con il farmaco; sono stati successivamente valutati l'indice di fusione delle cellule in differenziamento e i livelli proteici delle isoforme embrionali e adulte di MHC. Le SCDM trattate con il veicolo

generano miotubi ramificati e con un elevato numero di nuclei, le SCDM trattate con simvastatina danno origine a miotubi piccoli, sottili e con un ridotto numero di nuclei. Il trattamento con la statina inoltre previene la riduzione dei livelli di MHC embrionale e l'incremento delle isoforme adulte rapide e lente dell'MHC, eventi necessari per l'evolversi del processo riparativo del tessuto. Il co-trattamento con il mevalonato, prodotto della reazione catalizzata dall'HMGR, ripristina la morfologia dei miotubi e il pattern proteico delle isoforme dell'MHC (CFR fig. 2 *paper 3*).

Con il supporto dei risultati ottenuti *in vitro*, è stata studiata *in vivo* la risposta al danno muscolare indotto mediante iniezione di cardiottossina nel muscolo *tibialis anterior* di topi trattati quotidianamente, per 21 giorni, con iniezioni intraperitoneali di simvastatina (1,5 mg/kg comparabile alla dose massima impiegata nella terapia ipocolesterolemizzante) o di simvastatina e mevalonato. I dati ottenuti indicano che 3 settimane dopo l'insulto miotossico, la citoarchitettura dei muscoli tibiali anteriori dei topi sottoposti a trattamento con il veicolo e a co-trattamento con simvastatina e mevalonato è completamente ristabilita, contrariamente a quella dei muscoli prelevati dai topi trattati con la sola simvastatina, ove la rigenerazione delle fibre non è ultimata ma ancora in corso, come dimostrato dalla presenza di nuclei centrali all'interno delle fibre (CFR fig. 4 *paper 3*). Analisi condotte mediante Western-blot indicano inoltre che il livello delle isoforme adulte, rapide e lente, di MHC è ridotto nei muscoli di animali trattati con il farmaco rispetto ai veicoli e ai topi sottoposti a co-trattamento (CFR fig. 5 *paper 3*).

I dati ottenuti sia *in vitro* che *in vivo* pertanto indicano che l'inibizione dell'HMGR riduce il differenziamento delle SCDM e rallenta la riparazione del tessuto muscolare: gli esperimenti condotti mediante l'impiego di mevalonato dimostrano che gli effetti osservati sono riconducibili all'inibizione dell'enzima e non ad un effetto tossico provocato dal farmaco indipendentemente dal suo meccanismo d'azione.

#### HMGR e suoi prodotti finali nel muscolo adulto

*(Effects of myosin heavy chain (MHC) plasticity induced by HMG CoA-reductase inhibition on skeletal muscle functions. FASEB J. 2011 Nov;25(11):4037-47. Epub 2011 Jul 28) Paper 4*

Per comprendere il ruolo svolto dall'HMGR e dei suoi prodotti finali nel tessuto muscolare adulto, ratti Wistar di 3 mesi sono trattati con

iniezioni intraperitoneali di simvastatina (1,5 mg/kg) per 21 giorni, a conclusione dei quali gli animali sono stati sottoposti a test comportamentali e quindi sacrificati; il prelievo di sangue e muscoli ha consentito l'effettuazione di analisi biochimiche e meccaniche.

Gli esperimenti sono stati condotti sul muscolo *extensor digitorum longus* (EDL) poichè costituito prevalentemente da fibre glicolitiche, le più suscettibili agli effetti collaterali delle statine.

Il trattamento cronico con il farmaco non ha determinato cambiamenti significativi nel peso corporeo dei ratti, ma, come aspettato, una riduzione dei livelli plasmatici di colesterolo e trigliceridi a dimostrazione dell'efficacia del trattamento. La simvastatina ha inibito del 20% l'attività dell'HMGR nel muscolo scheletrico e conseguentemente incrementato i livelli del recettore LDL sulla membrana delle fibre (CFR fig. 1 e tabella 1 *paper* 4). Il trattamento non ha provocato danni muscolari, in termini di necrosi o apoptosi, come dimostrato dalla mancata variazione dei livelli di creatin chinasi plasmatiche e di PARP-1 nell'EDL (CFR fig. 2 *paper* 4). L'inibizione cronica dell'HMGR non ha causato variazioni nello stato d'attivazione della proteina prenilata RhoA, né nel contenuto muscolare di colesterolo e ubiquinone (CFR fig. 2 e tabella 2 *paper* 4).

Il trattamento con simvastatina ha tuttavia provocato una riduzione dei livelli proteici dell'isoforma rapida glicolitica MHCIIb ed un incremento delle isoforme rapide-ossidative MHCIIa/x (CFR fig. 4 *paper* 4). Per verificare se lo *shift* delle isoforme potesse determinare variazioni nella *performance* muscolare dell'EDL, il muscolo è stato sottoposto ad esperimenti meccanici che hanno consentito la valutazione di diversi parametri inerenti la contrazione. I risultati ottenuti dimostrano che l'inibizione cronica dell'HMGR riduce la potenza contrattile e la velocità di accorciamento delle fibre senza determinare alcun cambiamento nella forza isometrica, nell'affaticamento e nel recupero muscolare dell'EDL (CFR fig. 6, 7 e tabella 3 *paper* 4). Per valutare se la riduzione dei parametri meccanici causata dal trattamento con simvastatina potesse provocare modificazioni funzionali, sono state valutate la coordinazione motoria e l'attività locomotoria basale degli animali sottoponendo i ratti al test del rotarod e dell'*open field*. I dati ottenuti indicano che l'inibizione cronica dell'HMGR pur non modificando l'attività locomotoria basale, come dimostrato dall'assenza di variazioni nella frequenza di attraversamento dei quadrati in cui l'arena dell'*open field test* è stata suddivisa, peggiora tuttavia la capacità degli animali di sostenere condizioni che richiedano sforzi muscolari più intensi (CFR fig. 8, 9 *paper* 4).

Complessivamente i dati ottenuti in questa fase del progetto dimostrano che il trattamento cronico con simvastatina determina nel muscolo EDL uno *shift* delle isoforme rapide dell'MHC verso un fenotipo più lento, una conseguente riduzione della potenza e della velocità di accorciamento delle fibre, un peggioramento funzionale: questo potrebbe spiegare i fastidi muscolari di pazienti sottoposti a trattamento con statine privi di un incremento delle creatin chinasi plasmatiche.

### HMGR e suoi prodotti finali nel muscolo cardiaco

*(HMG CoA reductase inhibition gets rat  $\beta$ -Myosin Heavy Chain disappeared: a statin paradox. Submitted to Journal of Cellular Biochemistry) Paper 5*

Effetti avversi delle statine sono stati descritti anche a carico del muscolo cardiaco. Pisarenko e colleghi hanno dimostrato che il trattamento di un mese con lovastatina determina una riduzione dell'eiezione cardiaca e dell'indice di contrattilità: gli autori hanno attribuito gli effetti descritti alla riduzione dei livelli intratissutali di ubiquinone.

Poiché le statine, come precedentemente dimostrato, sono in grado di modificare il pattern d'espressione delle diverse isoforme di MHC, evento potenzialmente responsabile della modulazione delle proprietà contrattili del cuore, e poiché le conoscenze circa la capacità delle statine di ridurre i livelli intratissutali di ubiquinone sono limitate, sono stati valutati gli effetti dell'inibizione dell'HMGR sul fenotipo strutturale e metabolico delle fibre cardiache. Ratti Wistar di 3 mesi sono stati trattati con iniezioni intraperitoneali di simvastatina (1,5 mg/kg) per 21 giorni, a conclusione dei quali gli animali sono stati sacrificati; è seguito quindi il prelievo del sangue e del cuore per l'effettuazione di indagini biochimiche.

Dopo aver accertato l'efficacia del trattamento, dimostrato dalla riduzione dei livelli plasmatici di colesterolo e trigliceridi (CFR fig. 1 *paper* 5), è stato misurato, mediante HPLC, il contenuto di colesterolo e ubiquinone in omogenati di ventricoli cardiaci: l'inibizione cronica dell'HMGR determina un incremento dei livelli di colesterolo ed una riduzione di ubiquinone (CFR tabella 1 *paper* 5). La valutazione del pattern delle isoforme MHC ha dimostrato che nonostante non siano state individuate variazioni significative nel contenuto di MHC $\alpha$ , l'isoforma  $\beta$  subisce un gravoso decremento che tuttavia non si può escludere venga compensato da un aumento di  $\alpha$  (CFR fig. 2 *paper* 5). La mancata

rilevazione di variazioni significative dell'MHC $\alpha$  potrebbe essere riconducibile all'elevato contenuto di questa isoforma nel ventricolo e alla sensibilità del Western-blot come metodo di indagine; infatti piccole variazioni compensatorie potrebbero non essere apprezzate dalla metodica utilizzata. Inoltre, poiché MHC  $\alpha$  e  $\beta$  sono regionalmente distribuite nel tessuto muscolare cardiaco per rispondere alle esigenze strutturali e funzionali del cuore, variazioni anche minime dei livelli delle isoforme potrebbero determinare conseguenze funzionali: ne deriva che sebbene l'isoforma  $\beta$  sia poco rappresentata rispetto ad  $\alpha$  (5:95), la sua riduzione potrebbe tradursi in una insufficiente funzionalità tissutale.

I risultati ottenuti sembrano pertanto mettere in luce un paradosso: le statine, farmaci impiegati per ridurre la colesterolemia e per prevenire il rischio di malattie cardiovascolari, possono modificare le proprietà contrattili dell'organo che si suppone debbano proteggere: il cuore.

## **Conclusioni**

Nel complesso i dati ottenuti durante lo svolgimento del progetto di dottorato mettono in luce come l'HMGR e i suoi prodotti finali siano fondamentali per il corretto svolgimento di molti processi fisiologici che coinvolgono il muscolo scheletrico come lo sviluppo, la rigenerazione e la contrazione muscolare nonché nel mantenimento del fenotipo strutturale e metabolico delle fibre cardiache.

A causa della crescente incidenza delle malattie cardiovascolari il cui principale fattore di rischio è l'elevato livello di lipidi plasmatici, il controllo della colesterolemia, effettuato con farmaci come le statine, che inibiscono l'HMGR, enzima chiave della sintesi del colesterolo, è divenuto un'esigenza primaria per il mantenimento dello stato di salute.

Resta tuttavia da stabilire fino a che punto il rapporto rischio/beneficio suggerisca l'impiego di tali farmaci.

Pazienti sottoposti a trattamento con statine, infatti, potrebbero non soltanto lamentare fastidi alla muscolatura scheletrica, ma non essere in grado di riparare eventuali danni. Inoltre, seppur impiegate per ridurre il rischio di sviluppare malattie cardiovascolari, le statine possono alterare le funzioni cardiache.

Pertanto, considerando il ruolo cruciale dell'HMGR nella crescita, nella proliferazione, nel differenziamento e nella sopravvivenza cellulare e la necessità di mantenere a livelli ridotti il contenuto plasmatico di colesterolo per prevenire l'insorgenza di patologie cardiovascolari, dovrebbero essere impiegate nuove strategie terapeutiche nel trattamento

dell'ipercolesterolemia mirate all'inibizione esclusiva della sintesi di colesterolo a valle dell'HMGR la cui *down*regolazione e/o ridotta attività possono provocare effetti dannosi alla salute dell'uomo.

# INTRODUCTION

## 1. Mevalonate pathway

Mevalonate (Mva) pathway (Fig. 1) is an important metabolic pathway that provides cells with essential bioactive molecules, vital in multiple cellular processes. This pathway converts Mva into sterol isoprenoids, such as cholesterol, essential precursor of bile acids, lipoproteins, and steroid hormones, and into a number of hydrophobic molecules, nonsterol isoprenoids, among others dolichol, ubiquinone (CoQ) and isoprenes. These intermediates play important roles in the post-translational modification of a multitude of proteins involved in intracellular signaling and are essential in cell growth, differentiation, gene expression, protein glycosylation and cytoskeletal assembly (Buhaescu and Izzedine, 2007).

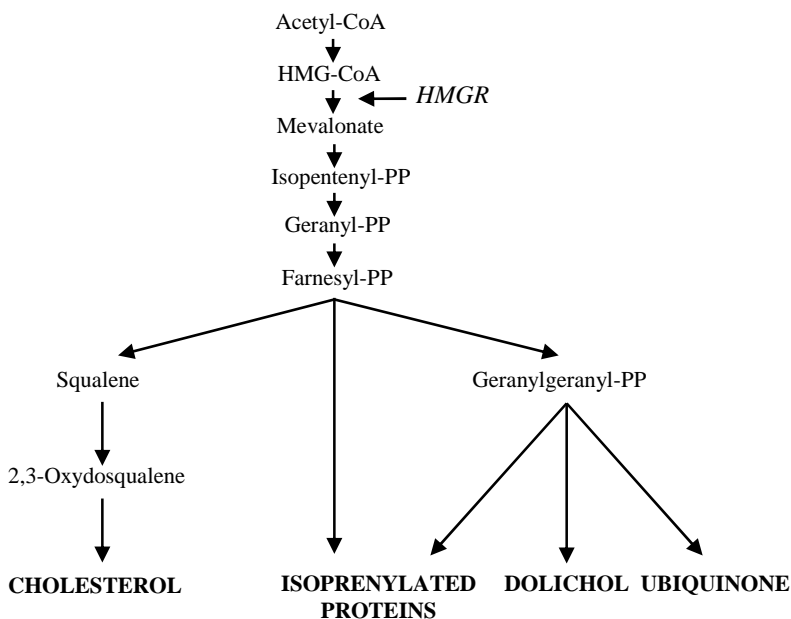


**Figure 1.** Scheme of mevalonate pathway.

Initially, the pathway involves repeated condensation of acetyl-CoA units, resulting in 3 $\beta$ -hydroxy 3 $\beta$ -methylglutharyl coenzyme A (HMG-CoA). The next reaction, which is a reduction of the substrate to mevalonate consuming two molecules of NADPH in a two-step reaction, is mediated by 3 $\beta$ -hydroxy 3 $\beta$ -methylglutharyl coenzyme A reductase (HMGR) (Fig. 2). This protein is considered to be the major regulatory enzyme in cholesterol biosynthesis and is one of the most intensively investigated proteins in biochemistry.

Mva is phosphorylated in two consecutive steps, which requires two molecules of ATP (Tanaka et al., 1990). Dehydration-decarboxylation of Mva-PP gives isopentenyl pyrophosphate (IPP), the basic building block for all products of the pathway (Rozman and Monostory, 2010). IPP can isomerize to dimethylallyl pyrophosphate via isopentenyl pyrophosphate isomerase (ILI1). IPP and dimethylallyl pyrophosphate condense to form the C-10 geranyl pyrophosphate which in turn condenses with a second molecule of isopentenyl pyrophosphate to produce the C-15 farnesyl pyrophosphate by farnesyl pyrophosphate synthase (FDPS) (Rozman and Monostory, 2010). The terminal steps of Mva pathway involve the branch-point enzymes that utilize FPP, i.e., squalene synthase, trans-prenyltransferase, cis-prenyltransferase and farnesyl- or geranylgeraniol-protein transferases for cholesterol, CoQ, dolichol and isoprenylated proteins, which are considered to be rate-limiting for the terminal portion of the biosynthetic sequences (Bentinger et al., 2011).

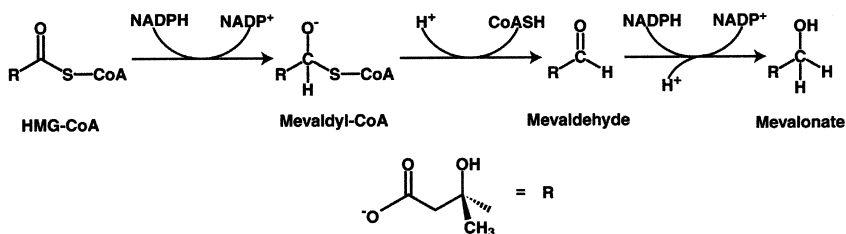


**Figure 2.** The reductive deacylation of HMG-CoA to mevalonate is thought to proceed in three steps, with mevaldyl-CoA and mevaldehyde as reaction intermediates (Istvan and Deisenhofer, 2000).



## 2. 3 $\beta$ -hydroxy 3 $\beta$ -methylglutharyl coenzyme A reductase

HMGR is the key and rate-limiting enzyme of Mva pathway, catalyzing a NADPH-dependent reduction of HMG-CoA to mevalonate, the first committed step in cholesterol biosynthesis (Rozman and Monostory, 2010). The enzyme is a transmembrane glycoprotein anchored to the endoplasmic reticulum (ER). The human HMGR protein consists of three domains: the N-terminal 339 residues form the membrane-associated domain; the C-terminal catalytic region (residues 460–888) located in the cytosol and the residues 340–459 of the linker domain that connect the two portions of the protein (Friesen and Rodwell, 2004).

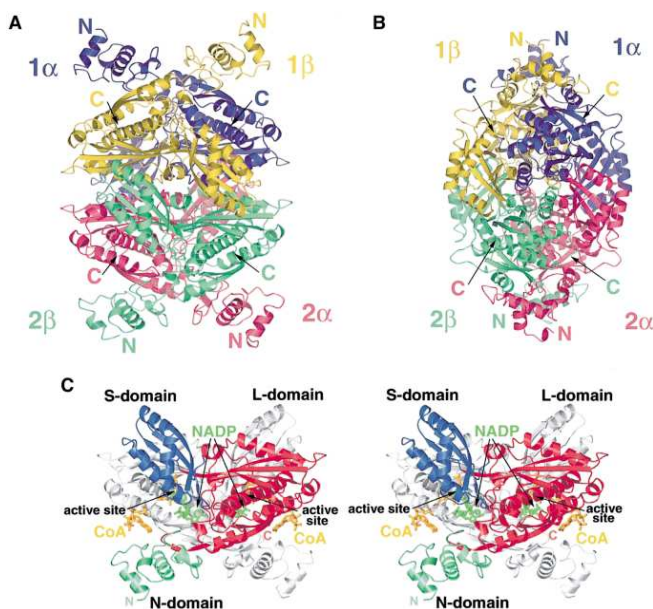


**Figure 3.** Ribbon diagrams of human HMGR. (A and B) Structure of the HMGR homotetramer. (C) Stereo diagram of the HMGR dimer structure (Istvan and Deisenhofer, 2000).

The functional enzyme is a tetramer with the dimeric active sites at the interface of the two monomers (Istvan and Deisenhofer, 2000) (Istvan et al., 2000). The HMG moiety of the substrate, which is bound to a single HMGR monomer, comes into proximity of the nicotinamide ring of a NADPH molecule, whose binding pocket is located in the neighbouring monomer. The substrate-binding pocket is characterized by a loop of residues 682–694. The cis-peptide (Cys688– Thr689) within this region is essential in the formation of the HMG-CoA binding site, and is critical in positioning the residues participating directly in HMGR mediated reduction (Istvan and Deisenhofer, 2000) (Istvan et al., 2000) (Fig. 3). The substrate-binding pocket also accommodates statin molecules upon competitive inhibition of the enzyme (Istvan and Deisenhofer, 2001) (Fig. 4).

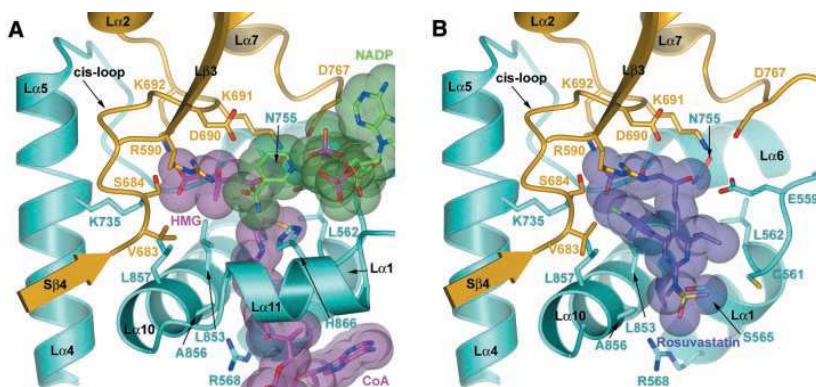


**Figure 4.** Statins exploit the conformational flexibility of HMGR to create a hydrophobic binding pocket near the active site. (A) Active site of human HMGR in complex with HMG-CoA, and NADP. (B) Binding of rosuvastatin to HMGR (Istvan and Deisenhofer, 2001).

As the central enzyme of the cholesterol biosynthetic pathway, HMGR is highly regulated (Goldstein and Brown, 1990). In particular, the enzyme undergoes short-term, long-term and hormonal regulations.

## 2.1. HMGR regulation

HMGR short term regulation is achieved by phosphorylation and dephosphorylation reactions both able to affect the enzyme activity (Fig. 5 A). The phosphorylation of enzyme's residue S872 decreases HMGR catalytic activity whereas the removal of the phosphate reactivates the enzyme (Beg et al., 1985). AMP activated kinase (AMPK) appears to be the major HMGR kinase in the liver, where the cholesterologenesis takes place. AMPK is known to be involved in the regulation of energy homeostasis responding to changes in cellular AMP to ATP ratio (Towler and Hardie, 2007). HMGR dephosphorylation (activation) is operated principally by Protein Phosphatase 2A (PP2A), an abundant cellular serine/threonine phosphatase that regulates a significant network of cellular events (Janssens and Goris, 2001). Aside from short-term regulation, HMGR is subjected to transcriptional, translational, and post-translational control (Xu et al., 2005).

To monitor levels of membrane sterols, cells employ in addition to HMGR another membrane-embedded protein of the ER, Scap (SREBP cleavage activating protein), both containing a polytopic intramembrane sequence called sterol-sensing domain (SSD).

Scap is an escort protein for Sterol Regulatory Element Binding Proteins (SREBPs), membrane bound transcription factors able to induce the expression of genes required for cholesterol synthesis and uptake, such as HMGR and Low Density Lipoprotein receptor (LDLr) (Brown and Goldstein, 1997). In sterol-deprived cells, Scap binds SREBPs and escorts them from the ER to the Golgi apparatus where SREBPs are proteolytically processed to yield active fragments that enter the nucleus and induce the expression of their target genes (Brown and Goldstein, 1999). When cholesterol builds up in ER membranes, the Scap/SREBP complex fails to exit the ER, the proteolytic processing of SREBPs is abolished and the transcription of the target genes declines. ER retention of Scap/SREBP is mediated by sterol-dependent binding of Scap/SREBP to Insig (INSulin Induced Gene), an ER resident protein (Fig. 5 B) (Yang et al., 2002). Intracellular accumulation of sterols induces HMGR to bind Insig: the interaction promotes the ubiquitination and proteasomal degradation of the enzyme (Sever et al., 2003) (Fig. 5 C) .

Several hormones, including insulin, glucagon, glucocorticoids, thyroid hormone, and estrogen, regulate the expression of hepatic HMGR in animals. Insulin likely stimulates HMGR expression by increasing its rate of transcription, while glucagon opposes this effect. Hepatic HMGR activity undergoes significant diurnal variations due to changes in the levels of immunoreactive proteins, which are primarily mediated by changes in

insulin and glucagon levels. Thyroid hormone increases hepatic HMGR levels by acting to increase both transcription and mRNA stability, while glucocorticoids decrease hepatic HMGR expression by destabilizing HMGR mRNA. The effects of estrogen on HMGR expression are still debated. Some studies suggest that estrogens act to increase hepatic HMGR activity primarily by stabilizing HMGR mRNA and that deficiencies in those hormones that act to increase hepatic *HMGR* gene expression lead to elevated serum cholesterol levels (Ness and Chambers, 2000). On the other hand, studies using the DLD1 cell line suggest that estrogens induce an early increase in LDLr at both mRNA and protein level and later cause decreases in HMGR activity and protein expression (Messa et al., 2005).

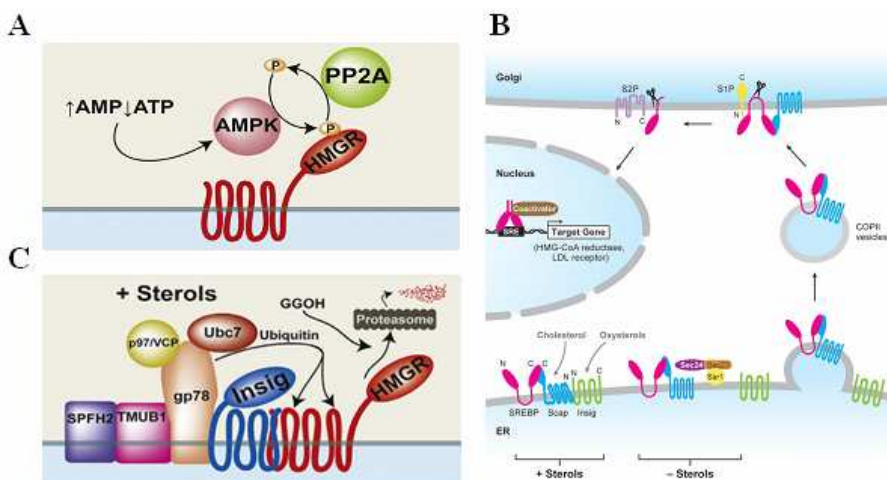


**Figure 5.** Schematic illustration of HMGR short (A) and long (B, C) term regulations. In particular, panel B and C show the regulation of HMGR transcription (B) and degradation (C) as a function of intracellular sterol amount and of cholesterol uptake (Burg and Espenshade, 2011).

### 3. Mevalonate pathway's main end-products

#### 3.1.1. Cholesterol

Cholesterol (Cholest-5-en-3-ol) is the most abundant sterol in vertebrates. First isolated from bile stones by Poulletier de La Salle in 1770, cholesterol was later isolated from unsaponifiable fraction of animal fats by Chevreul (1815), who named it Cholesterine (Greek χόλη, bile and στέρεος, solid). The exact formula of cholesterol ( $C_{27}H_{46}O$ ) was proposed by Reinitzer in 1880, and the right structure and exact steric representation were elucidated between 1900 and 1932, mainly by works from Wieland and Windaus. Meanwhile, Schmidt (1914) measured for the first time high serum cholesterol levels in patients with xanthomatosis, thus recognised it as essential hypercholesterolemia. By the early 1950s, Lynen demonstrated that the acetylation of Coenzyme A is the key first step in a chain of reactions that result in the formation of cholesterol and fatty acids. Together with Bloch, Lynen successively received the Nobel price for medicine (1954) and Nobel price for physiology and medicine (1964) for their discoveries concerning the mechanism and regulation of cholesterol and fatty acids metabolism (pathway from “activated acetic acid” to terpenes and fatty acids). Meanwhile, Tavormina et al. (1956) discovered that mevalonic acid is quantitatively incorporated in cholesterol in cell-free systems with loss of carbon dioxide. The biological function of cholesterol gained insights from work by Fisher (1976) who, by freeze-fracture and biochemical analysis in human erythrocytes, demonstrated that cholesterol is asymmetrically distributed across the plane of the membrane, being more present on the exterior side than on the interior side. Works to elucidate the very nature and metabolism of cholesterol were just starting that it was already pointed for its involvement in atherosclerogenesis. The first hint came from work by Windaus who reported that atherosclerotic plaques from aortas of human subjects contained 20- to 26- fold higher concentrations of cholesterol than did normal aortas. This observation opened nearly a century of research, which led to the recognition of the cholesterol carrying low density lipoprotein (LDL) particles as the primary cause of atherosclerosis (Rader et al., 2003). With the discovery of the mevalonic aciduria as first inborn error of cholesterol biosynthesis (Hoffmann et al., 1986), a new era of cholesterol history started, era in which cholesterol was no longer considered just as heart breaking molecule, but also as a key player in developmental processes.

One of the sources for the acquisition of cholesterol by animals and human beings is the absorption of sterol ingested in the diet. During

digestion, cholesterol esters are broken into unesterified cholesterol and long chain fatty acids; such monomers of unesterified cholesterol can diffuse directly up to the microvillus border of the intestinal epithelial cell and be absorbed passively (Dietschy, 1984). After entering the enterocytes, approximately half of the cholesterol molecules move to the endoplasmic reticulum (ER) where cholesterol is esterified by acyl-CoA:cholesterol acyltransferase (ACAT) before incorporation into nascent chylomicron (CM), particles produced by the small intestine soon after a meal. CMs carry a lot of triglycerides (TGs) as well. These particles are released from the base of the intestinal epithelial cell and enter the intestinal lymphatic vessels, where they interact with high-density lipoprotein (HDL) to acquire apoproteins C and E (Havel, 1982). The liver is the most important site for body synthesis, but all organs in the body are capable of significant rates of cholesterol synthesis (Dietschy, 1984). The rate of cholesterol synthesis in the liver varies inversely with the amount of dietary cholesterol reaching it in the CMs (Nervi et al., 1975). Hence, sterol synthesis within the intestinal hepatic axis tends to accommodate to changing rates of dietary cholesterol entrance into the body. Cholesterol moves out of the liver largely carried in VLDL (Very Low Density Lipoproteins) that are gradually converted into IDL (intermediate-density lipoproteins) and LDL. Cells that have a demand for cholesterol bind LDL through their LDLr and then take up the complete particle through receptor-mediated endocytosis. This type of transport is mediated by depressions in the membrane (“coated pits”), the interior of which is lined with the protein clathrin. After LDL binding, clathrin promotes invagination of the pits and pinching off of vesicles (“coated vesicles”). The clathrin then dissociates off and is reused (Brown and Goldstein, 1985). After fusion of the vesicle with lysosomes, the LDL particles are broken down, and cholesterol and other lipids are used by the cells. The HDLs also originate in the liver. They return the excess cholesterol formed in the tissues to the liver. While it is being transported, cholesterol is acylated by lecithin cholesterol acyltransferase (LCAT). Formed cholesterol esters are no longer amphipathic and can be transported in the core of the lipoproteins. In addition, HDLs promote CM and VLDL turnover by exchanging lipids and apoproteins with them (Nilsson and Duan, 2006).

### 3.1.2. Cholesterol function in vertebrates

The cholesterol molecule consists of three main parts: a rigid lipophilic steroid core, which can trigger anchoring to lipid bilayer, a non-polar hydrocarbon tail that can undergo oxidation, and a polar hydroxyl head, which can take part in several esterification reactions (Fig. 6). As can be predicted from its molecular structure, the biochemistry of cholesterol covers a wide spectrum of biological processes, a lot of which is still to be understood.

More than 80% of the cellular pool of cholesterol is located in the plasma membrane (Hoekstra and van ISC, 2000), in which it accounts for 20 to 25% of the lipid molecules (Dietschy and Turley, 2001). The plasma membrane (PM) cholesterol functions not only as a structural entity, but influences many properties of the PM. In addition to generally affecting membrane fluidity and permeability (Khan et al., 2003), as well as integral protein function, cholesterol-induced membrane packing in lateral microdomains (rafts) can provide a scaffold for variety of membrane associated signalling proteins (Tabas, 2002). Rafts are small platforms, composed of sphingolipids and cholesterol in the outer exoplasmic leaflet, and connected to phospholipids and cholesterol in the inner cytoplasmic leaflet of the lipid bilayer. These assemblies are fluid but more ordered and tightly packed than the surrounding bilayer. The presence of this liquid-ordered microdomains in cells transforms the classical membrane fluid mosaic model into a more complex system, where proteins and lipid rafts diffuse laterally within a two-dimensional liquid.

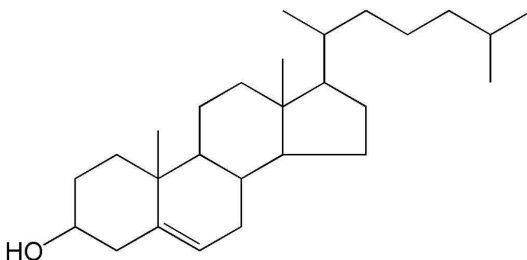


**Figure 6.** Structure of cholesterol molecule.





Following its isolation and characterization in 1955, CoQ was originally shown to be a necessary component of the mitochondrial respiratory chain two years later. It functions as an electron carrier from complex I and II to complex III and, according to Mitchell's protonmotive Q cycle, production of ubisemiquinone accounts for the energy conservation occurring at coupling site 2 of the respiratory chain (Mitchell, 1975). It is hypothesized that disruption of ubiquinone production may lead to dysfunction of the electron transport chain, which could reduce muscle cell ATP levels, thus affecting muscle contraction, increase radical production and lead to apoptosis.

Today, several other important functions are also associated with this lipid.

1. The PM of most cells contains a CoQ-dependent NADH-oxidase which regulates the cytosolic  $\text{NAD}^+/\text{NADH}$  ratio and ascorbate reduction and is involved in regulation of cell growth and differentiation (Gomez-Diaz et al., 1997).

2. CoQ is our only lipid-soluble antioxidant synthesized endogenously, and efficiently prevents oxidation of proteins, lipids and DNA. Effective enzymatic systems strive continuously to maintain this compound in its active reduced form (Bentinger et al. 2011).

3. Opening of the mitochondrial membrane transition pore allows the translocation of molecules as large as 1500 Da in size, which leads to a collapse of mitochondrial functions. CoQ10 is one of the compounds that prevent such pore opening, thereby it is counteracting apoptotic events such as ATP depletion, release of cytochrome c into the cytosol, caspase-9 activation, depolarization of the mitochondrial membrane potential and DNA fragmentation (Papucci et al., 2003).

4. Uncoupling proteins present in the inner mitochondrial membrane can translocate protons from the outside to the inside of this membrane as a result of which the proton gradient formed by the respiratory chain is uncoupled from oxidative phosphorylation and heat is produced instead. These protons are delivered from fatty acids to the uncoupling proteins with the assistance of oxidized CoQ, which is thus an obligatory cofactor in this process (Echtay et al., 2001).

5. CoQ exerts multiple anti-inflammatory effects by influencing the expression of NF $\kappa$ B1-dependent genes (Schmelzer et al., 2007). Apparently, uptake of CoQ into lymphocytes and monocytes initiates the release of mediators and signal substances into the blood that subsequently modify such expression in a variety of tissues (Bentinger et al., 2011).

6. By protecting LDL from oxidation, this lipid has also anti-atherosclerotic properties. Moreover, it reduces the levels of lipid peroxides associated with lipoproteins in atherosclerotic lesions, as well as the size of such lesions in the aorta. Furthermore, CoQ decreases the levels of  $\beta$ 2-integrin CD11b in monocytes, which counteracts monocyte–endothelial cell interactions (Thomas et al., 1996).

7. CoQ helps counteract endothelial dysfunction by stimulating endothelial release of nitric oxide (Hamilton et al., 2007).

8. CoQ mediates both oxidation of sulfide in yeast and the introduction of disulfide bonds into bacterial proteins (Bentinger et al., 2011).

### 3.3. Dolichol

Dolichol is widely distributed in all tissues and membranes and besides carrying a terminal free hydroxyl group it exists in a phosphorylated, dephosphorylated or in an esterified form (Holstein and Hohl, 2004) (Fig 8). Although knowledge on dolichol function is limited, it has been proposed as a biomarker for ageing (Parentini et al., 2005).

Briefly, the unesterified dolichol was shown to modify the organization and packing of phospholipids in model membranes (Vigo et al., 1984), the free and the phosphorylated forms were found to be mediators of protein N-linked glycosylation or as sugar carriers (Houten et al., 2003), the lipophilic molecule dolichol intercalates into the bilayer of cell membranes and interacts with the phospholipids (Parentini et al., 2005).

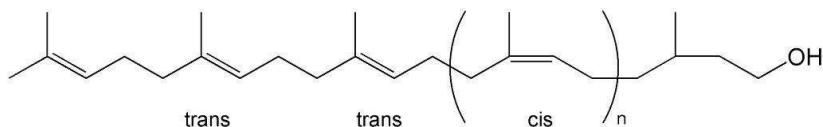


**Figure 8.** Structure of dolichol molecule.

In particular, it was found that alteration of cell-surface glycoproteins, using oligosaccharide-processing inhibitors that interfered with the synthesis of the high-mannose type of N-linked oligosaccharide, resulted in the inhibition of both the fusion reaction and biochemical differentiation of rat

skeletal muscle precursors, L6 myoblasts. Ketoconazole, compactin, and lovastatin, which affect dolichol and cholesterol biosynthesis, were also potent fusion inhibitors. These observations, coupled with earlier studies on the characterization of fusion-defective myoblast cell lines defective in glycoprotein biosynthesis, point to the importance of surface glycoproteins in cellular recognition in L6 myoblasts (Jamieson et al., 1992) (Belo et al., 1993).

In comparison to dolichol phosphate, the role of the free alcohol and its carboxylic ester is less established. An important question is the effect of these lipids on the physical properties of biological membranes. Biophysical studies have shown that dolichol and dolichol phosphates destabilize the bilayer structure of model membranes, and also increase their fluidity (Valtersson et al., 1985).

Furthermore dolichol enhances vesicle fusion whereas dolichol phosphate stimulates the fusion of rat liver microsomes. In this way, dolichol might play a more general role in membrane trafficking. Some studies (Sato et al., 1999) (Belgareh-Touze et al., 2003) suggest that free dolichol is involved in vesicle trafficking, a function in agreement with an enrichment of the Golgi apparatus for this lipid. A specific role for the dolichol-ester has not been clearly established. Besides an effect on membrane properties, the esterified form was suggested to be necessary for intracellular dolichol transport (Tollbom and Dallner, 1986). An oxidized derivative of dolichol, dolichoic acid has also been identified in human brain (Ward et al., 2007): it is speculated to result from dolichol catabolism, but its exact function is unknown (Cantagrel and Lefeber, 2011).

### **3.4. Prenylated proteins**

Protein prenylation is a post-translational modification that consists of the addition of 15 (farnesyl) or 20 (geranylgeranyl) carbon isoprenoid units to specific cysteine residues positioned near the C-terminus of a protein (Fig. 9) (Shepherd et al., 1995). Based on labelling experiments with tritiated Mva, it has been estimated that 2% of the mammalian proteome is prenylated (Anderson et al., 1995). Thus, essentially all signal transduction pathways involve prenylated proteins. The frequent occurrence of this modification, coupled with its crucial role in regulating cellular processes has generated intense interest in the enzymology and function of protein prenylation. The “CAAX” box is the recognition sequence for prenylation. The mature isoprenylated protein arises from a three-step process that consists of prenylation, followed by proteolysis of the “AAX” sequence,

and methyl esterification of the new C-terminal cysteine. Progress has also been made in understanding the function of protein prenylation. In some cases, isoprenylation serves to direct membrane association, (Ridker et al., 2001) whereas in other situations, the prenyl group is involved in mediating protein-protein interactions (Yamazaki et al., 1995).

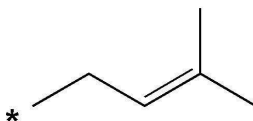


**Figure 9.** Structure of a prenyl group.

Thus, protein isoprenylation allows the covalent attachment, subcellular localization, and intracellular trafficking of membrane-associated proteins. Importantly, members of Ras and Rho GTPase family are major substrates for posttranslational modification by prenylation. Ras translocation from the cytoplasm to the plasma membrane is dependent on farnesylation, whereas Rho translocation is dependent on geranylgeranylation (Nakagami et al., 2003).

Concerning the role played by prenylated proteins in muscle function, GTP RhoA interacts and activates the phosphotransferase activity of Rho-kinase. Rho-kinase is able to regulate the phosphorylation of myosin light chain (MLC), a component of the muscle contractile protein myosin, by both the direct phosphorylation of MLC, and by the inactivation of myosin phosphatase through the phosphorylation of MBS (Myosin Binding Subunit of myosin phosphatase). Rho-kinase and myosin phosphatase thus coordinately regulate the phosphorylation-state of MLC, which is thought to induce smooth muscle contraction and stress fiber formation in non-muscle cells (Amano et al., 1996).

Moreover, Fortier and co-workers (2008) showed that RhoE, a member of Rho family, accumulates in elongated, aligned myoblasts prior to fusion and that its expression is also increased during injury-induced skeletal muscle regeneration. Furthermore, although RhoE is not required for myogenesis induction, it is essential for myoblast elongation and alignment before fusion and for M-cadherin expression and accumulation at the cell-cell contact sites. RhoE physiological upregulation is also

responsible for the decrease of RhoA and Rho-kinase activities, which are required for myoblast fusion process (Fortier et al., 2008).

#### **4. Muscle tissue**

Muscle is a very specialized tissue that has both the ability to conduct electrical impulses and to contract. Muscles are classified both structurally as either striated or smooth and functionally as either voluntary or involuntary. From this, three types of muscles emerge: skeletal muscle associated with the body's voluntary movements, cardiac muscle whose cells are joined to one another by intercalated discs which allow the synchronization of the heart beat, and smooth muscle, the intrinsic component of the wall of internal organs and blood vessels.

The prime mechanical functions of skeletal muscle are to produce force, to generate power and to act as a brake. Skeletal muscle maintains the integrity of the skeleton, allows walking, running, jumping, talking, eating, breathing and undertaking activities essential for life and living. These highly diverse requirements of muscle are met through a number of factors, such as the intricate neural control mechanisms, the different architectural arrangements, the heterogeneity of fiber types, and the ability to use different sources of fuel to keep the muscle machine working. However, within the basic functional unit of contraction, the sarcomere, there are a multitude of different structural, regulatory and contractile proteins, many of which exist as different isoforms, giving skeletal muscle a multiplicity of isoform expression (Schiaffino and Reggiani, 1996). The ability to increase the number of sarcomeres (i.e. muscle size), together with an ability to alter protein isoform expression, gives muscle the ability to adapt to the different challenges that may be placed upon it (Harridge, 2007).

Several classification techniques differentiate fibers based on their physiologic capabilities and their content of different isoforms of myosin, the sarcomere protein forming the thick filaments (Barany, 1967).

Myosin is a hexameric protein (molecular mass 480 kDa) comprising two myosin heavy chains (MHC) and four myosin light chains (MLC). At the COOH terminus, the myosin molecule is rod-shaped, as a result of the dimerization of the two heavy chains (molecular mass 200 kDa) into a 200-nm  $\alpha$ -helical tail (the S-2 fragment). Bundled together, this portion of the MHC forms the thick filament backbone. At the NH<sub>2</sub> terminus, the heavy chains separate and branch out to form two distinct heads (the S1 fragment), which contain both actin and nucleotide binding domains.

Chemomechanical transduction occurs at the S1-actin interface, where the intramolecular conformational change in the S1 structure induced by cleavage of the  $\gamma$ -phosphate of ATP is reversed by strong binding of the S1 fragment to the actin molecule (strongly bound cross-bridge formation) and subsequent release of ATP hydrolysis products ( $P_i$  and ADP) (Gordon et al., 2000). The detailed mechanisms of the actomyosin ATPase reaction have been extensively studied in solution in permeabilized skeletal muscle fibers (Cooke, 1997).

Studies on chemically skinned single human fibers showed that, as with rodent muscle, it is the MHC isoform the prime determinant of the velocity at which the peak power of contraction occurs (Bottinelli et al., 1996) as well as the rate of force development (Harridge, 2007) in a fully active fiber.

According to the majority of MHC isoforms found in adult mammalian skeletal muscles, the following pure fiber types exist: slow type I with MHCI, and three fast types, namely type IIA with MHCIIa, type IIX with MHCIIx, and type IIB with MHCIIb. The coexpression of specific pairs of these major MHC isoforms results in the formation of hybrid fibers, which can be subdivided based on the predominant MHC isoform. Fiber type-specific programs of gene expression are not restricted to the MHC isoforms, but exist for many other muscle proteins (Pette and Staron, 1997). For example, fiber type-specific isoforms exist for the essential and regulatory myosin light chains (MLC), the three troponin subunits, tropomyosin,  $\alpha$ -actinin, and various  $Ca^{2+}$  regulatory proteins (e.g., sarcoplasmic reticulum  $Ca^{2+}$  ATPase, calsequestrin, and the  $\alpha$ -subunit of the dihydropyridine receptor) (Pette and Staron, 1997). In addition to these qualitative differences, the expression levels of some proteins vary in a fiber type-specific manner.

Muscle fibers can be classified as a function of their metabolic pathways that can be either aerobic/oxidative, anaerobic/glycolytic. This kind of classification leads to 3 fiber types: fast-twitch glycolytic (FG), fast-twitch oxidative (FOG), and slow-twitch oxidative (SO) (Pette and Staron, 1997). Although a good correlation exists between type I and SO fibers, the correlations between type IIA and FOG and type IIB and FG fibers are more varied. (Hamalainen and Pette, 1995).

In cardiac myocytes, the two MHCs are encoded by two separate genes, designated as  $\alpha$  and  $\beta$  genes (Jostarndt-Fogen et al., 1998). The two MHCs,  $\alpha$  and  $\beta$ , generate three myosin isoforms in the ventricles, named V1, V2, and V3, based upon their electrophoretic mobility in the native state. The three myosin isoforms differ in the composition of  $\alpha$  and  $\beta$

MHCs, but have the same two pairs of MLCs, refereed as essential (LC-1) and regulatory (LC-2) light chains. The V1 myosin isoform is an  $\alpha\alpha$  homodimer and V3 is a  $\beta\beta$  homodimer, whereas V2 is an  $\alpha/\beta$  heterodimer. The atria contain a separate myosin isoform (Va) that is made up of two  $\alpha$ MHCs and a separate set of light chains (LC-1a and LC-2a) (Matsuoka et al., 1991) (Saez et al., 1987).

#### 4.1. Skeletal muscle development

The development of skeletal muscle is a multi-step process by which new muscle fibers are formed from precursor muscle cells.

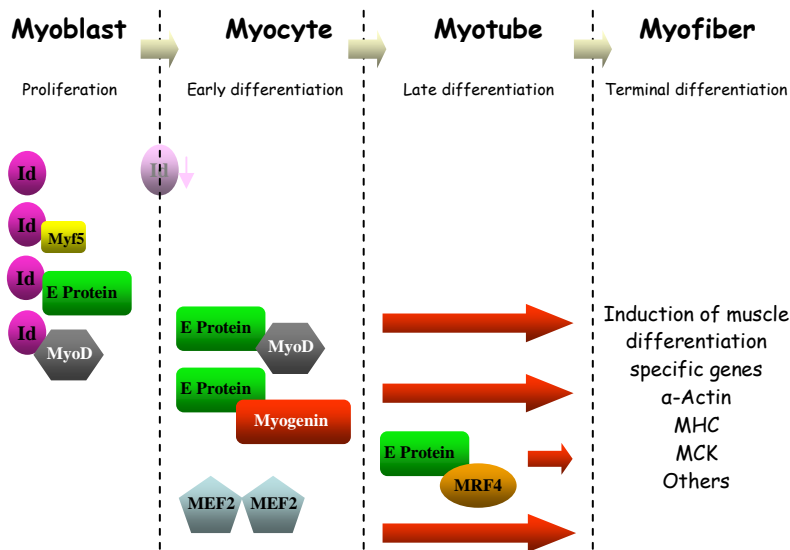


**Figure 10.** Control of skeletal myogenesis by *bHLH* and *MEF2* transcription factors (modified from Lluís et al., 2006).

Mononucleated undifferentiated myoblasts grow in proliferating conditions, characterized by a high mitogen content (proliferation); upon mitogen

withdrawal, myoblasts differentiate into mononucleated myocytes (early differentiation) that subsequently start to fuse into multinucleated myotubes expressing muscle-specific proteins (late differentiation), to form the mature muscle. Progression through the different myogenic stages is controlled by the sequential activation of four myogenic regulatory factors (MRFs) belonging to the basic helix–loop–helix (bHLH) family of transcription factors (Myf5, MyoD, myogenin and MRF4), which cooperate with the ubiquitously expressed E proteins (the E2A gene products E12 and E47, and HEB) and myocyte enhancer factor 2 (MEF2), transcriptional regulators to activate the transcription of muscle-specific genes, coding for structural and enzymatic muscle proteins such as  $\alpha$ -actin, MHC or muscle creatine kinase (MCK) (Fig. 10).

Studies using both primary cultures of skeletal muscle and established muscle cell lines (which partially recapitulate myogenesis, thus being extensively used as myogenic model systems) have confirmed the expression of MyoD and Myf5 in undifferentiated myoblasts, whereas myogenin and MRF4 are activated at early and late differentiation stages, respectively. In proliferating myoblasts, MRFs and E proteins associate with the HLH protein Id (inhibitor of differentiation). Id expression is downregulated at the onset of differentiation, allowing the formation of the functional MRF–E-protein heterodimers (Lluis et al., 2006).

#### **4.2. Skeletal muscle regeneration**

As previously reported, mammalian skeletal muscles consist of multinucleated myofibers which are formed during development by fusion of mononucleated muscle progenitors, some of which remain associated to adult myofibers as satellite cells, a specific type of stem cells located under the basal lamina of muscle fibers. The satellite cells are responsible for both muscle growth and regeneration, a process that in many but not all respects recapitulates the sequence of events observed during embryonic myogenesis.

Following muscle damage, myofibers are sheared or torn exposing the intracellular contents to the extracellular environment. Activation of calcium-dependent proteases leads to the rapid disintegration of the myofibrils whereas the activation of the complement cascade induces chemotactic recruitment of neutrophils and later macrophages who begin the process of digestion of the necrotic myofibers and cellular debris by phagocytosis. The neutrophils and macrophages release cytokines that amplify the inflammatory response and recruit the satellite cells.



Satellite cell proliferation leads to the formation of both new stem cells, which maintain an undifferentiated state, and of committed myogenic precursors which express the MyoD family regulators of muscle determination and differentiation (MRFs), including MyoD, Myf5, myogenin and MRF4. The transition from the quiescent to the activated state is rapidly followed by muscle differentiation, with expression of MHCs and fusion of myoblasts to each other forming myotubes.

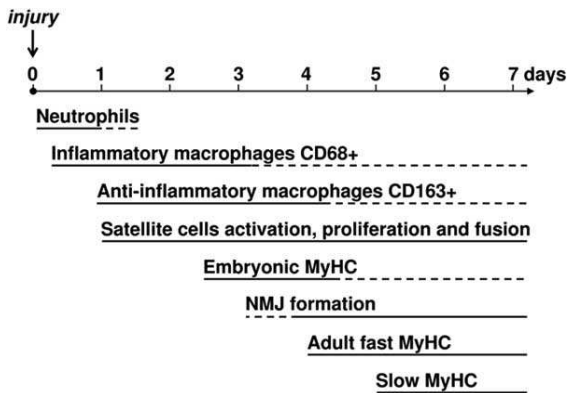


**Figure 11. Major events in muscle regeneration.** Schematic representation of the temporal sequence of inflammatory and regenerative events following muscle injury (Ciciliot and Schiaffino, 2010).

The growth of regenerated muscle may vary according to various factors, including the type of muscle injury, the involvement of blood vessels and the re-establishment of neuromuscular and myotendinous connections. A crucial factor for successful muscle regeneration is the maintenance of the basal lamina of muscle fibers. Within the intact basal lamina satellite cells can proliferate and generate myoblasts which fuse to form almost normal muscle fibers in a short time period. Regenerated fibers can be recognized by the presence of centrally located nuclei which in rodents, but not in human muscle, are a hallmark of previous muscle regeneration (Ciciliot and Schiaffino, 2010).

## **5. HMGCR inhibitors: the statins**

Statins competitively inhibit HMGCR occupying the catalytic portion of the enzyme, specifically the binding site of HMG-CoA, thus blocking access of this substrate to the active site (Istvan, 2002) (Istvan, 2003). The structures of the catalytic domains of the enzyme in complex with statin molecules have been identified (Istvan and Deisenhofer, 2000).

By interrupting cholesterol synthesis in the liver, statins activate the production of microsomal HMGCR and cell surface LDLr (Lennernas and Fager, 1997). This results in a predictable increased clearance of LDL from the bloodstream and a decrease in blood LDL cholesterol levels that may range from 20% to 55% (Jones et al., 1998) (Jones et al., 2003). Statins have shown strong evidence-based capacity of decreasing the cardiovascular morbidity and mortality both in primary (Shepherd et al., 1995) (Downs et al., 1998), and secondary prevention settings (Sacks et al., 1996) (Tonkin et al., 2000). Because of these properties, statins are amongst the most widely used pharmaceutical agents in the world (Golomb and Evans, 2008).

Although statins are generally well-tolerated, they have potentially serious adverse effects on skeletal muscle. While fatal rhabdomyolysis is a rare event, with 0,15 deaths per million prescriptions, rhabdomyalgia and myositis are much more common, with an estimated occurrence in 1-5% of patients (Draeger et al., 2006).

The development of myopathy can impact daily living and quality of life by affecting the patient's ability to accomplish even simple tasks or may prevent participation in once enjoyable physical activities. Currently, the only treatment for statin-induced myopathy is the discontinuation of statin use in affected patients, in which symptoms are most often reversible (Dirks and Jones, 2006).

Moreover a range of cases have now been reported in which statin use has "uncovered" previously clinically silent or clinically tolerated conditions, including McArdle disease, myotonic dystrophy (Tsivgoulis et al., 2006) acid maltase deficiency (Voermans et al., 2005) and possible Kennedy disease (Tsivgoulis et al., 2006). Statin has also exacerbated known muscle conditions, such as myasthenia gravis. In case of mitochondrial myopathies, the relative degree to which statins have unmasked versus induced disease may not always be clear (Golomb and Evans, 2008).

The pathogenesis of muscle damage is not known, nor it is clear why skeletal muscle should be thus affected (Draeger et al., 2006). However, given that cholesterol-lowering drugs in general can elicit myalgia, several

investigators have postulated that the loss of cholesterol destabilizes the membrane (Gharavi et al., 1994; Langer and Levy, 1968). Other authors have suggested that muscle damage is induced either by a dearth of interim products that are essential for the prenylation of small GTP-binding regulatory proteins, involved in cell growth and maintenance (Flint et al., 1997), or by a reduction in the levels of isoprenoids or farnesyl pyrophosphate levels, which could lead to mitochondrial dysfunction (Ghirlanda et al., 1993). In any case, the mechanisms underlying statin-induced myopathies are still debated.

## References

- Amano M, Ito M, Kimura K, Fukata Y, Chihara K, Nakano T, Matsuura Y, Kaibuchi K. 1996. Phosphorylation and activation of myosin by Rho-associated kinase (Rho-kinase). *J Biol Chem* 271(34):20246-20249.
- Anderson TJ, Meredith IT, Yeung AC, Frei B, Selwyn AP, Ganz P. 1995. The effect of cholesterol-lowering and antioxidant therapy on endothelium-dependent coronary vasomotion. *N Engl J Med* 332(8):488-493.
- Barany M. 1967. ATPase activity of myosin correlated with speed of muscle shortening. *J Gen Physiol* 50(6):Suppl:197-218.
- Beg ZH, Stonik JA, Brewer HB, Jr. 1985. Phosphorylation of hepatic 3-hydroxy-3-methylglutaryl coenzyme A reductase and modulation of its enzymic activity by calcium-activated and phospholipid-dependent protein kinase. *J Biol Chem* 260(3):1682-1687.
- Belgareh-Touze N, Corral-Debrinski M, Launhardt H, Galan JM, Munder T, Le Panse S, Haguenaue-Tsapis R. 2003. Yeast functional analysis: identification of two essential genes involved in ER to Golgi trafficking. *Traffic* 4(9):607-617.
- Belo RS, Jamieson JC, Wright JA. 1993. Studies on the effect of mevinolin (lovastatin) and mevastatin (compactin) on the fusion of L6 myoblasts. *Mol Cell Biochem* 126(2):159-167.
- Bentinger M, Tekle M, Dallner G. 2011. Coenzyme Q--biosynthesis and functions. *Biochem Biophys Res Commun* 396(1):74-79.
- Bottinelli R, Canepari M, Pellegrino MA, Reggiani C. 1996. Force-velocity properties of human skeletal muscle fibres: myosin heavy chain

- isoform and temperature dependence. *J Physiol* 495 ( Pt 2):573-586.
- Brown MS, Goldstein JL. 1985. The LDL receptor and HMG-CoA reductase--two membrane molecules that regulate cholesterol homeostasis. *Curr Top Cell Regul* 26:3-15.
- Brown MS, Goldstein JL. 1997. The SREBP pathway: regulation of cholesterol metabolism by proteolysis of a membrane-bound transcription factor. *Cell* 89(3):331-340.
- Brown MS, Goldstein JL. 1999. A proteolytic pathway that controls the cholesterol content of membranes, cells, and blood. *Proc Natl Acad Sci U S A* 96(20):11041-11048.
- Buhaescu I, Izzedine H. 2007. Mevalonate pathway: a review of clinical and therapeutical implications. *Clin Biochem* 40(9-10):575-584.
- Burg JS, Espenshade PJ. 2011. Regulation of HMG-CoA reductase in mammals and yeast. *Prog Lipid Res* 50(4):403-410.
- Cantagrel V, Lefeber DJ. 2011. From glycosylation disorders to dolichol biosynthesis defects: a new class of metabolic diseases. *J Inherit Metab Dis* 34(4):859-867.
- Carozzi AJ, Ikonen E, Lindsay MR, Parton RG. 2000. Role of cholesterol in developing T-tubules: analogous mechanisms for T-tubule and caveolae biogenesis. *Traffic* 1(4):326-341.
- Ciciliot S, Schiaffino S. 2010. Regeneration of mammalian skeletal muscle. Basic mechanisms and clinical implications. *Curr Pharm Des* 16(8):906-914.
- Cooke R. 1997. Actomyosin interaction in striated muscle. *Physiol Rev* 77(3):671-697.
- Dietschy JM. 1984. Regulation of cholesterol metabolism in man and in other species. *Klin Wochenschr* 62(8):338-345.
- Dietschy JM, Turley SD. 2001. Cholesterol metabolism in the brain. *Curr Opin Lipidol* 12(2):105-112.
- Dirks AJ, Jones KM. 2006. Statin-induced apoptosis and skeletal myopathy. *Am J Physiol Cell Physiol* 291(6):C1208-1212.
- Downs JR, Clearfield M, Weis S, Whitney E, Shapiro DR, Beere PA, Langendorfer A, Stein EA, Kruyer W, Gotto AM, Jr. 1998. Primary prevention of acute coronary events with lovastatin in men and women with average cholesterol levels: results of AFCAPS/TexCAPS. Air Force/Texas Coronary Atherosclerosis Prevention Study. *JAMA* 279(20):1615-1622.
- Draeger A, Monastyrskaya K, Mohaupt M, Hoppeler H, Savolainen H, Allemann C, Babiychuk EB. 2006. Statin therapy induces

- ultrastructural damage in skeletal muscle in patients without myalgia. *J Pathol* 210(1):94-102.
- Echtay KS, Winkler E, Frischmuth K, Klingenberg M. 2001. Uncoupling proteins 2 and 3 are highly active H(+) transporters and highly nucleotide sensitive when activated by coenzyme Q (ubiquinone). *Proc Natl Acad Sci U S A* 98(4):1416-1421.
- Flint OP, Masters BA, Gregg RE, Durham SK. 1997. Inhibition of cholesterol synthesis by squalene synthase inhibitors does not induce myotoxicity in vitro. *Toxicol Appl Pharmacol* 145(1):91-98.
- Fortier M, Comunale F, Kucharczak J, Blangy A, Charrasse S, Gauthier-Rouviere C. 2008. RhoE controls myoblast alignment prior fusion through RhoA and ROCK. *Cell Death Differ* 15(8):1221-1231.
- Friesen JA, Rodwell VW. 2004. The 3-hydroxy-3-methylglutaryl coenzyme-A (HMG-CoA) reductases. *Genome Biol* 5(11):248.
- Gharavi AG, Diamond JA, Smith DA, Phillips RA. 1994. Niacin-induced myopathy. *Am J Cardiol* 74(8):841-842.
- Ghirlanda G, Oradei A, Manto A, Lippa S, Uccioli L, Caputo S, Greco AV, Littarru GP. 1993. Evidence of plasma CoQ10-lowering effect by HMG-CoA reductase inhibitors: a double-blind, placebo-controlled study. *J Clin Pharmacol* 33(3):226-229.
- Goldstein JL, Brown MS. 1990. Regulation of the mevalonate pathway. *Nature* 343(6257):425-430.
- Golomb BA, Evans MA. 2008. Statin adverse effects : a review of the literature and evidence for a mitochondrial mechanism. *Am J Cardiovasc Drugs* 8(6):373-418.
- Gomez-Diaz C, Rodriguez-Aguilera JC, Barroso MP, Villalba JM, Navarro F, Crane FL, Navas P. 1997. Antioxidant ascorbate is stabilized by NADH-coenzyme Q10 reductase in the plasma membrane. *J Bioenerg Biomembr* 29(3):251-257.
- Gordon AM, Homsher E, Regnier M. 2000. Regulation of contraction in striated muscle. *Physiol Rev* 80(2):853-924.
- Hamalainen N, Pette D. 1995. Patterns of myosin isoforms in mammalian skeletal muscle fibres. *Microsc Res Tech* 30(5):381-389.
- Hamilton SJ, Chew GT, Watts GF. 2007. Therapeutic regulation of endothelial dysfunction in type 2 diabetes mellitus. *Diab Vasc Dis Res* 4(2):89-102.
- Harridge SD. 2007. Plasticity of human skeletal muscle: gene expression to in vivo function. *Exp Physiol* 92(5):783-797.

- Havel RJ. 1982. Approach to the patient with hyperlipidemia. *Med Clin North Am* 66(2):319-333.
- Hoekstra D, van ISC. 2000. Lipid trafficking and sorting: how cholesterol is filling gaps. *Curr Opin Cell Biol* 12(4):496-502.
- Hoffmann G, Gibson KM, Brandt IK, Bader PI, Wappner RS, Sweetman L. 1986. Mevalonic aciduria--an inborn error of cholesterol and nonsterol isoprene biosynthesis. *N Engl J Med* 314(25):1610-1614.
- Holstein SA, Hohl RJ. 2004. Isoprenoids: remarkable diversity of form and function. *Lipids* 39(4):293-309.
- Houten SM, Frenkel J, Waterham HR. 2003. Isoprenoid biosynthesis in hereditary periodic fever syndromes and inflammation. *Cell Mol Life Sci* 60(6):1118-1134.
- Istvan E. 2003. Statin inhibition of HMG-CoA reductase: a 3-dimensional view. *Atheroscler Suppl* 4(1):3-8.
- Istvan ES. 2002. Structural mechanism for statin inhibition of 3-hydroxy-3-methylglutaryl coenzyme A reductase. *Am Heart J* 144(6 Suppl):S27-32.
- Istvan ES, Deisenhofer J. 2000. The structure of the catalytic portion of human HMG-CoA reductase. *Biochim Biophys Acta* 1529(1-3):9-18.
- Istvan ES, Deisenhofer J. 2001. Structural mechanism for statin inhibition of HMG-CoA reductase. *Science* 292(5519):1160-1164.
- Istvan ES, Palnitkar M, Buchanan SK, Deisenhofer J. 2000. Crystal structure of the catalytic portion of human HMG-CoA reductase: insights into regulation of activity and catalysis. *EMBO J* 19(5):819-830.
- Jamieson JC, Wayne S, Belo RS, Wright JA, Spearman MA. 1992. The importance of N-linked glycoproteins and dolichyl phosphate synthesis for fusion of L6 myoblasts. *Biochem Cell Biol* 70(6):408-412.
- Janssens V, Goris J. 2001. Protein phosphatase 2A: a highly regulated family of serine/threonine phosphatases implicated in cell growth and signalling. *Biochem J* 353(Pt 3):417-439.
- Jones P, Kafonek S, Laurora I, Hunninghake D. 1998. Comparative dose efficacy study of atorvastatin versus simvastatin, pravastatin, lovastatin, and fluvastatin in patients with hypercholesterolemia (the CURVES study). *Am J Cardiol* 81(5):582-587.
- Jones PH, Davidson MH, Stein EA, Bays HE, McKenney JM, Miller E, Cain VA, Blasetto JW. 2003. Comparison of the efficacy and safety of rosuvastatin versus atorvastatin, simvastatin, and

- pravastatin across doses (STELLAR\* Trial). *Am J Cardiol* 92(2):152-160.
- Jostarndt-Fogen K, Djonov V, Draeger A. 1998. Expression of smooth muscle markers in the developing murine lung: potential contractile properties and lineal descent. *Histochem Cell Biol* 110(3):273-284.
- Khan N, Shen J, Chang TY, Chang CC, Fung PC, Grinberg O, Demidenko E, Swartz H. 2003. Plasma membrane cholesterol: a possible barrier to intracellular oxygen in normal and mutant CHO cells defective in cholesterol metabolism. *Biochemistry* 42(1):23-29.
- Langer T, Levy RI. 1968. Acute muscular syndrome associated with administration of clofibrate. *N Engl J Med* 279(16):856-858.
- Lennernas H, Fager G. 1997. Pharmacodynamics and pharmacokinetics of the HMG-CoA reductase inhibitors. Similarities and differences. *Clin Pharmacokinet* 32(5):403-425.
- Lluis F, Perdiguero E, Nebreda AR, Munoz-Canoves P. 2006. Regulation of skeletal muscle gene expression by p38 MAP kinases. *Trends Cell Biol* 16(1):36-44.
- Matsuoka R, Beisel KW, Furutani M, Arai S, Takao A. 1991. Complete sequence of human cardiac alpha-myosin heavy chain gene and amino acid comparison to other myosins based on structural and functional differences. *Am J Med Genet* 41(4):537-547.
- Messa C, Notarnicola M, Russo F, Cavallini A, Pallottini V, Trentalancia A, Bifulco M, Laezza C, Gabriella Caruso M. 2005. Estrogenic regulation of cholesterol biosynthesis and cell growth in DLD-1 human colon cancer cells. *Scand J Gastroenterol* 40(12):1454-1461.
- Mitchell P. 1975. Protonmotive redox mechanism of the cytochrome b-c1 complex in the respiratory chain: protonmotive ubiquinone cycle. *FEBS Lett* 56(1):1-6.
- Nakagami H, Jensen KS, Liao JK. 2003. A novel pleiotropic effect of statins: prevention of cardiac hypertrophy by cholesterol-independent mechanisms. *Ann Med* 35(6):398-403.
- Nervi FO, Weis HJ, Dietschy JM. 1975. The kinetic characteristics of inhibition of hepatic cholesterologenesis by lipoproteins of intestinal origin. *J Biol Chem* 250(11):4145-4151.
- Ness GC, Chambers CM. 2000. Feedback and hormonal regulation of hepatic 3-hydroxy-3-methylglutaryl coenzyme A reductase: the concept of cholesterol buffering capacity. *Proc Soc Exp Biol Med* 224(1):8-19.

- Nilsson A, Duan RD. 2006. Absorption and lipoprotein transport of sphingomyelin. *J Lipid Res* 47(1):154-171.
- Nowicka B, Kruk J. 2010. Occurrence, biosynthesis and function of isoprenoid quinones. *Biochim Biophys Acta* 1797(9):1587-1605.
- Papucci L, Schiavone N, Witort E, Donnini M, Lapucci A, Tempestini A, Formigli L, Zecchi-Orlandini S, Orlandini G, Carella G, Brancato R, Capaccioli S. 2003. Coenzyme q10 prevents apoptosis by inhibiting mitochondrial depolarization independently of its free radical scavenging property. *J Biol Chem* 278(30):28220-28228.
- Parentini I, Cavallini G, Donati A, Gori Z, Bergamini E. 2005. Accumulation of dolichol in older tissues satisfies the proposed criteria to be qualified a biomarker of aging. *J Gerontol A Biol Sci Med Sci* 60(1):39-43.
- Pette D, Staron RS. 1997. Mammalian skeletal muscle fiber type transitions. *Int Rev Cytol* 170:143-223.
- Rader DJ, Cohen J, Hobbs HH. 2003. Monogenic hypercholesterolemia: new insights in pathogenesis and treatment. *J Clin Invest* 111(12):1795-1803.
- Ridker PM, Rifai N, Clearfield M, Downs JR, Weis SE, Miles JS, Gotto AM, Jr. 2001. Measurement of C-reactive protein for the targeting of statin therapy in the primary prevention of acute coronary events. *N Engl J Med* 344(26):1959-1965.
- Rozman D, Monostory K. 2010. Perspectives of the non-statin hypolipidemic agents. *Pharmacol Ther* 127(1):19-40.
- Sacks FM, Pfeffer MA, Moye LA, Rouleau JL, Rutherford JD, Cole TG, Brown L, Warnica JW, Arnold JM, Wun CC, Davis BR, Braunwald E. 1996. The effect of pravastatin on coronary events after myocardial infarction in patients with average cholesterol levels. Cholesterol and Recurrent Events Trial investigators. *N Engl J Med* 335(14):1001-1009.
- Saez LJ, Gianola KM, McNally EM, Feghali R, Eddy R, Shows TB, Leinwand LA. 1987. Human cardiac myosin heavy chain genes and their linkage in the genome. *Nucleic Acids Res* 15(13):5443-5459.
- Sato M, Sato K, Nishikawa S, Hirata A, Kato J, Nakano A. 1999. The yeast RER2 gene, identified by endoplasmic reticulum protein localization mutations, encodes cis-prenyltransferase, a key enzyme in dolichol synthesis. *Mol Cell Biol* 19(1):471-483.



- Schiaffino S, Reggiani C. 1996. Molecular diversity of myofibrillar proteins: gene regulation and functional significance. *Physiol Rev* 76(2):371-423.
- Schmelzer C, Lindner I, Vock C, Fujii K, Doring F. 2007. Functional connections and pathways of coenzyme Q10-inducible genes: an in-silico study. *IUBMB Life* 59(10):628-633.
- Sever N, Yang T, Brown MS, Goldstein JL, DeBose-Boyd RA. 2003. Accelerated degradation of HMG CoA reductase mediated by binding of insig-1 to its sterol-sensing domain. *Mol Cell* 11(1):25-33.
- Shepherd J, Cobbe SM, Ford I, Isles CG, Lorimer AR, MacFarlane PW, McKillop JH, Packard CJ. 1995. Prevention of coronary heart disease with pravastatin in men with hypercholesterolemia. West of Scotland Coronary Prevention Study Group. *N Engl J Med* 333(20):1301-1307.
- Tabas I. 2002. Cholesterol in health and disease. *J Clin Invest* 110(5):583-590.
- Tanaka RD, Schafer BL, Lee LY, Freudenberger JS, Mosley ST. 1990. Purification and regulation of mevalonate kinase from rat liver. *J Biol Chem* 265(4):2391-2398.
- Thomas SR, Neuzil J, Stocker R. 1996. Cosupplementation with coenzyme Q prevents the prooxidant effect of alpha-tocopherol and increases the resistance of LDL to transition metal-dependent oxidation initiation. *Arterioscler Thromb Vasc Biol* 16(5):687-696.
- Tollbom O, Dallner G. 1986. Dolichol and dolichyl phosphate in human tissues. *Br J Exp Pathol* 67(5):757-764.
- Tonkin AM, Colquhoun D, Emberson J, Hague W, Keech A, Lane G, MacMahon S, Shaw J, Simes RJ, Thompson PL, White HD, Hunt D. 2000. Effects of pravastatin in 3260 patients with unstable angina: results from the LIPID study. *Lancet* 356(9245):1871-1875.
- Towler MC, Hardie DG. 2007. AMP-activated protein kinase in metabolic control and insulin signaling. *Circ Res* 100(3):328-341.
- Tsivgoulis G, Spengos K, Karandreas N, Panas M, Kladi A, Manta P. 2006. Presymptomatic neuromuscular disorders disclosed following statin treatment. *Arch Intern Med* 166(14):1519-1524.
- Valtersson C, van Duyn G, Verkleij AJ, Chojnacki T, de Kruijff B, Dallner G. 1985. The influence of dolichol, dolichol esters, and dolichyl phosphate on phospholipid polymorphism and fluidity in model membranes. *J Biol Chem* 260(5):2742-2751.

- Vigo C, Grossman SH, Drost-Hansen W. 1984. Interaction of dolichol and dolichyl phosphate with phospholipid bilayers. *Biochim Biophys Acta* 774(2):221-226.
- Voermans NC, Lammens M, Wevers RA, Hermus AR, van Engelen BG. 2005. Statin-disclosed acid maltase deficiency. *J Intern Med* 258(2):196-197.
- Ward WC, Guan Z, Zucca FA, Fariello RG, Kordestani R, Zecca L, Raetz CR, Simon JD. 2007. Identification and quantification of dolichol and dolichoic acid in neuromelanin from substantia nigra of the human brain. *J Lipid Res* 48(7):1457-1462.
- Xu F, Rychnovsky SD, Belani JD, Hobbs HH, Cohen JC, Rawson RB. 2005. Dual roles for cholesterol in mammalian cells. *Proc Natl Acad Sci U S A* 102(41):14551-14556.
- Yamazaki T, Komuro I, Kudoh S, Zou Y, Shiojima I, Mizuno T, Takano H, Hiroi Y, Ueki K, Tobe K, et al. 1995. Angiotensin II partly mediates mechanical stress-induced cardiac hypertrophy. *Circ Res* 77(2):258-265.
- Yang T, Espenshade PJ, Wright ME, Yabe D, Gong Y, Aebersold R, Goldstein JL, Brown MS. 2002. Crucial step in cholesterol homeostasis: sterols promote binding of SCAP to INSIG-1, a membrane protein that facilitates retention of SREBPs in ER. *Cell* 110(4):489-500.

## AIM

The main end-products of Mva pathway play a pivotal role in cell physiology and metabolism. In particular, in skeletal muscle, cholesterol is essential for the maintenance of a proper membrane structure, CoQ is an electron carrier of the mitochondrial respiratory chain, ensuring ATP production (Thompson et al., 2003). Oligoprenyl groups are necessary for post-translational modification of proteins such as RhoA which is known to be involved in myogenesis and in the regulation of smooth muscle contraction (Amano et al., 1996). Lastly, dolichol is needed for *N*-linked glycosylation of proteins such as the fusogenic proteins responsible for the fusion of myoblasts into multinucleated syncytia (Belo et al., 1993).

Clinical and epidemiological studies provide evidence for myopathy in patients given lipid lowering drugs such as the statins, competitive HMGR inhibitors. Although the molecular mechanisms underlying muscle adverse effects of statins are poorly understood, it is likely that the partial deficiency of HMGR main end-products following the administration of the drugs, could account for them.

Besides affecting adult muscle fibers, HMGR inhibition seems to impair skeletal muscle development preventing the fusion of muscle progenitor cells (Belo et al., 1993). Even though the above reported data suggest a pivotal role exerted by HMGR in muscle physiology, the majority of the studies in literature are limited to the definition of statin-induced myotoxicity without investigating whether and how HMGR activity influences muscle physiology.

Thus, the PhD project was primarily aimed at providing a comprehensive analysis of the role played by the enzymes and the main end-products of cholesterol biosynthetic pathway in rodent skeletal muscle differentiation, repair and functions.

Additionally, although less investigated, statin side effects on cardiac muscle were detected (Pisarenko et al., 2001) emphasising even more the necessity of extending such kind of research to cardiac muscle. Therefore, the analysis of the effects of HMGR inhibition on rat cardiac ventricle is among the objects of the PhD project.

The initial section of the thesis, namely the first three reported papers, are addressed to the evaluation of the role played by HMGR and its main end-products both in myogenesis and muscle repair through *in vitro* and *in vivo* experiments carried out in feasible models of muscle differentiation and regeneration.

The second part which comprises the last two papers, is dedicated to the analysis of the impact that HMGR inhibition exerts on skeletal muscle mechanical performance and on skeletal and cardiac muscle fiber phenotype.

Considering the elevated percentage of statin users due to the high incidence of cardiovascular disease, understanding the extent of mevalonate pathway involvement in muscle functions appears useful for the purpose of treating patients.

## References

- Amano M, Ito M, Kimura K, Fukata Y, Chihara K, Nakano T, Matsuura Y, Kaibuchi K. 1996. Phosphorylation and activation of myosin by Rho-associated kinase (Rho-kinase). *J Biol Chem* 271(34):20246-20249.
- Belo RS, Jamieson JC, Wright JA. 1993. Studies on the effect of mevinolin (lovastatin) and mevastatin (compactin) on the fusion of L6 myoblasts. *Mol Cell Biochem* 126(2):159-167.
- Pisarenko OI, Studneva IM, Lankin VZ, Konovalova GG, Tikhaze AK, Kaminnaya VI, Belenkov YN. 2001. Inhibitor of beta-hydroxy-beta-methylglutaryl coenzyme A reductase decreases energy supply to the myocardium in rats. *Bull Exp Biol Med* 132(4):956-958.
- Thompson PD, Clarkson P, Karas RH. 2003. Statin-associated myopathy. *JAMA* 289(13):1681-1690.

## **PAPERS CONCERNING PhD PROJECT**

# 3-Hydroxy 3-Methylglutaryl Coenzyme A Reductase Increase Is Essential for Rat Muscle Differentiation

CHIARA MARTINI,<sup>1</sup> LAURA TRAPANI,<sup>1</sup> LAURA NARCISO,<sup>2</sup> MARIA MARINO,<sup>1</sup> ANNA TRENTALANCE,<sup>1</sup> AND VALENTINA PALLOTTINI<sup>1</sup>\*

<sup>1</sup>Department of Biology, University of "Roma Tre," Rome, Italy

<sup>2</sup>Department of Environment and Primary Prevention, Istituto Superiore di Sanità, Rome, Italy

3-Hydroxy 3-methylglutaryl coenzyme A reductase (HMG-CoAR) is the key and rate-limiting enzyme of cholesterol biosynthetic pathway. Although HMG-CoAR activity has already been related to the differentiation of some cellular lines there are no studies that analyze the role of HMG-CoAR, and the pathway it is involved with in a fully characterized muscle differentiation model. Thus, the aim of this work is to evaluate such role and delineate the pathway involved in foetal rat myoblasts (L6) induced to differentiate by insulin—a standard and feasible model of the myogenic process. The results obtained by biochemical and morphological approaches demonstrate that (i) HMG-CoAR increase is crucial for differentiation induction, (ii) p21<sup>waf</sup>, whose increase is a necessary requisite for differentiation to occur, rises downstream HMG-CoAR activation, (iii) the main role of p38/MAPK as key regulator also for HMG-CoAR. Pathologies characterized by muscle degeneration might benefit from therapeutic programmes committed to muscle function restoration, such as modulation and planning myoblast differentiation. Thus, the important role of HMG-CoAR in muscular differentiation providing new molecular basis for the control of muscle development can help in the design of therapeutic treatment for diseases characterized by the weakening of muscular fibers and aging-related disorders (sarcopenia).

J. Cell. Physiol. 220: 524–530, 2009. © 2009 Wiley-Liss, Inc.

Myogenic differentiation is a process that begins with the commitment of mononucleated precursors to withdraw from the cell cycle, and continues with their planned progression towards specific cell types. Myogenesis can therefore be seen as a two-state process consisting of commitment and progression of myoblasts, both requiring the interplay of positive and negative regulatory signals. As they elongate, myoblasts align with each other, guided in this by mutual membrane recognition. Such alignment is followed by cell fusion, and by the formation of long and striated multinucleated myotubes (Mermelstein et al., 2007).

One of the major intracellular signaling pathways activated during the differentiation of myogenic cell lines is p38/mitogen-activated protein kinase (MAPK). By modifying p38 activity in myoblasts, the pathway has been proved essential for the expression of muscle-specific genes. p38 affects the activities of transcription factors of the MyoD and MEF2 families, and participates in the remodeling of chromatin at the level of specific muscle-regulatory regions. p38 cooperates with the myogenic transcription factors in the activation of a subset of late-transcribed genes, thus contributing to the progressive expression of genes during differentiation. p38/MAPK signaling has been also described as an inductor of the expression of the cyclin-dependent inhibitor p21<sup>waf</sup> in myoblasts, supporting p38's role in regulating cell cycle withdrawal of myoblasts at the G1 stage. Such withdrawal is considered a necessary condition for differentiation to occur (Keren et al., 2006).

3-Hydroxy 3-methylglutaryl coenzyme A reductase (HMG-CoAR) is the key and rate-limiting enzyme of the mevalonate pathway that leads to the production of cholesterol and isoprenoids (Goldstein and Brown, 1990). The enzyme is subjected to short- and long-term regulations. Short-term modulation is carried out by phosphorylation/dephosphorylation mechanisms operated, respectively, by AMP activated kinase (AMPK) (Hardie, 1992; Fisslthaler et al., 2007) and Protein Phosphatase 2 A (PP2A) (Gaussin et al.,

1997). Long-term regulation concerns the modulation of HMG-CoAR protein levels by several factors, which include Sterol Regulatory Elements Binding Protein (SREBP) and INSulin Induced Gene (INSIG)—both able to affect enzyme transcription and degradation (Goldstein et al., 2006).

It has been demonstrated that, some HMG-CoAR end-products derivatives of mevalonate such as farnesyl-pyrophosphate (FPP) and geranyl-pyrophosphate (GGPP) are essential compounds for survival, proliferation, and differentiation of cells through the activation of small GTPases, such as Ras and RhoA (Allal et al., 2000; Prendergast and Oliff, 2000; van de Donk et al., 2005). RhoA, in particular, has been shown to trigger the myogenic potential of mouse embryo fibroblasts, to accelerate myoblast differentiation and to promote actin gene expression through serum response factor activation (Castellani et al., 2006). Moreover, it has been demonstrated that HMG-CoAR activity inhibiting statins Mevinolin and Mevastatin are able to inhibit myoblast fusion by impairing the synthesis of fusogenic cell surface N-linked glycoproteins, probably by affecting the synthesis of dolichol phosphate-oligosaccharides that are required as intermediates in N-linked glycoprotein biosynthesis (Belo et al., 1993).

Contract grant sponsor: University of Roma Tre, CLAR 2007–2008.

\*Correspondence to: Valentina Pallottini, Department of Biology, University of Roma Tre, Viale Marconi, 446-00146 Rome, Italy. E-mail: vpallott@uniroma3.it

Received 12 January 2009; Accepted 30 March 2009

Published online in Wiley InterScience  
(www.interscience.wiley.com.), 22 April 2009.  
DOI: 10.1002/jcp.21810

Sterolic and non-sterolic isoprenoids products of HMG-CoAR biosynthetic pathway play an important role in several cellular processes. In most of the previous studies, only cholesterologenesis has been thoroughly analyzed because of the implication of its main product—cholesterol—in cardiovascular diseases. Yet several and clinical experimental data suggest that other compounds derived from this enzyme are essential for cellular growth and differentiation, and that HMG-CoAR could play an important role in these physiological states.

Although HMG-CoAR activity has already been related to the differentiation of some cellular lines (Ogura et al., 2007; Viccica et al., 2007), there are no studies that analyze the role of HMG-CoAR, and the pathway it is involved with in a fully characterized muscle differentiation model. Thus, the aim of this work is to evaluate such role and delineate the pathway involved in the differentiation of foetal rat myoblasts (L6)—a standard and feasible model of the myogenic process, similar to the one followed by myoblasts derived from activated satellite cells (Molinaro et al., 1998).

## Materials and Methods

### Materials

All materials used were obtained from commercial sources and of the highest quality available. All materials with no specified source are obtained from Sigma-Aldrich (Milan, Italy).

### Cell culture

Rat L6 skeletal muscle cells were used as experimental models. Undifferentiated myoblast L6 cells were purchased from the ATCC (Manassas, VA) and maintained in air containing 5% CO<sub>2</sub> in DMEM containing 10% fetal calf serum, L-glutamine (2 mM), gentamicin (0.1 mg/ml), and penicillin (100 U/ml). Cells were plated in six well plates or 25 cm<sup>2</sup> flasks at 5,000 cells/cm<sup>2</sup> in DMEM containing 10% FBS and were grown to ~70% confluence and then stimulated with 10<sup>-8</sup> M insulin to induce differentiation. To study HMG-CoAR involvement in insulin-induced L6 differentiation, 3  $\mu$ M Mevinolin (Mev) or 25  $\mu$ M 25-Hydroxy-Cholesterol (25OH-cho) were used. To study the role of p38 the specific inhibitor SB203580 was used (Calbiochem, San Diego, CA).

### Protein levels analysis

Protein levels were analyzed by Western blotting. Analysis of HMG-CoAR (Upstate, Lake Placid, NY), myogenin (Abcam, Cambridge, UK), Myosin Heavy Chain (MHC) (Abcam), RhoA (Santa Cruz Biotechnology, Santa Cruz, CA), p21waf (Santa Cruz Biotechnology), P-p38 and p38 (Cell Signaling Technology, Denver, MA) was performed on total lysates according to Martini et al. (2007). Twenty micrograms of protein were resolved by 12% (for myogenin, RhoA, P-p38, p38, and p21waf) and 7% (for MHC and HMG-CoAR) SDS-PAGE at 100 V for 60 min. The proteins were subsequently transferred electrophoretically onto nitrocellulose for 80 min at 100 V. The nitrocellulose was treated with 3% BSA in 138 mM NaCl, 27 mM KCl, 25 mM Tris-HCl, 0.05% Tween-20 (pH 6.8), and probed at 4°C overnight with primary antibodies, then 1 h with the secondary ones (UCS Diagnostic, Rome, Italy). The nitrocellulose was stripped by Restore Western Blot Stripping Buffer (Pierce Chemical, Rockford, IL) for 10 min at room temperature and then probed with anti-tubulin antibody (MP Biomedicals, Solon, OH). Bound antibodies were visualized using enhanced chemoluminescence detection (GE Healthcare, Milan, Italy). All the images derived from Western blotting were analyzed by ImageJ (NIH, Bethesda, MD) software for Windows, as arbitrary units.

### Cellular cholesterol analysis

Cells from 25 cm<sup>2</sup> flasks were harvested with trypsin (1%, v/v) and homogenized in chloroform/methanol/H<sub>2</sub>O 4:2:1 (v/v). The mixture was stirred on a vortex mixer for 2 min and then left for 15 min at room temperature. The samples were then centrifuged for 10 min at 600g. The chloroform fraction was transferred and dried under N<sub>2</sub>, then the samples were dissolved in 100  $\mu$ l ethyl ether and chromatographed on a thin layer chromatography silica gel 60 Å, 20  $\times$  20 (Whatman, Maidstone, England), previously activated at 100°C for 60 min. Samples were developed in petroleum ether/ethyl ether/acetic acid 75:25:1 (v/v); bands were visualized with iodine vapor and compared with the standard (cholesterol). All the spots visualized with iodine vapor were analyzed by ImageJ (NIH) software for Windows, as arbitrary units.

### Prenylated protein analysis

Three hours after stimulation, L6 myoblast were incubated with 30  $\mu$ M Mev and 3  $\mu$ Ci [3-<sup>3</sup>H]-MVA. Cells were then washed three times with ice-cold phosphate-buffered saline (PBS), harvested with trypsin and resuspended in PBS containing protease inhibitor cocktail. Proteins were precipitated with 1 ml of ice-cold acetone for 30 min. Samples were then washed three times with ice-cold acetone, three times with chloroform/methanol 2:1 (v/v), and last twice ethanol 95%. Samples were solubilized in 0.25 mM Tris-HCl,

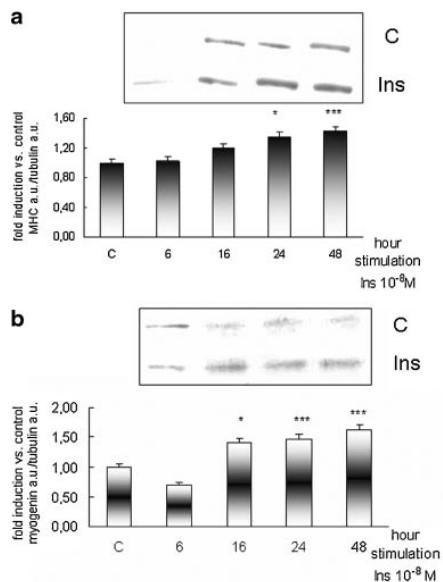


**Fig. 1.** Myogenin and Myosin Heavy Chain levels in insulin-induced L6 myoblast differentiation. The figure represents a time course (6–48 h) of 10<sup>-8</sup> M insulin treatment on myogenin (part a) and MHC (part b) protein level. On the top a typical Western blotting is shown, on the bottom the densitometric analysis of three different experiments performed in duplicate. For details see the main text. \**P* < 0.05, \*\*\**P* < 0.0001 as from a ANOVA followed by Tukey–Kramer post-test versus 0 h Ins treatment.

(pH = 6.8) containing 20% (w/v) SDS, protease inhibitor cocktail. The radioactivity was counted and normalized for the protein content of each sample.

# Immunofluorescence analysis

Treated L6 myoblasts were fixed in 4% paraformaldehyde in PBS (v/v) for 10 min and permeabilized with 0.2% Triton X-100 in PBS (v/v) for 10 min. The analysis of myotube formation was performed by incubating cells with anti-MHC antibody (produced by Dr. Crescenzi, ISS, Rome, Italy) and with anti-mouse Alexa488-conjugated antibody (Invitrogen, Carlsbad, CA). Cells were counterstained with DAPI dye.

Differentiation index was calculated performing the ratio between nuclei number observed in MHC positive cells and total nuclei number; fusion index was calculated performing the ratio between nuclei number observed in MHC positive cells and total MHC positive cells.

# Results

The main objective of this work was to understand the role played by HMG-CoAR during rat muscle differentiation. To this end, the insulin-induced differentiation of L6 rat skeletal muscle cells was studied by monitoring the expression of myogenin and MHC, that are early and late markers of muscular

differentiation, respectively. Insulin is well known to induce myoblast differentiation (Pontecorvi et al., 1988).

Firstly, a time course of myogenin and MHC induction by insulin was performed. As Figure 1 illustrates, myogenin levels showed a significant increase at 16 h, after insulin treatment (part a), whereas the increase of MHC was detected at 24 h post-stimulation (part b).

To ascertain if HMG-CoAR is subject to some modulation during insulin-induced muscular differentiation, the levels of this enzyme and the end-products critical for cellular functions, that is, prenylated proteins and cholesterol, were measured. Part a in Figure 2 illustrates the time course of the insulin effect on HMG-CoAR protein levels. An increase in protein levels was detected after 6 h, remained constant up to 16 h, and then decreased below control levels at 72 h after insulin addition. The changes in cholesterol and prenylated protein levels (parts b,c) followed a kinetics similar to that of HMG-CoAR. The prenylated protein RhoA that is involved in the differentiation process presented also a similar trend (part d).

HMG-CoAR changes during myoblast differentiation suggested that this enzyme could play a role in this process. In line with this hypothesis, differentiation was affected by interfering with either the activity or the protein levels of HMG-CoAR. As shown in Figure 3, myogenin and MHC levels were reduced when HMG-CoAR activity was blocked by Mev

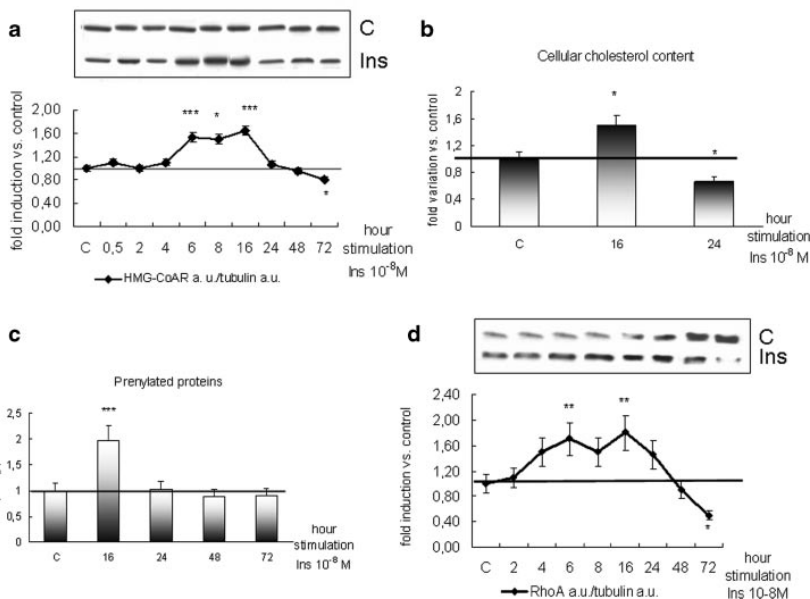


**Fig. 2.** HMG-CoAR and RhoA protein levels, cellular cholesterol and prenylated protein levels. Part a illustrates a time course (0–72 h) of 10<sup>-8</sup> M insulin treatment on HMG-CoAR protein level. On the top a typical Western blotting is shown, on the bottom the densitometric analysis of three different experiments performed in duplicate. Part b shows cellular cholesterol amount obtained by densitometric analysis of three different experiments performed through TLC (for details see the main text) on L6 myoblasts treated with 10<sup>-8</sup> M insulin for 0, 16, and 24 h. Part c represents a time course of prenylated protein amount after 10<sup>-8</sup> M insulin treatment. Part d illustrates a time course (0–72 h) of RhoA protein level after 10<sup>-8</sup> M insulin treatment. On the top a typical Western blotting is shown, on the bottom the densitometric analysis of three different experiments performed in duplicate. \**P* < 0.05, \*\*\**P* < 0.0001 as from a ANOVA followed by Tukey–Kramer post-test versus 0 h Ins treatment.



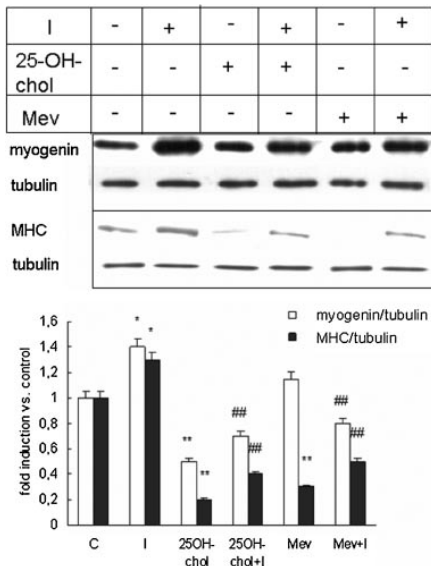


Fig. 3. 25OH-cholesterol and Mevinolin effects in insulin-induced L6 myoblast differentiation. The figure illustrates on the top a typical Western blotting and on the bottom the densitometric analysis of three different experiments performed in duplicate. Three micromolars Mev and 25  $\mu$ M 25OH-chol were administered immediately before insulin treatment. Myogenin levels were detected after 16 h of insulin treatment while MHC after 24 h insulin treatment. \* $P$  < 0.05 and \*\* $P$  < 0.001 as from a ANOVA followed by Tukey–Kramer post-test versus C. ### $P$  < 0.001 as from a ANOVA followed by Tukey–Kramer post-test versus Ins.

or when 25OH-chol interfered with its transcription and degradation. These results were also confirmed by morphological analysis. As shown in Figure 4, Mev and 25OH-chol treatment prevented myoblasts' fusion. In addition, the treatment with these inhibitors caused a significant decrease of the differentiation and fusion indexes over control (Table 1). Altogether these data suggest that HMG-CoAR participates in the differentiation process.

The correlation between HMG-CoAR and cell differentiation generated an interest in understanding which insulin-induced signal transduction pathway is involved in HMG-CoAR modulation during myoblast differentiation.

It is well established that the p38/MAPK pathway is one of the main regulatory pathways of muscular differentiation. In fact, in myoblasts p38 is able to induce p21waf, the CDK inhibitor that plays a central role in the switch of the differentiation process (Keren et al., 2006). It is also worth noting that p21waf is a SREBP1-dependent gene hence strictly correlated to the HMG-CoAR regulatory pathway (Inoue et al., 2005).

In order to elucidate the involvement of these two factors, p38 phosphorylation and p21waf induction were analyzed in L6 myoblasts during insulin-stimulated differentiation. Figure 5 shows that p38 phosphorylation is detectable 4 h after insulin stimulation, and reaches a plateau at 6 h post-stimulation

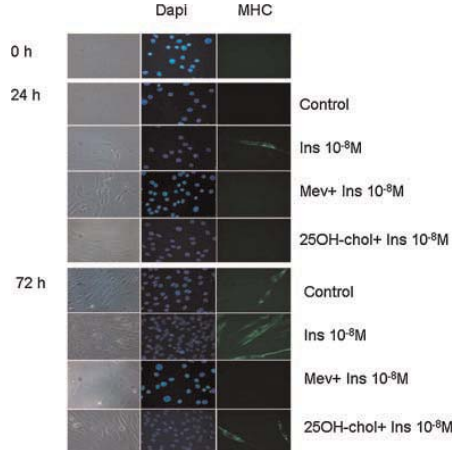


Fig. 4. Morphological analysis of L6 myoblasts during insulin-induced differentiation in presence and in absence of HMG-CoAR inhibitors. The figure represents phase contrast, Dapi staining and anti-MHC immunostaining of L6 myoblast in absence (Control) or in presence of HMG-CoAR inhibitors for 24 and 72 h. Three micromolars Mev and 25  $\mu$ M 25OH-chol were administered immediately before 10<sup>-8</sup> insulin treatment. For details see the main text.

(part a). On the contrary, the levels of p21waf are low up to 8 h post-insulin stimulation, increase at 16 and 24 h, and then fall down at 72 h (part b).

To analyze the involvement of p38 in HMG-CoAR regulation, L6 myoblasts were pre-treated with the p38 inhibitor, SB203580, and stimulated for 16 h with insulin; subsequently, HMG-CoAR levels were checked. As indicated in Figure 6, the block of p38 phosphorylation impairs the rise of HMG-CoAR (part a) and prenylated protein (part b), whilst reducing the prenylated RhoA (part c).

Cross-talk among p38, p21waf, RhoA, and HMG-CoAR was then studied by performing experiments that blocked either p38 or HMG-CoAR and p21waf was measured. In the case of HMG-CoAR inhibition also RhoA was measured. Data show

TABLE 1. Differentiation index and fusion index in L6 myoblasts treated with insulin (I) for 24 and 72 h

	Stimulation	Differentiation index	Fusion index
24 h	C	0	0
	Ins	0.014 <sup>a</sup>	1.6 <sup>b</sup>
	Mev + Ins	0 <sup>b</sup>	0 <sup>b</sup>
	25OH-chol + Ins	0 <sup>b</sup>	0 <sup>b</sup>
72 h	C	0.042	1.5
	Ins	0.07 <sup>a</sup>	3.3 <sup>a</sup>
	Mev + Ins	0 <sup>b</sup>	0 <sup>b</sup>
	25OH-chol + Ins	0.013 <sup>b</sup>	1 <sup>b</sup>

L6 myoblasts were treated with 3  $\mu$ M Mev and 25  $\mu$ M 25OH-chol immediately before insulin treatment. The differentiation and fusion indexes were calculated as indicated in Materials and Methods Section.

<sup>a</sup> $P$  < 0.001 as from ANOVA followed by Tukey–Kramer post-test with the respect to control (C).

<sup>b</sup> $P$  < 0.001 as from ANOVA followed by Tukey–Kramer post-test with the respect to Ins.

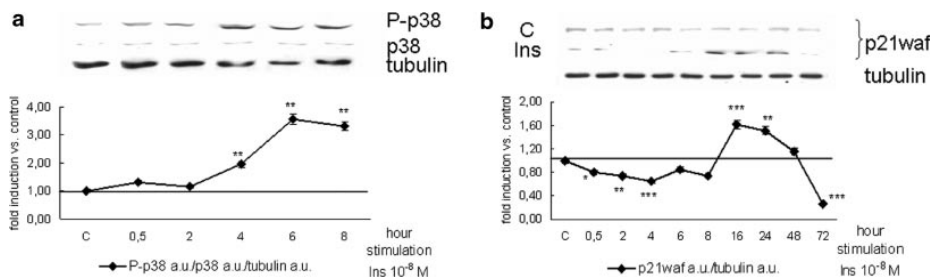


Fig. 5. Time course of p38 activation state and p21waf protein level during insulin-induced L6 myoblast differentiation. Part a illustrates a time course (0–8 h) of p38 phosphorylation state after  $10^{-8}$  M insulin treatment. Part b shows a time course (0–72 h) of p21waf protein level after  $10^{-8}$  M insulin treatment. On the top a typical Western blotting is shown, on the bottom the densitometric analysis of three different experiments performed in duplicate. \* $P < 0.05$ , \*\* $P < 0.001$ , \*\*\* $P < 0.0001$  as from a ANOVA followed by Tukey–Kramer post-test versus 0 h Ins treatment.

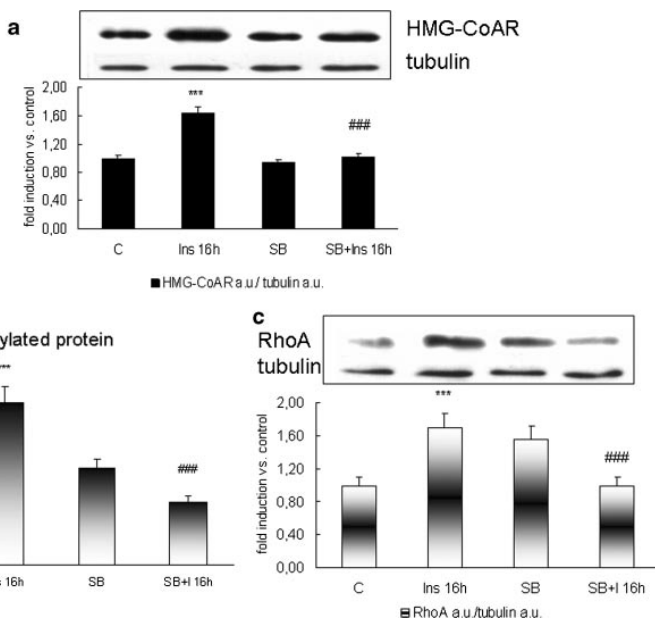
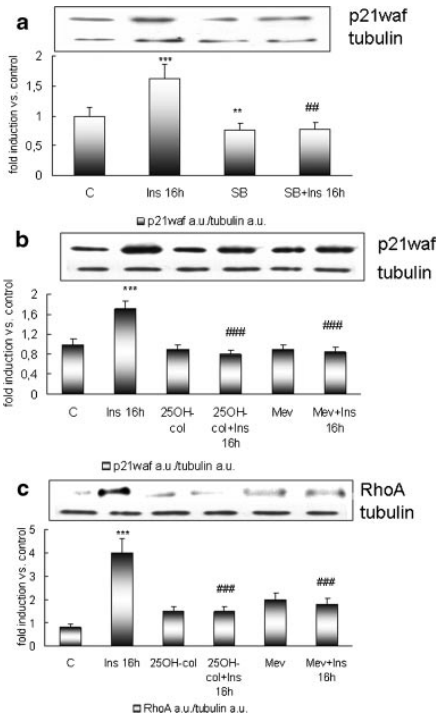


Fig. 6. Effects of p38 inhibitor SB203580 on HMG-CoAR, RhoA, and Prenylated protein levels. Part a illustrates 5  $\mu$ M SB203580 effects on HMG-CoAR protein level after 16 h  $10^{-8}$  M insulin treatment. On the top a typical Western blotting is shown, on the bottom the densitometric analysis of three different experiments performed in duplicate. Part b represents prenylated protein amount in presence of SB203580 after  $10^{-8}$  M insulin treatment. Part c illustrates RhoA protein level in presence of SB203580 after  $10^{-8}$  M insulin treatment. On the top a typical Western blotting is shown, on the bottom the densitometric analysis of three different experiments performed in duplicate. \*\*\* $P < 0.0001$  as from a ANOVA followed by Tukey–Kramer post-test versus C; #### $P < 0.0001$  as from a ANOVA followed by Tukey–Kramer post-test versus Ins.



**Fig. 7.** p38 and HMG-CoAR involvement in insulin-induced p21waf and RhoA protein increase. Part a shows the effect of p38 inhibitor, part b shows HMG-CoAR inhibitor effects on p21waf increase after 16 h insulin treatment. Part c represents the effects of HMG-CoAR inhibitors on RhoA protein levels. On the top a typical Western blotting is shown, on the bottom the densitometric analysis of three different experiments performed in duplicate. \*\* $P < 0.001$ , \*\*\* $P < 0.0001$  as from a ANOVA followed by Tukey–Kramer post-test versus C; #### $P < 0.0001$ , ### $P < 0.001$  as from a ANOVA followed by Tukey–Kramer post-test versus Ins.

that SB203580, Mev, and 25OH-cholesterol impair insulin-induced p21waf rise (Fig. 7 parts a,b). Moreover, HMG-CoAR impairment blocks the increase of RhoA (Fig. 7 part c).

Lastly, L6 myoblasts were pre-treated with SB203580, and myogenin and MHC levels tested, so as to verify the ability of p38 inhibition to block insulin-induced differentiation processes in this experimental model. Figure 8 shows that p38 inhibition effectively impairs insulin-induced L6 myoblast differentiation as shown by myogenin and MHC increase inhibition.

## Discussion

Muscle is a relatively stable tissue composed by differentiated muscle fibers containing post-mitotic nuclei. Growth and repair of mammalian muscle is inextricably linked to the action of a group of myogenic precursor cells called satellite cells, initially identified in amphibian muscle (Mauro, 1961). The muscle

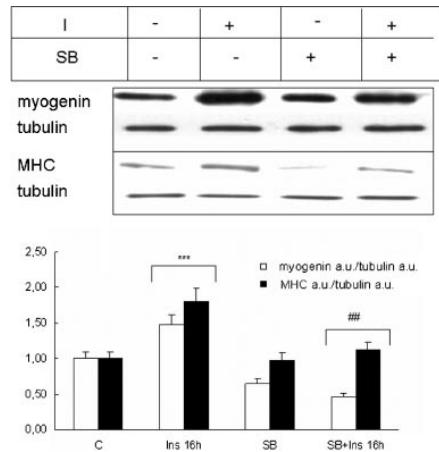


**Fig. 8.** p38 inhibitor effect on insulin-induced L6 myoblast differentiation. The figure represents protein level of myogenin and MHC after 16 h of  $10^{-8}$  M insulin treatment in presence of  $5 \mu\text{M}$  SB203580. On the top a typical Western blotting is shown, on the bottom the densitometric analysis of three different experiments performed in duplicate. For details see the main text. \*\*\* $P < 0.0001$  as from a ANOVA followed by Tukey–Kramer post-test versus C, ### $P < 0.001$  as from a ANOVA followed by Tukey–Kramer post-test versus Ins.

satellite cell fulfils the basic definition of a stem cell in that it can give rise to a differentiated cell type and also maintain itself by self-renewal (Zammit et al., 2006). Upon activation, most satellite cells go through a series of stages where they proliferate and differentiate into myoblasts; myoblasts are able to further differentiate and fuse with existing myofibers to repair damaged muscle and/or facilitate an increase in its size (Harridge, 2007).

Over the last 20 years, developments in molecular and cell biology have helped researchers increase knowledge of the mechanisms regulating muscle differentiation, but further work is required better to elucidate this process while providing therapeutic targets.

The aim of the research presented in this article was to study the putative involvement of the rate-limiting enzyme of cholesterol biosynthetic pathway HMG-CoAR during insulin-induced rat myoblast (L6) differentiation. The definition of this topic has been supported by experimental and clinical evidence demonstrating how HMG-CoAR strong inhibiting statins, widely used in therapies against hypercholesterolemia, occasionally cause myopathy characterized by weakness, pain, and elevated serum creatine phosphokinase (Ogura et al., 2007). This suggests an important role for HMG-CoAR in muscular physiology.

The data presented indicate that p21waf, whose increase is a necessary requisite for differentiation to occur (Keren et al., 2006), rises downstream HMG-CoAR activation; and that the inhibition or down-regulation of enzyme completely blocks p21waf increase, also impairing muscle differentiation. Therefore, the enzyme appears to be crucial in the withdrawal of myoblasts from the G1 stage.

The main HMG-CoAR end-products implicated in the differentiation process are prenylated proteins. The level of RhoA, a prenylated protein with an established role in the occurrence of differentiation, was checked. RhoA level appears to have initially increased and then progressively and specifically down-regulated in parallel to HMG-CoAR level changes. This result is consistent with the findings of Castellani et al. (2006) describing the importance of RhoA content down-regulation for proper muscle-specific gene expression, execution of tissue specific morphogenetic events such as fusion into multinucleated syncytia, and maintenance of the terminally differentiated phenotype. Against this broader experimental framework, HMG-CoAR appears to be up-regulated at an early stage and down-regulated at a later one in order for myoblast differentiation to start.

This study was also focused on the signal transduction pathway involved in insulin-induced L6 differentiation, and assessed the main role of p38/MAPK as key regulator also for HMG-CoAR. This is demonstrated by p38 inhibition's ability to block both insulin-induced HMG-CoAR modulation and p21waf induction. The observation of HMG-CoAR involvement in muscular differentiation processes is supported also by the findings of Belo et al. (1993), which suggest that another product of mevalonate pathway, the dolichol phosphate, could be involved in L6 myotube fusion. On the other hand, Mermelstein et al. (2007) and Portilho et al. (2007) speculate that cholesterol depletion, in myoblast, induces recognition and fusion into multinucleated myotubes. Portilho et al. (2007) shows that M $\beta$ CD-conditioned media accelerate myogenesis. This data are not in contrast with our findings; in fact, membrane cholesterol depletion is a signal that induce the expression and the activation of HMG-CoAR. Furthermore, in our model it seems that the production of prenylated proteins is important for the induction of differentiation rather than the induction of cholesterol biosynthesis.

From the data generated, it can also be assumed that the lack of the main products of HMG-CoAR biosynthetic pathway is related to statin-induced myotoxicity. Some effects could be structural, and functional to membrane modifications induced by cholesterol decrease and/or to alteration of intracellular signal transduction pathway caused by the reduced levels of prenylated metabolites (Christopher-Stine, 2006). The identification of the strict relationship between HMG-CoAR and muscular differentiation suggests that, in the case of muscular damage, statin treatment of hypercholesterolemic patients could prevent myotube formation impairing proper muscular repair.

Muscular differentiation could also be linked to metabolic variation of the cell; in fact, HMG-CoAR activity is tightly and rapidly regulated by AMPK, a cellular fuel sensor, particularly in skeletal muscle cells (Hardie and Sakamoto, 2006). The connection envisaged could be supported by the observation that AMPK modulation regulates adipocyte differentiation (Tong et al., 2008).

Pathologies characterized by muscle cells degeneration might benefit from therapeutic programmes committed to muscle function restoration, such as modulation and planning myoblast differentiation. The comprehension of the mechanisms involved in both the myogenic process and its regulation could help find new therapeutic targets in this field.

The important role of HMG-CoAR in muscular differentiation providing new molecular basis for the control of muscle development can be helpful in the design of therapeutic

treatment for diseases characterized by the weakening of muscular fibers and aging-related disorders such as sarcopenia.

## Acknowledgments

The authors are gratefully indebted to Dr. Eugenia Dogliotti, (Department of Environment and Primary Prevention, Istituto Superiore di Sanità, Rome, Italy) for the hospitality in her laboratory and for the helpful discussion. The generous gifts of MHC antibody for immunocytochemical experiments from Dr. M. Crescenzi (Department of Environment and Primary Prevention, Istituto Superiore di Sanità, Viale Regina Elena 299, 00161 Rome, Italy), and RhoA antibody from Prof. V. Casavola (Department of General and Environmental Physiology, University of Bari, 70126 Bari, Italy) are gratefully acknowledged. This work was supported by University of Roma Tre, CLAR 2007-2008 to V.P. and A.T.

## Literature Cited

- Allal C, Favre G, Coudere B, Salicio S, Sikou S, Hamilton AD, Sebi SM, Lajoie-Mazenc I, Pradines A. 2000. RhoA prenylation is required for promotion of cell growth and transformation and cytoskeleton organization but not for induction of serum response element transcription. *J Biol Chem* 275:31001-31008.
- Belo RS, Jamieson JC, Wright JA. 1993. Studies on the effect of mevinolin (lovastatin) and mevastatin (compactin) on the fusion of L6 myoblasts. *Mol Cell Biochem* 126:159-167.
- Castellani L, Salvati E, Alema S, Falcone G. 2006. Fine regulation of RhoA and Rock is required for skeletal muscle differentiation. *J Biol Chem* 281:15249-15257.
- Christopher-Stine L. 2006. Statin myopathy: An update. *Curr Opin Rheumatol* 18:647-653.
- Fisthalter B, Fleming L, Keseru B, Walsh K, Busse R. 2007. Fluid shear stress and NO decrease the activity of the hydroxy-methylglutaryl coenzyme A reductase in endothelial cells via the AMP-activated protein kinase and FoxO1. *Circ Res* 100:e12-621.
- Gaussin V, Skarlas P, Chung YP, Hardie DG, Hue L. 1997. Distinct type-2A protein phosphatases activate HMGCoA reductase and acetyl-CoA carboxylase in liver. *FEBS Lett* 413:115-118.
- Goldstein JL, Brown MS. 1990. Regulation of the mevalonate pathway. *Nature* 343:425-430.
- Goldstein JL, DeBose-Boyd RA, Brown MS. 2006. Protein sensors for membrane sterols. *Cell* 124:35-46.
- Hardie DG. 1992. Regulation of fatty acid and cholesterol metabolism by the AMP-activated protein kinase. *Biochim Biophys Acta* 1123:231-238.
- Hardie DG, Sakamoto K. 2006. AMPK: A key sensor of fuel and energy status in skeletal muscle. *Physiology (Bethesda)* 21:48-60.
- Harridge SD. 2007. Plasticity of human skeletal muscle: Gene expression to in vivo function. *Exp Physiol* 92:783-797.
- Inoue N, Shimano H, Nakakuki M, Matsuzaka T, Nakagawa Y, Yamamoto T, Sato R, Takahashi A, Sone H, Yahagi N, Suzuki H, Toyoshima H, Yamada N. 2005. Lipid synthesis transcription factor SREBP-1a activates p21WAF1/CIP1, a universal cyclin-dependent kinase inhibitor. *Mol Cell Biol* 25:8938-8947.
- Keren A, Tamir Y, Bengali E. 2006. The p38 MAPK signaling pathway: A major regulator of skeletal muscle development. *Mol Cell Endocrinol* 252:224-229.
- Martini C, Palotini V, Cavallini G, Donati A, Bergamini E, Trentalance A. 2007. Caloric restrictions affect some factors involved in age-related hypercholesterolemia. *J Cell Biochem* 101:235-243.
- Mauro A. 1961. Satellite cell of skeletal muscle fibers. *J Biophys Biochem Cytol* 9:493-495.
- Mermelstein CS, Portilho DM, Mendes FA, Costa ML, Abreu JG. 2007. Wnt/beta-catenin pathway activation and myogenic differentiation are induced by cholesterol depletion. *Differentiation* 75:184-192.
- Molinaro M, Rizzoli C, Siracusa G, Stefanini M. 1998. Istologia di V. Monesi. IV edition. Italy: Piccin, 767 p.
- Ogura T, Tanaka Y, Nakata T, Namikawa T, Kataoka H, Ohtsubo Y. 2007. Simvastatin reduces insulin-like growth factor-I signaling in differentiating C2C12 mouse myoblast cells in an HMG-CoA reductase inhibition-independent manner. *J Toxicol Sci* 32:57-67.
- Pontecorvi A, Tata JR, Phyllisier M, Robbins J. 1988. Selective degradation of mRNA: The role of short-lived proteins in differential destabilization of insulin-induced creatine phosphokinase and myosin heavy chain mRNAs during rat skeletal muscle L6 cell differentiation. *EMBO J* 7:1489-1495.
- Portilho DM, Martins ER, Costa ML, Mermelstein CS. 2007. A soluble and active form of Wnt-3a protein is involved in myogenic differentiation after cholesterol depletion. *FEBS Lett* 581:5787-5795.
- Prendergast GC, Cliff A. 2000. Farnesyltransferase inhibitors: Antineoplastic properties, mechanisms of action, and clinical prospects. *Semin Cancer Biol* 10:443-452.
- Tong J, Zhu MJ, Underwood KR, Hess BW, Ford SP, Du M. 2008. AMP-activated protein kinase and adipogenesis in sheep fetal skeletal muscle and 3T3-L1 cells. *J Anim Sci* 86:1296-1305.
- van de Donk NW, Lokhorst HM, Nijhuis EH, Kamphuis MM, Bloem AC. 2005. Geranylgeranylated proteins are involved in the regulation of myeloma cell growth. *Clin Cancer Res* 11:429-439.
- Viccia G, Vignali E, Marocchi C. 2007. Role of the cholesterol biosynthetic pathway in osteoblastic differentiation. *J Endocrinol Invest* 30:8-12.
- Zammit PS, Partridge TA, Yablonsky-Reuveni Z. 2006. The skeletal muscle satellite cell: The stem cell that came in from the cold. *J Histochem Cytochem* 54:1177-1191.

## Mechanism Underlying Long-Term Regulation of 3-Hydroxy-3-Methylglutaryl Coenzyme A Reductase During L6 Myoblast Differentiation

Laura Trapani, Chiara Martini, Anna Trentalance, and Valentina Pallottini\*

*Department of Biology, University Roma Tre, Viale Marconi, 446-00146 Rome, Italy*

### ABSTRACT

3-Hydroxy 3-methylglutaryl Coenzyme A reductase (HMG-CoAR) and its end-products are crucial for insulin-induced differentiation of fetal rat myoblasts (L6) both at early and terminal stages of development. Inhibition of HMG-CoAR activity and reduction of the enzyme levels impair the expression of L6 differentiation markers and prevent myoblast fusion into multinucleated syncytia. The mechanism underlying the modulation of this crucial enzyme so that muscular differentiation can occur is poorly understood. Thus, the aim of this work was to explore the long-term regulation of HMG-CoAR in an attempt to provide a new molecular basis for the control of muscle development. All experiments were performed in L6 rat myoblasts induced to differentiate utilizing insulin. The results indicate the following: (i) at early stages of L6 differentiation, the increase in HMG-CoAR protein levels is probably due to transcriptional induction and a decrease in the enzyme degradation rate; (ii) the subsequent reduction of HMG-CoAR protein levels is related both to an increased degradation rate and reduced gene transcription, as indicated by the rise of Insig-1 levels and the subsequent decrease in the amount of n-SREBP-1; (iii) in the terminal stages of myogenesis, reduced protein levels of HMG-CoAR could be ascribed to the decrease in gene transcription while its degradation rate is not affected. By highlighting the mechanisms involved in HMG-CoAR long-term regulation during myogenesis, this work provides useful information for searching for tools to improve the regenerative ability of muscle tissue and for the development of new pharmacological treatments of myopathies. *J. Cell. Biochem.* 110: 392–398, 2010. © 2010 Wiley-Liss, Inc.

**KEY WORDS:** HMG-CoAR; INSIG; MUSCULAR DIFFERENTIATION; SREBP

Products derived from the cholesterol biosynthetic pathway, such as ubiquinone, dolichol, and prenyls, are essential compounds for survival, proliferation, and differentiation of cells [Ogura et al., 2007; Viccica et al., 2007]. Thus, the key rate-limiting enzyme of this pathway [Goldstein and Brown, 1990], 3-hydroxy-3-methylglutaryl coenzyme A reductase (HMG-CoAR), must play an important role in these physiological processes.

HMG-CoAR, which catalyzes the conversion of HMG-CoA to mevalonate, a four-electron oxidoreduction [Friesen and Rodwell, 2004], is a highly regulated enzyme, subject to transcriptional, translational, and post-translational control [Xu and Simoni, 2003]. It can induce up to 200-fold changes in enzyme levels as a function of intracellular sterol and cholesterol uptake by Low Density Lipoprotein receptor (LDLr) [Goldstein et al., 2006].

To monitor levels of membrane sterols, cells employ another membrane-embedded protein of the endoplasmic reticulum, (ER)-Scap (SREBP cleavage activating protein), in addition to HMG-

CoAR, both containing a polytopic intramembrane sequence called sterol-sensing domain (SSD).

Scap is an escort protein for Sterol Regulatory Element Binding Proteins (SREBPs), membrane bound transcription factors able to induce expression of genes required for the synthesis and uptake of cholesterol, such as *HMG-CoAR* and *LDLr* [Brown and Goldstein, 1997; Horton et al., 2002]. In sterol-deprived cells, Scap binds SREBPs and escorts them from the ER to the Golgi apparatus where SREBPs are proteolytically processed to yield active fragments that enter the nucleus and induce expression of their target genes [Brown and Goldstein, 1999]. When cholesterol builds up in ER membranes, the Scap/SREBP complex fails to exit the ER, the proteolytic processing of SREBPs is abolished and the transcription of target genes declines.

ER retention of Scap/SREBP is mediated by sterol-dependent binding of Scap/SREBP to Insig (INSulin Induced Gene), an ER resident protein [Yang et al., 2002]. Intracellular accumulation of

Additional Supporting Information may be found in the online version of this article.

\*Correspondence to: Valentina Pallottini, Department of Biology, University Roma Tre, Viale Marconi, 446-00146 Rome, Italy. E-mail: vpallott@uniroma3.it

Received 7 May 2009; Accepted 26 January 2010 • DOI 10.1002/jcb.22544 • © 2010 Wiley-Liss, Inc.

Published online 24 March 2010 in Wiley InterScience (www.interscience.wiley.com).

sterols induces HMG-CoAR to bind Insig, promoting ubiquitination and proteasomal degradation [Sever et al., 2003].

It has been recently shown that HMG-CoAR and its end-products are crucial for myogenesis both at early and terminal stages in insulin-induced fetal rat myoblast (L6) differentiation [Martini et al., 2009]. Myogenesis is a dynamic process where undifferentiated mononuclear myoblasts proliferate at first, then withdraw from the cell cycle and finally differentiate and fuse to form mature multinucleated muscle fibers. This process is controlled by members of a family of muscle-specific basic helix-loop-helix (bHLH) proteins that, in concert with members of the ubiquitous E2A and myocyte enhancer factor-2 (MEF2) families, activate the differentiation program by inducing the transcription of muscle-specific regulatory and structural genes [Lluis et al., 2006].

The important role of the HMG-CoAR pathway in muscle physiology is demonstrated by the observations that the inhibition of HMG-CoAR activity and transcription and the induction of HMG-CoAR degradation result not only a decrease in Myogenin (Myo) and Myosin Heavy Chain (MHC) protein levels (known as early and late markers of myoblast differentiation), but also inhibit myoblast fusion into multinucleated syncytia [Martini et al., 2009]. Moreover, experimental and clinical studies show that HMG-CoAR inhibitors known as statins, which are widely used in hypercholesterolemia therapies, could cause myopathy characterized by weakness, pain and elevated serum creatine phosphokinase [Christopher-Stine, 2006]. Thus, pathologies characterized by muscular weakness or damage could be improved by stimulating myogenesis through the modulation of HMG-CoAR activity and protein levels. Although the crucial role of HMG-CoAR in differentiating L6 cells has been recently demonstrated, the molecular mechanisms of long-term HMG-CoAR regulation during insulin-induced rat myoblast differentiation is completely unknown. In fact, identification of the factors involved in long-term HMG-CoAR regulation could provide useful information in the development of new pharmacological treatments for myopathies. Thus, the aim of this work was to study the steps of such regulation during skeletal muscle differentiation in an attempt to find new tools to enhance the regenerative ability of muscle tissue. To analyze the protein network regulating HMG-CoAR, we used the well-characterized insulin-induced L6 rat myoblast differentiation model. In this model, HMG-CoAR long-term regulation and the factors involved in, studied.

## MATERIALS AND METHODS

### MATERIALS

All materials were obtained from commercial sources and were of the highest quality available. All materials with no specified source were obtained from Sigma-Aldrich (Milan, Italy).

### CELL CULTURE

Rat L6 skeletal muscle cells were used in all experiments. Undifferentiated L6 myoblasts were purchased from ATCC (Manassas, VA) and were cultured in DMEM containing 10% fetal calf serum, L-glutamine (2 mM), gentamicin (0.1 mg/ml) and penicillin (100 U/ml) at 5% CO<sub>2</sub>. Cells were plated in six-well plates or 25-cm<sup>2</sup>

flasks at a density of 5,000 cells/cm<sup>2</sup> in DMEM containing 10% FBS, grown to ~70% confluence and then stimulated with 10<sup>-8</sup> M insulin to induce differentiation. To analyze whether long term HMG-CoAR regulation was affected by the modulation of transcription and/or the modulation of protein translation, L6 myoblasts were stimulated with insulin in the presence of actinomycin (ACT) (1 µg/ml) and cycloheximide (CHX) (10 µg/ml), which are transcription and protein translation inhibitors, respectively.

### PROTEIN LEVELS ANALYSIS

Protein levels were analyzed by Western blotting. Analysis of HMG-CoAR, Insig-1, and nSREBP-1 was performed on cell lysates according to Martini et al. [2007]. Twenty micrograms of protein were resolved by 12% (for Insig-1) and 10% (for HMG-CoAR and nSREBP-1) SDS-PAGE at 100 V for 60 min. The proteins were subsequently transferred onto nitrocellulose membranes for 80 min at 100 V. Membranes were treated with 3% BSA in 138 mM NaCl, 27 mM KCl, 25 mM Tris-HCl, 0.05% Tween-20 (pH 6.8), and probed at 4°C overnight with primary antibodies. Membranes were then incubated with secondary probes for 1 h. Membranes were stripped by Restore Western Blot Stripping Buffer (Pierce Chemical, Rockford, IL) for 10 min at room temperature and then probed with anti-tubulin antibody (MP Biomedicals, Solon, OH). Bound antibodies were visualized using enhanced chemiluminescence detection (GE Healthcare, Milan, Italy). All images were analyzed as arbitrary units by ImageJ (NIH, Bethesda, MD) software for Windows.

Antibodies were obtained as follows: SREBP-1 (Santa Cruz Biotechnology, Santa Cruz, CA), secondary goat anti-rabbit conjugated to HRP (UCS Diagnostic, Rome, Italy); Insig-1 (Novus Biologicals, Littleton, CO), secondary goat anti-rabbit conjugated to HRP (UCS Diagnostic); HMG-CoAR (Upstate, Lake Placid, NY), secondary goat anti-rabbit conjugated to HRP (UCS Diagnostic); Tubulin (MP Biomedicals), secondary goat anti-mouse conjugated to HRP (UCS Diagnostic).

### RNA ISOLATION AND QUANTITATIVE RT-PCR ANALYSIS (qRT-PCR)

The sequences for gene-specific forward and reverse primers were designed using the Primer Express program by Applied Biosystems. The following primers were used: for rat HMG-CoAR (GenBank Accession NM\_013134), 5'-CCTTGACGCTCTGTGGGAAT-3' (forward) and 5'-CCTGACATGGTGCCCAACTCC-3' (reverse), for rat Insig-1 (GenBank Accession NM\_022392), 5'-TGCAGATCCAGCGGAATGT-3' (forward) and 5'-CCAGGCGGAGGAGAAGATG-3' (reverse), and for tubulin (GenBank Accession AB\_011679) 5'-GTGGAATGG-ATCCCCAACAA-3' (forward) and 5'-CCGTGCTGTTCCGATGAA-3' (reverse). Total RNA was extracted from L6 cells using TRIzol Reagent (Invitrogen, Carlsbad, CA) according to the manufacturer's instructions. To determine Insig-1 gene expression levels, cDNA synthesis and qPCR were performed using a one-step qRT-PCR kit ("SuperScript<sup>TM</sup> III Platinum<sup>®</sup> - SYBR<sup>®</sup> Green One-Step" kit; Invitrogen) according to the manufacturer's instructions. cDNA synthesis and qPCR were carried out as follows: first strand cDNA synthesis was performed at 50°C for 5 min, followed by an automatic hot-start *Taq* DNA Polymerase activation step at 95°C for 5 min, and then by 25 cycles of denaturation at 95°C for 15 s, annealing at 60°C



for 30 s, and elongation at 40°C for 1 min. Gene expression was verified by 2% agarose gel electrophoresis. Each sample was tested in duplicate and the experiment repeated three times.

HMG-CoA REDUCTASE DEGRADATION IN VITRO ASSAYS

L6 myoblasts treated with insulin for 4, 16, 24, and 48 h were suspended in ice-cold 10 mM Tris-HCl (pH 7.4), 150 mM sucrose, sonicated three times and then incubated at 37°C [Pallottini et al., 2004].

The protein concentration was determined as per Lowry et al. [1951]. At certain established times (0, 4, 16, 24, and 48 h), the incubation was blocked by the addition of an equal volume of sample buffer (final concentration 0.125 M Tris-HCl (pH 6.8) containing 10% SDS, 1 mM phenylmethylsulphonyl fluoride); samples were boiled for 2 min, and the proteins were separated by SDS-PAGE on 10% polyacrylamide gels. The proteins were transferred to nitrocellulose membranes, and HMG-CoA reductase was detected using anti-HMG-CoAR antibody (Upstate). Detection of bound antibody was performed using anti-rabbit IgG and the ECL Western blotting Kit (GE Healthcare).

RESULTS

The objective of this work was to understand the mechanisms involved in long term HMG-CoAR regulation during the myogenic process. In other studies, authors used L6 myoblasts growing in 10% serum (the “proliferation” medium). To induce quiescence and promote the differentiation, the serum content was lowered to 2%. In our experimental model, L6 myoblast differentiation was induced by insulin stimulation [Pontecorvi et al., 1988]. Although in 2% serum-culture conditions the differentiation process is well controlled and the differentiation index is high, we opted for a “non-standard” method to induce L6 myogenesis since variation in HMG-CoAR levels is observed when cellular lipid composition is changed [Goldstein et al., 2006], and moreover, L6 cells are able to initiate the differentiation process even in the presence of 10% FBS (data not shown).

It has already been shown that, in our experimental model, inhibition of HMG-CoAR activity and reduction in protein levels completely prevents L6 myoblast differentiation [Martini et al., 2009]. To confirm these data we performed a time-course of insulin’s effects on HMG-CoAR levels, inhibited enzyme activity using mevinolin and decreased HMG-CoAR levels by adding 25-OH cholesterol to the culture medium. As shown in Figure 1a, enzyme levels increased at 6 h, remained constant up to 16 h, and then decreased below control levels at 72 h after insulin treatment; moreover, mevinolin and 25-OH cholesterol addition completely prevented the increase of differentiation markers (Myogenin an Myosin Heavy Chain), as shown in Figure 1b.

INSIG mRNA AND PROTEIN LEVELS

As mentioned above, long term HMG-CoAR regulation depends on enzyme transcription and degradation. Both processes were analyzed in detail by evaluating the levels of the proteins involved in the HMG-CoAR regulatory network. Since Insig-1 is able to affect

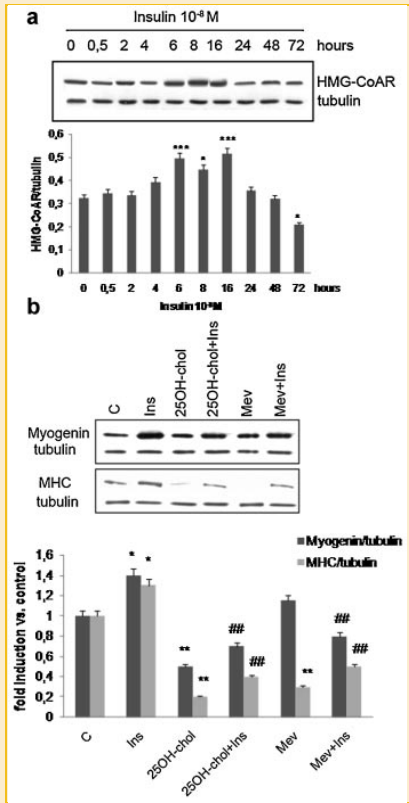


Fig. 1. HMG-CoAR time course and effects of 25-OH cholesterol and Mevinolin in insulin-treated L6 myoblasts. Panel a: The figure illustrates the time course (0–72 h) of 10<sup>−8</sup> M insulin treatment on HMG-CoAR protein levels. Twenty micrograms of protein were resolved by SDS–PAGE, followed by Western blotting with HMG-CoAR antibody. The tubulin level was used as a protein loading control. For details, see the main text. Top: a typical Western blot, Bottom: densitometric analysis of three different experiments performed in duplicate. Panel b: Effects of 25-OH cholesterol and Mevinolin in insulin-induced L6 myoblast differentiation. Top: A typical Western blot, Bottom: densitometric analysis. 3 μM Mev and 25 μM 25-OH cholesterol were administered immediately before insulin treatment. Myogenin levels were detected after 16 h post-insulin treatment while MHC levels were detected 24 h post-insulin treatment. Three different experiments were performed in duplicate. \*P < 0.05, \*\*P < 0.001, and \*\*\*P < 0.0001 as determined by ANOVA followed by Tukey–Kramer post-test versus C. ##P < 0.001 as determined by ANOVA followed by Tukey–Kramer post test versus Ins.

HMG-CoAR protein levels by inhibiting the expression of the gene coding the enzyme and by inducing HMG-CoAR degradation, Insig-1 mRNA and protein levels were analyzed in insulin-treated L6 cells. As illustrated in Figure 2a, Insig-1 mRNA levels increase by 8 h after

insulin stimulation and significantly decrease at 16 h, reaching control levels at 24 h. On the other hand, Insig-1 protein levels were decreased 8 h after insulin addition, increased by 16 h and diminished once again at 72 h (Fig. 2b). Comparative analysis of these results indicates that Insig-1 mRNA and protein levels change in an opposite way, in agreement with previously published data [Goldstein et al., 2006].

## HMG-CoAR DEGRADATION

Insig-1 mRNA and protein level variations suggested the involvement of both degradative and transcriptional mechanisms in long term HMG-CoAR regulation. Thus, *in vitro* degradation assays were performed in L6 myoblasts following insulin addition.

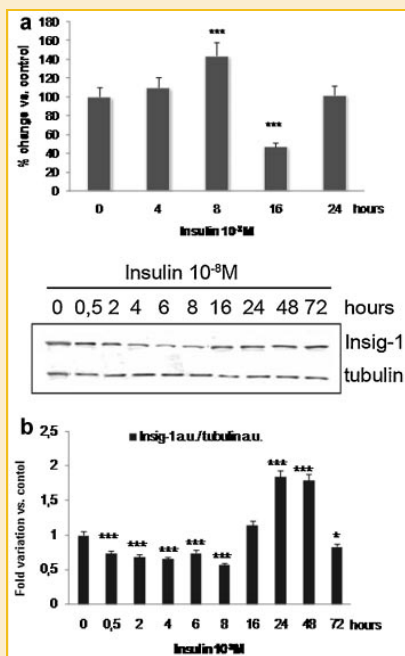


Fig. 2. Insig-1 mRNA and protein levels in insulin-induced L6 myoblast differentiation. Panel a: Relative Insig-1 mRNA levels between stimulated and control cells. qRT-PCR analysis was performed on total RNA extracted from L6 cells treated with insulin ( $10^{-8}$  M) at the times indicated. Insig-1 mRNA levels are expressed as % change versus control samples. Data are presented as the mean values  $\pm$  SD of three different experiments. Panel b: Time course (0–72 h) of  $10^{-8}$  M insulin treatment on Insig-1 protein levels. Twenty micrograms of protein were resolved by SDS-PAGE, followed by Western blotting with Insig-1 antibody. Tubulin level was used as protein loading control. For details, see the main text. Top: a typical Western blot, Bottom: densitometric analysis of three different experiments performed in duplicate. For details, see the main text. \* $P < 0.001$ , \*\*\* $P < 0.0001$  as determined by ANOVA followed by Tukey–Kramer post test versus C.

The variation in HMG-CoAR protein levels from *in vitro* degradation assays in L6 myoblasts stimulated at different times with insulin are shown separately in Figure 3a; the data were fitted using a linear regression. The slopes obtained are shown in Figure 3b; the results indicate that the rate of HMG-CoAR degradation does not change between 16 and 48 h, declines at 4 h, and increases at 24 h after insulin stimulation.

The reduced degradation rate observed at 4 h post-stimulation could account for the precocious increase in enzyme levels, while the increase in HMG-CoAR degradation rate at 24 h after insulin addition could explain the reduction of enzyme protein levels. Thus, HMG-CoAR variations appear to be functionally related to Insig-1 protein levels.

## HMG-CoAR EXPRESSION

To examine whether HMG-CoAR variations were also due to transcriptional or translational modulation, enzyme protein levels were evaluated in L6 myoblasts stimulated with insulin in presence of ACT and CHX, transcription and protein translation inhibitors, respectively. HMG-CoAR levels were checked at 6 h after insulin stimulation, when the rise in the enzyme was observed. The results shown in Figure 4 indicate that inhibition of transcription and translation by ACT and CHX, respectively, resulted in a decrease in HMG-CoAR protein levels.

The reduction in HMG-CoAR levels in presence of ACT, along with the pattern of Insig-1 expression, suggested transcriptional modulation of the enzyme; thus a time-course of SREBP-1 (HMG-CoAR transcription factor) induction by insulin was analyzed. As Figure 5 illustrates, SREBP-1 protein levels increase after 4 h, remain constant up to 8 h and then drop below control levels at 24 h.

A similar trend was observed for HMG-CoAR and Insig-1, the expression of which was reduced by SREBP-1. This suggests that SREBP-1 induces expression of HMG-CoAR followed by Insig-1 at an early stage of myogenesis.

To ascertain the involvement of transcriptional mechanisms in long term HMG-CoAR regulation, mRNA levels were measured in L6 myoblasts at 4 and 48 h after insulin treatment. Those times were chosen based on the HMG-CoAR protein levels variations previously observed. As shown in Figure 6, HMG-CoAR mRNA levels were significantly elevated at 4 h and decreased at 48 h post-stimulation, in agreement with our observed variations in HMG-CoAR protein levels.

## DISCUSSION

Skeletal muscle damage is known to depend on traumatic, ischemic, pharmaceutical, toxic, metabolic, or infectious cell damage that influences the integrity of the plasma membrane (sarcolemma) and leads to the release of toxic intracellular material into systemic circulation and to muscular fiber necrosis. These pathological conditions could benefit from an enhancement in myogenesis.

Myogenesis consists of commitment and progression of myoblasts, both processes requiring the interplay of positive and negative regulatory signals. As they elongate, myoblasts align with each other, guided in this process by mutual membrane recognition.



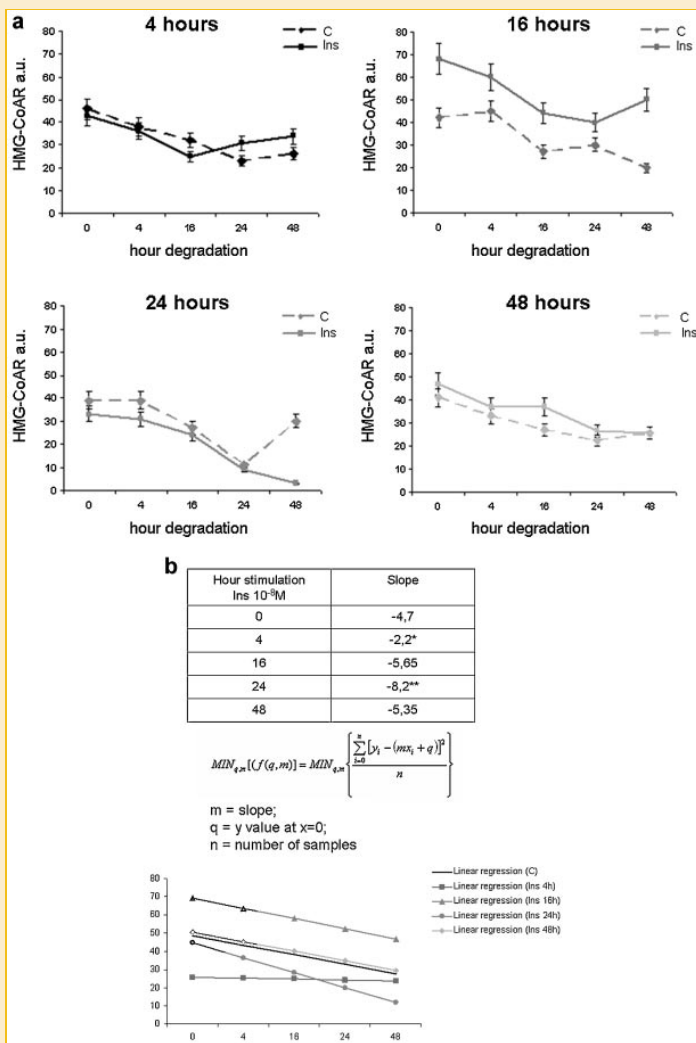


Fig. 3. HMG-CoAR degradation rate in insulin-treated L6 myoblasts. Panel a: Time courses of in vitro HMG-CoAR degradation in L6 myoblasts treated with insulin  $10^{-9}$  M for 4, 16, 24, and 48 h. At the end of each insulin stimulation, each sample was sonicated and then incubated at  $37^{\circ}\text{C}$  in a specific buffer (detailed in the text). From these samples, lysates were collected at 4, 16, 24, and 48 h. Degradation was blocked in cold lysis buffer and HMG-CoAR levels were analyzed. HMG-CoAR protein levels were evaluated by Western blot. Twenty micrograms of protein were resolved by SDS-PAGE, followed by Western blotting with HMG-CoAR antibody. Data are presented as the mean values  $\pm$  SD of three different experiments. The data were fitted using a linear regression shown in panel b.

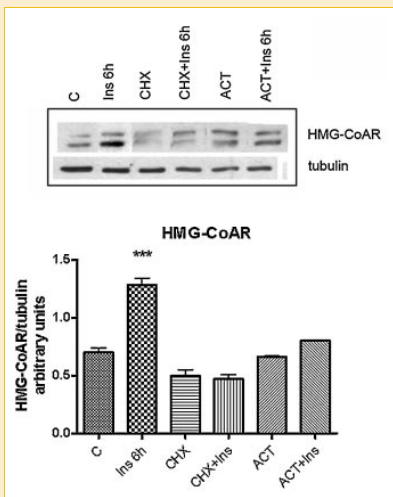


Fig. 4. Effects of actinomycin and cycloheximide in insulin-induced L6 myoblast differentiation. Top: a typical Western blot, Bottom: densitometric analysis of three different experiments performed in duplicate, cycloheximide (CHX) (10  $\mu$ g/ml) and actinomycin (ACT) (1  $\mu$ g/ml) were administered to cells 60 and 30 min before insulin treatment, respectively. HMG-CoAR protein levels were detected after 6 h of insulin treatment. Twenty micrograms of protein were resolved by SDS-PAGE, followed by western blotting with HMG-CoAR antibody. Tubulin level was used as protein loading control. For details, see the main text. \*\*\* $P$  < 0.05 as determined by ANOVA followed by Tukey-Kramer post test versus C.

Alignment is followed by cell fusion and by the formation of long, striated multinucleated myotubes [Mermelstein et al., 2007].

As recently demonstrated, HMG-CoAR appears to be up-regulated at an early stage of myogenesis and down-regulated later, moreover, inhibition of enzyme activity prevents L6 myoblast differentiation [Martini et al., 2009]. These data underline the important role for HMG-CoAR modulation in muscular differentiation. Thus, elucidation of the mechanisms responsible for HMG-CoAR modulation during muscular differentiation could be helpful in designing therapies for treatment of diseases characterized by the weakening of muscular fibers.

The data presented here demonstrate that different mechanisms are involved in long-term modulation of enzyme levels during myogenesis. At early stages of differentiation, the increase in HMG-CoAR protein levels seems to be due to transcriptional induction (parallel increase in nSREBP1 and HMG-CoAR mRNA) and to a reduction of enzyme degradation rates. These data are in agreement with the reduced amount of Insig-1, allowing both an increase in active nSREBP-1 levels and a decline in HMG-CoAR degradation rate. It is interesting to note that this induction seems dependent only on SREBP-1; in fact, no variations in SREBP-2 levels were observed (data not shown).

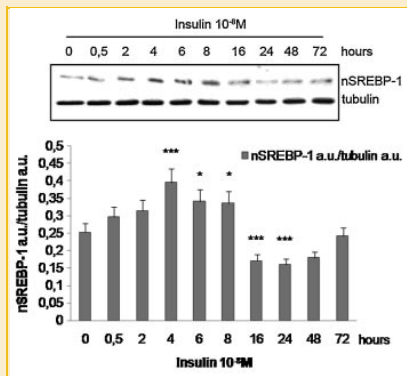


Fig. 5. SREBP-1 protein levels in insulin-induced L6 myoblast differentiation. Time course (0–72 h) of  $10^{-8}$  M insulin treatment on SREBP-1 protein levels. Twenty micrograms of protein were resolved by SDS-PAGE, followed by Western blotting with SREBP-1 antibody. Tubulin level was used as protein loading control. For details, see the main text. Top: a typical Western blot, Bottom L densitometric analysis of three different experiments performed in duplicate. For details, see the main text. \* $P$  < 0.05; \*\*\* $P$  < 0.0001 as determined by ANOVA followed by Tukey-Kramer post test versus C.

The subsequent reduction (24 h post insulin stimulation) in HMG-CoAR protein levels is likely due to accelerated degradation and to reduced transcription of the enzyme, both paralleled by elevated Insig-1 levels and a consequent decrease in n-SREBP-1 levels.

In the terminal stages of muscular differentiation considered in this study (48–72 h post-insulin stimulation), reduced protein levels of HMG-CoAR seem to be due solely to a decrease in transcription, as the degradation rate was unaltered. In this phase of the myogenic process, although Insig-1 levels were high, thus reducing nSREBP-1 levels, it was not able to accelerate the rate of HMG-CoAR degradation. This could be dependent on the low cholesterol levels

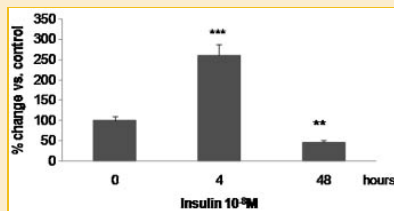


Fig. 6. HMG-CoAR mRNA levels in insulin-induced L6 myoblast differentiation. Relative levels of HMG-CoAR mRNA between stimulated and control cells. qRT-PCR analysis was performed on total RNA extracted from L6 cells treated with insulin ( $10^{-8}$  M) at the times indicated. Data are presented as the mean values  $\pm$  SD of three different experiments. For details, see the main text. \* $P$  < 0.05; \*\* $P$  < 0.001 as determined by ANOVA followed by Tukey-Kramer post test versus C.

observed in this phase of the process [Martini et al., 2009] and necessary for Insig's binding to HMG-CoAR [Espenshade and Hughes, 2007].

It is interesting to note that although Insig-1 mRNA is rapidly up-regulated by insulin stimulation [Kast-Woelbern et al., 2004], the protein levels are lower than the controls in the first stage of muscular differentiation and begin to rise only at 24 h after stimulation. These observations combine to highlight the crucial role played by Insig in HMG-CoAR regulation [Sever et al., 2003], and in turn, muscular differentiation, which has already been reported [Martini et al., 2009].

Thus, the strong relationship between the modulation of HMG-CoAR activity and muscle cell differentiation previously observed [Martini et al., 2009] is consistent with the potential role of HMG-CoAR to increase the regenerative ability of damaged muscle tissue. In conclusion, our data provide the mechanisms involved in long-term HMG-CoAR regulation during myoblast differentiation and point out new targets for the design of therapeutic treatments to improve the regenerative ability of muscle tissue in degenerative myopathies and age-related muscular disorders. Modulation of Insig-1 levels could be a functionally relevant target for improving the regenerative ability of muscle cells.

## ACKNOWLEDGMENTS

This research was supported by grants from the University of Roma Tre 2007–2008 to A.T. and V.P.

## REFERENCES

- Brown MS, Goldstein JL. 1997. The SREBP pathway: Regulation of cholesterol metabolism by proteolysis of a membrane-bound transcription factor. *Cell* 89:331–340.
- Brown MS, Goldstein JL. 1999. A proteolytic pathway that controls the cholesterol content of membranes, cells, and blood. *Proc Natl Acad Sci USA* 96:11041–11048.
- Christopher-Stine L. 2006. Statin myopathy: An update. *Curr Opin Rheumatol* 18:647–653.
- Espenshade PJ, Hughes AL. 2007. Regulation of sterol synthesis in eukaryotes. *Annu Rev Genet* 41:401–427.
- Friesen JA, Rodwell VW. 2004. The 3-hydroxy-3-methylglutaryl coenzyme-A (HMG-CoA) reductases. *Genome Biol* 5:248–252.
- Goldstein JL, Brown MS. 1990. Regulation of the mevalonate pathway. *Nature* 343:425–430.
- Goldstein JL, DeBose-Boyd RA, Brown MS. 2006. Protein sensors for membrane sterols. *Cell* 124:35–46.
- Horton JD, Goldstein JL, Brown MS. 2002. SREBPs: Activators of the complete program of cholesterol and fatty acid synthesis in the liver. *J Clin Invest* 109:1125–1131.
- Kast-Woelbern HR, Dana SL, Cesario RM, Sun L, de Grandpre LY, Brooks ME, Osburn DL, Reifel-Miller A, Klausning K, Leibowitz MD. 2004. Rosiglitazone induction of Insig-1 in white adipose tissue reveals a novel interplay of peroxisome proliferator-activated receptor gamma and sterol regulatory element-binding protein in the regulation of adipogenesis. *J Biol Chem* 279:23908–23915.
- Lluís F, Perdiguer E, Nebreda AR, Muñoz-Cánoves P. 2006. Regulation of skeletal muscle gene expression by p38 MAP kinases. *Trends Cell Biol* 16:36–44.
- Lowry OH, Rosenbrough NJ, Farr AL, Randall RJ. 1951. Protein measurement with the Folin phenol reagent. *J Biol Chem* 193:265–275.
- Martini C, Pallottini V, Cavallini G, Donati A, Bergamini E, Trentalance A. 2007. Caloric restrictions affect some factors involved in age-related hypercholesterolemia. *J Cell Biochem* 101:235–243.
- Martini C, Trapani L, Narciso L, Marino M, Trentalance A, Pallottini V. 2009. 3-Hydroxy 3-methylglutaryl Coenzyme A reductase increase is essential for rat muscle differentiation. *J Cell Physiol* 220:524–530.
- Mermelstein CS, Portillo DM, Mendes FA, Costa ML, Abreu JG. 2007. Wnt/beta-catenin pathway activation and myogenic differentiation are induced by cholesterol depletion. *Differentiation* 75:184–192.
- Ogura T, Tanaka Y, Nakata T, Namikawa T, Kataoka H, Ohtsubo Y. 2007. Simvastatin reduces insulin-like growth factor-1 signaling in differentiating C2C12 mouse myoblast cells in an HMG-CoA reductase inhibition-independent manner. *J Toxicol Sci* 32:57–67.
- Pallottini V, Montanari L, Cavallini G, Bergamini E, Gori Z, Trentalance A. 2004. Mechanisms underlying the impaired regulation of 3-hydroxy-3-methylglutaryl coenzyme A reductase in aged rat liver. *Mech Age Dev* 125:633–639.
- Pontecorvi A, Tata JR, Phyllaier M, Robbins J. 1988. Selective degradation of mRNA: The role of short-lived proteins in differential destabilization of insulin-induced creatine phosphokinase and myosin heavy chain mRNAs during rat skeletal muscle L6 cell differentiation. *EMBO J* 5:1489–1495.
- Sever N, Yang T, Brown MS, Goldstein JL, DeBose-Boyd RA. 2003. Accelerated degradation of HMG CoA reductase mediated by binding of Insig-1 to its sterol-sensing domain. *Mol Cell* 1:25–33.
- Viccia G, Vignali E, Marocchi C. 2007. Role of the cholesterol biosynthetic pathway in osteoblastic differentiation. *J Endocrinol Invest* 30:8–12.
- Xu L, Simoni RD. 2003. The inhibition of degradation of 3-hydroxy-3-methylglutaryl coenzyme A (HMG-CoA) reductase by sterol regulatory element binding protein cleavage-activating protein requires four phenylalanine residues in span 6 of HMG-CoA reductase transmembrane domain. *Arch Biochem Biophys* 414:232–243.
- Yang T, Espenshade PJ, Wright ME, Yabe D, Gong Y, Aebersold R, Goldstein JL, Brown MS. 2002. Crucial step in cholesterol homeostasis: Sterols promote binding of SCAP to INSIG-1, a membrane protein that facilitates retention of SREBPs in ER. *Cell* 110:489–500.

# **3-Hydroxy 3-methylglutaryl Coenzyme A reductase inhibition impairs muscle regeneration**

(Pending Editorial Decision: *Journal of Cellular Physiology*)

Laura Trapani, Marco Segatto, Piergiorgio La Rosa, Francesca Fanelli,  
Sandra Moreno, Maria Marino, Valentina Pallottini\*

Department of Biology, University Roma Tre, Viale Marconi 446, 00146,  
Rome, Italy

\*Corresponding author: Valentina Pallottini, Department of Biology,  
University of Roma Tre, Viale Marconi 446, 00146, Rome, Italy  
Tel. +39.06.57336320  
Fax: +39.06.57336321  
e-mail: vpallott@uniroma3.it

**Running title:** Simvastatin affects skeletal muscle regeneration

**Key words:** HMG-CoA reductase, muscle regeneration, myosin heavy chain, satellite cells, statins.

## **Abstract**

Skeletal muscle has the ability to regenerate new muscle fibers after injury. The process of new muscle formation requires that quiescent mononuclear muscle precursor cells (myoblasts) become activated, proliferate, differentiate, and fuse into multinucleated myotubes which, in turn, undergo further differentiation and mature to form functional muscle fibers. Previous data demonstrated the crucial role played by 3-hydroxy 3-methylglutaryl Coenzyme A reductase (HMGR), the rate limiting enzyme of cholesterol biosynthetic pathway, in fetal rat myoblast (L6) differentiation. This finding, along with epidemiological studies assessing the myotoxic effect of statins, HMGR inhibitors, allowed us to speculate that HMGR could be strongly involved in skeletal muscle repair. Thus, our research was aimed at evaluating such involvement: *in vitro* and *in vivo* experiments were performed on both adult satellite cell derived myoblasts (SCDM) and mouse muscles injured with cardiotoxin. Results demonstrate that HMGR inhibition by the statin simvastatin reduces SCDM fusion index, fast MHC protein levels by 60% and slow MHC by 40%. Most importantly, HMGR inhibition delays skeletal muscle regeneration *in vivo*. Thus, besides complaining of myopathies, patients given simvastatin could also undergo an impairment in muscle repair.

## **Introduction**

Skeletal muscle is the most abundant tissue of our body. Apart from its essential role in locomotion, it is also the main store of carbohydrates and proteins in the body as well as a body heat generator. The proper maintenance and function of skeletal muscle are, therefore, essential for body homeostasis. A severe, acute loss of muscle function is potentially lethal and the debilitating effects of chronic decline in mobility are commonplace experience. The maintenance of a working skeletal musculature is conferred by its remarkable ability to regenerate. Indeed, upon muscle damage a finely orchestrated set of cellular responses is activated, resulting in the regeneration of a well-innervated, fully vascularized, and contractile muscle apparatus (Charge and Rudnicki, 2004).

Following muscle damage, myofibers are sheared or torn exposing the intracellular contents to the extracellular environment. Activation of calcium-dependent proteases leads to the rapid disintegration of myofibrils, whereas the activation of the complement cascade induces chemotactic recruitment of neutrophils and then later of macrophages who begin the process of digestion of the necrotic myofibers and cellular debris by phagocytosis. Neutrophil- and macrophage-released cytokines amplify the inflammatory response and recruit satellite cells (as reviewed in Turner and Badylak, 2011) muscle-specific stem cells located under the basal lamina of muscle fibers (Mauro, 1961), responsible for muscle regeneration (Iani et al., 1994; Zammit et al., 2006).

Normally quiescent in adult skeletal muscle, satellite cells become activated when muscle is injured and proliferate to generate a pool of muscle precursor cells or myoblasts (SCDM). These cells can then either repair damaged segments of fibers or fuse together to generate entirely new multinucleated muscle fibers (as reviewed in Boldrin et al., 2010).

Muscle regeneration from satellite cells has long been believed to recapitulate, at least partially, the process of embryonic myogenesis. Supportive evidence includes the findings that proliferating and differentiating satellite cells re-express myogenic regulatory factors (MRFs, namely *MyoD*, *Myf5*, *Myogenin*, and *MRF4*) and embryonic myofibrillar genes (e.g., the embryonic isoform of myosin heavy chain, *eMHC*) during muscle regeneration (Zhao and Hoffman, 2004).

It was recently shown that 3-hydroxy 3-methylglutaryl Coenzyme A reductase (HMGR), the key and rate limiting enzyme of cholesterol biosynthetic pathway, and its main end-products (e.g. prenyls, dolichol) are

crucial for the myogenesis to occur: indeed, in insulin-induced fetal rat myoblast (L6) differentiation, HMGR down-regulation or inhibition by the statin mevinolin lead both to a decreased expression of myogenin (myo) and eMHC and to a reduction of myoblast fusion into multinucleated syncytia (Martini et al., 2009). In fact, HMGR inhibition could lead to a reduction of prenyls needed for the lipidation and the consequent activation of Rho small G protein family members, some of which (RhoA and RhoE) are known to be involved in the myogenic process (Martini et al., 2009; Fortier et al., 2008). Moreover, the statin-induced reduction of dolichol, can affect the glycosylation of proteins implicated in myoblast fusion (Belo et al., 1993). Although the involvement of HMGR in myoblast differentiation had been postulated and well characterized, little or nothing is known about the role played by the enzyme in the differentiation and maturation of adult satellite cell derived myocytes (SCDM) responsible for muscle regeneration.

Statins, HMGR competitive inhibitors, besides the beneficial effects on plasma lipid profile in patients suffering from hypercholesterolemia, have been shown to cause myopathy characterized by weakness, pain, elevated serum creatine phosphokinase and, to a lesser extent (0.05%), rhabdomyolysis, which is a life-threatening condition (Cheng et al., 2005).

The hypothesized mechanisms underlying the statin myotoxicity include structural and functional membrane modifications, mitochondria dysfunction and alteration of intracellular signal transduction pathway due to the impairment of cholesterol, ubiquinone and prenyl synthesis respectively (Draeger et al., 2006). Thus, statin-induced myopathy and the strict relationship between mevalonate pathway and myogenesis suggests that HMGR end-products are essential for skeletal muscle homeostasis maintenance. Indeed myoblast differentiation occurs not only in pathological conditions but also after common traumas occurring in many sports (Jarvinen et al., 2005): in case of muscle damage, a dysregulation of HMGR pathway can interfere with the proper muscle repair.

Thus, this research was aimed at assessing the putative involvement of HMGR in muscle regeneration by analyzing the effects of the enzyme inhibition both *in vitro* on differentiating SCDM and *in vivo* on cardiotoxin (CTX) injured mouse muscles.

### **Materials and Methods**

All materials used were obtained from commercial sources and of the highest quality available. All materials with no specified source are obtained from Sigma-Aldrich (Milan, Italy).

## **Cells**

Adult primary satellite cells were a generous gift of Dr. Marco Crescenzi of Italian National Institute of Health. The cells were grown on gelatin-coated dishes in 77% Nutrient mixture F-10 Ham (N6908, Sigma) with Pen/Strep solution (penicillin 100U/ml and streptomycin 0,1mg/ml), 20% Fetal Bovine Serum, 3% chicken embryo extract (prepared in Hank's Balanced Solution) and 2,5 ng/mL basic Fibroblast Growth Factor (Peprotech, Rocky Hill, NJ, USA). Cells were cultured at 37°C in a humidified incubator containing 5% CO<sub>2</sub>. For differentiation, cells were seeded at high density ( $2,5 \times 10^5$ ) in gelatin-coated 35mm dishes and, after cell attachment, growth medium was replaced with DMEM (D5796, Sigma) and Pen/Strep solution (penicillin 100U/ml and streptomycin 0,1mg/ml) supplemented with 10% Fetal Bovine Serum. Medium was changed every 24 h. In order to study the involvement of HMGR in cell differentiation, 1μM simvastatin (Sim) (in DMSO) and/or 100μM mevalonate (Mva) were used daily. Control cells were treated with DMSO (Veh) at the same volume of Simvastatin. Cell lysates were carried out as previously described (Martini et al., 2007).

## **Immunofluorescent staining**

For immunofluorescent staining, SCDM were grown on 18mm glass coverslips in 6-well plates ( $2,5 \times 10^5$  cells/well/coverslip). Treated cells were washed with phosphate-buffered saline (PBS, pH 7.4), fixed for 20 minutes in 4% paraformaldehyde and then permeabilized for 3 minutes with Triton X-100 (0,2% in PBS). Cells were washed, blocked in 2% BSA for 1h at room temperature, and incubated with phalloidin (0,2% in BSA 2%) for 20 minutes. SCDM were then rinsed 3 times with PBS for 10 minutes each. Nuclear stain was performed incubating cells with DAPI (5% in PBS) for 15 minutes. The slides were mounted with Prolong antifade reagent (Invitrogen, Carlsbad, CA, USA). Fluorescence images were obtained using an Olympus BX51 fluorescent microscope. At least 10 fields for each sample were examined. Differentiation index was calculated performing the ratio between nuclei number observed in phalloidin positive myotubes and total number of myotubes. For microscopic analysis, 3 independent experiments were performed for each condition.

## **Animals and treatments**

Five-month-old female C57BL/6 mice (Harlan Nossan, S. Pietro al Natisone, Italy) were housed under controlled temperature ( $20 \pm 1^\circ\text{C}$ ), humidity ( $55 \pm 10\%$ ), and illumination (lights on for 12 hours daily, from 7 A.M. to 7 P.M.). Food and water were provided *ad libitum*. The experiments were performed according to the ethical guidelines for the conduct of animal research (Ministero della Salute, Official Italian



Regulation No. 116/92, Communication to Ministero della Salute no. 391/121).

The mice (Total number = 18) were anaesthetized with ether fume woods, and 40µl of 10µM cardiotoxin (CTX) (CalBiochem, Merck KGaA, Darmstadt, Germany) in PBS were injected into the right *tibialis anterior* muscle (Delaunay et al., 2008). Three mice were treated daily for 21 days with IP injection of Simvastatin (1,5mg/kg/die in DMSO), 3 mice with IP injection of Simvastatin (1,5mg/kg/die) and Mevalonate (150mg/kg/die in H<sub>2</sub>O), 12 mice received DMSO (Veh) at the same volume of Simvastatin.

The animals were sacrificed with IP injection of urethane in H<sub>2</sub>O (1g/kg). Control mice were sacrificed at 0, 3, 10, 21 days after being injured by CTX, whereas Simvastatin and Simvastatin plus Mva treated mice were sacrificed 21 days after CTX injection.

For morphological analysis, tibial muscles from both sides of the mice, were dissected and fixed by immersion in PBS containing 4% freshly depolymerized paraformaldehyde, overnight at 4°C.

#### **Morphological analysis**

Fixed muscles were dehydrated in graded ethanol, transferred to Bioclear (BioOptica, Milan, Italy), then to a 1:1 mixture of Bioclear and paraffin, and finally embedded in paraffin. Transverse, 7-µm-thick sections were cut by a microtome and collected on Superfrost Plus slides (BioOptica). For each treatment group, a minimum of 10 sections were deparaffinized, rehydrated and stained by hematoxylin-eosin (H&E), then dehydrated and mounted with Eukitt (Kindler GmbH & Co., Freiburg, Germany). Slides were observed under an Olympus BX 51 microscope, equipped with a Leica DFC 420 camera; electronic images were captured by a Leica Application Suite system, and composed in an Adobe Photoshop CS2 format.

#### **Protein analysis**

##### *Tibialis anterior lysate preparation*

Total lysate was obtained as follows: 100 mg *tibialis anterior* muscle were homogenized in 0.01 M Tris-HCl, 0.001 M CaCl<sub>2</sub>, 0.15 M NaCl, 0.001 M PMSF, pH 7.5. An aliquot of homogenate was solubilized by sonication in Sample Buffer (0.125 M Tris-HCl (pH 6.8) containing 10% SDS), centrifuged for 5 min at 15,600 g and the supernatant was transferred in microtubes. Protein concentration was determined by the method of Lowry and co-workers (Lowry et al., 1951). All samples were boiled for 3 min before loading for protein analysis.

##### *Western blotting analysis*

Protein profiles were analysed by Western blotting. 20 µg of protein from lysates were resolved by 7% SDS-PAGE at 100V for 60 minutes. The proteins were subsequently electrophoretically transferred to nitrocellulose

for 90 minutes at 100V. The nitrocellulose membrane was blocked at room temperature with 3% BSA in Tris-buffered saline (138 mM NaCl, 27 mM KCl, 25 mM Tris-HCl, 0.05% Tween-20, pH 6.8), and probed at 4°C overnight with primary antibodies (HMGR -Upstate, Lake Placid, NY, USA, eMHC -Abcam, Cambridge, UK, fast MHC MY-32 and slow MHC NOQ7.5.4D -Sigma) followed by incubation for 1h with secondary IgG antibodies coupled to horseradish peroxidase (Bio-Rad Laboratories, Milan, Italy). The nitrocellulose membrane was then re-probed with anti-tubulin ( $\alpha$ -tubulin DM-1A, Sigma) antibody. Bound antibodies were visualized using enhanced chemoluminescence detection (GE Healthcare). All images derived from Western blotting were analyzed with ImageJ (NIH, Bethesda, MD, USA) software for Windows. Each reported value was derived from the ratio between arbitrary units obtained by the protein band and the respective tubulin band.

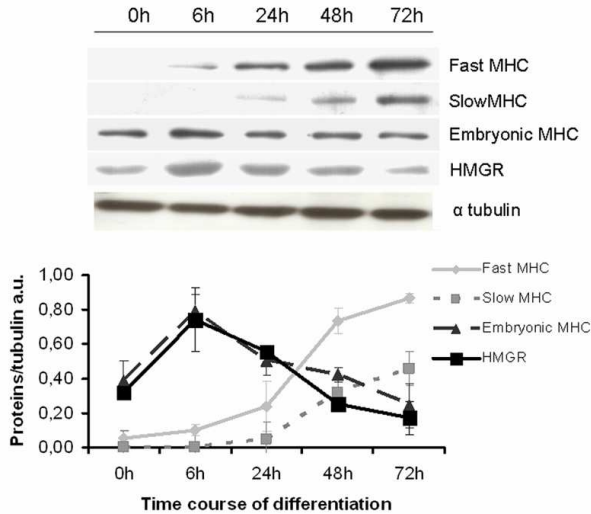
### **Statistical analysis**

Data are expressed as mean  $\pm$  SD. The difference of parameters was statistically tested for significance with one way ANOVA followed by Dunnett post-test.  $P < 0.05$  was considered statistically significant. Statistical analysis was performed using GraphPad Instat3 (GraphPad software, Inc., La Jolla, CA, USA) software for Windows. The significance of the difference was indicated by \* for  $P < 0.05$ , \*\* for  $P < 0.01$  and \*\*\* for  $P < 0.001$ .

### **Results**

Our previous work highlighting the crucial role played by HMGR and its main end-products in fetal rat myoblast (L6) myogenic process (Martini et al., 2009) allowed us to speculate that the enzyme inhibition could affect the differentiation of SCDM responsible for muscle regeneration and impair proper muscular repair.

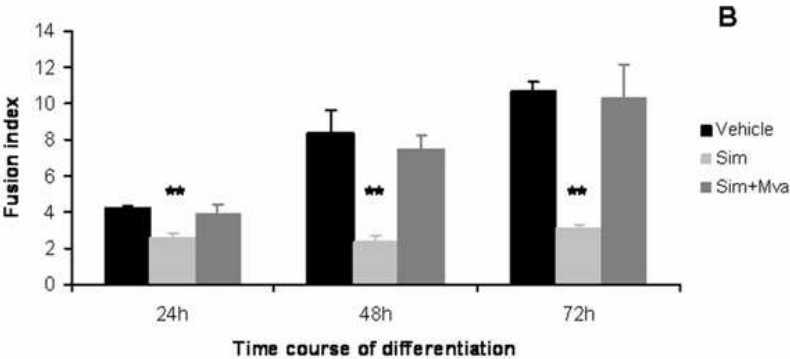
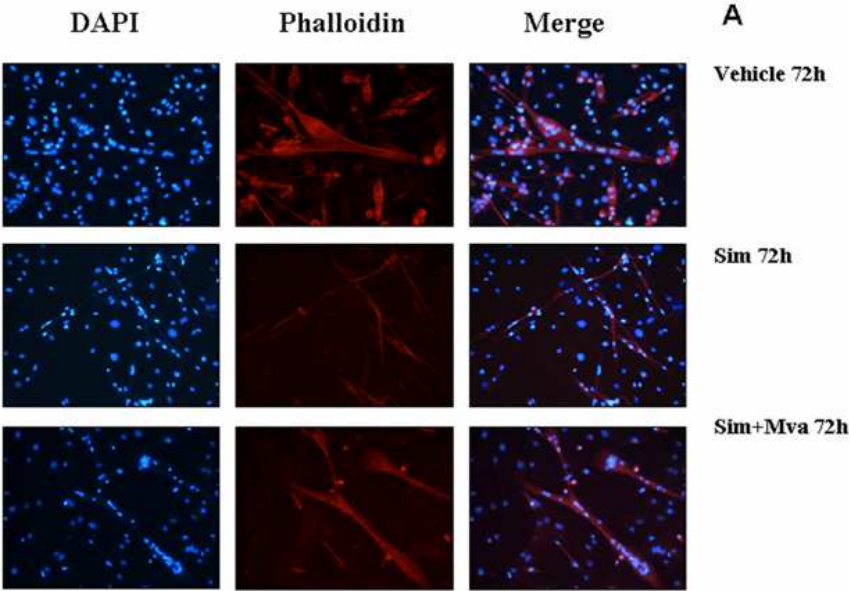
Figure 1 illustrates that both HMGR and eMHC protein levels increase 6 hours after the induction of differentiation and later decrease up to 72h. On the contrary, the rise of both fast and slow MHC isoforms (fMHC, sMHC) was observed 24h after the induction of differentiation even though the fMHC was barely detectable at 6h. The similar modulation of HMGR protein levels in both fetal L6 rat myoblasts (Martini et al., 2009) and in SCDM, allowed us to confirm an involvement of HMGR in SCDM differentiation. Our results were in agreement with the time dependent expression of the different MHC isoforms occurring in muscle regeneration.



**Figure 1. Time course of differentiation of HMGR and embryonic, fast and slow MHC in SCDM.** The figure shows a typical Western blotting and the densitometric analysis of a time course ranging from 0 to 72h of HMGR, eMHC, fMHC and sMHC protein levels in SCDM induced to differentiate through the replacement of the growth medium with that of differentiation. Data are expressed as the mean  $\pm$  SD of at least three different experiments. For details see the main text.

Proliferating Simvastatin- and Vehicle (Veh)-treated SCDM had a very similar morphology in growth medium (data not shown), but 72 h after the induction of differentiation, the myotubes derived from both types of culture showed striking differences (Fig. 2A). Indeed, Veh-treated cells formed large branched myotubes with a high number of nuclei, whereas the myotubes from the Simvastatin-treated cells were much smaller and thinner and had a relatively small number of nuclei per myotube. On the contrary, the myotubes deriving from the differentiation and fusion of SCDM treated both with Simvastatin and Mevalonate were morphologically very similar to the vehicles (Fig. 2A).

Interestingly, the fusion index (Fig. 2B) was much lower in Simvastatin-treated culture than in Veh at 24, 48, 72h treatment. In fact 72h after the replacement of the medium and the beginning of statin treatment, the fusion index decrease achieved 60%.



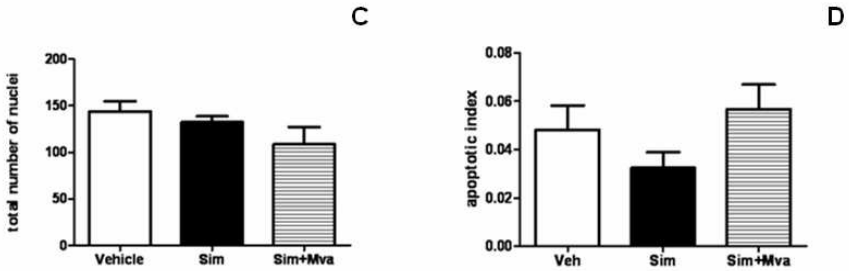


**Figure 2. Immunofluorescent staining, differentiation and apoptotic indexes of Veh, Sim, and Sim+Mva treated SCDM.** **A)** The figure shows phalloidin staining, Dapi staining and merged images of Veh, Sim, and Sim+Mva treated SCDM 72h after the induction of differentiation. **B)** Fusion index of Veh, Sim, and Sim+Mva treated SCDM 24, 48, and 72h after the induction of differentiation. The fusion index was calculated performing the ratio between nuclei number observed in phalloidin positive myotubes and total number of myotubes. Data are expressed as the ratio between Sim or Sim+Mva versus Veh sample of each time considered. **\*\*** $P < 0.01$  as from ANOVA followed by Dunnett post-test versus Veh sample of each time. **C)** Total number of nuclei of Veh, Sim, and Sim+Mva treated SCDM 72h after the induction of differentiation. At least 10 fields were observed for each experimental condition. Each column represents the mean  $\pm$  SD of at least three different experiments. **D)** Apoptotic index was calculated as ratio between apoptotic nuclei and total number of nuclei observed. A minimum of 1000 nuclei was counted for each experimental condition. Each column represents the mean  $\pm$  SD of at least three different experiments.

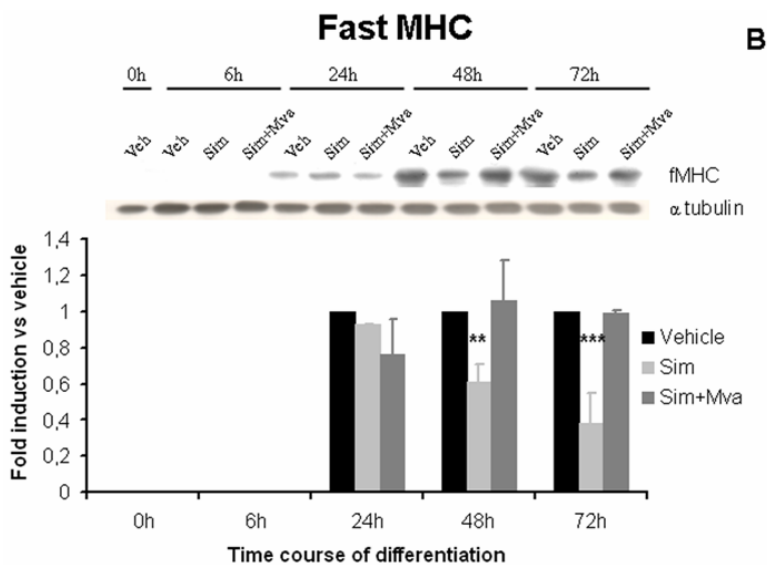
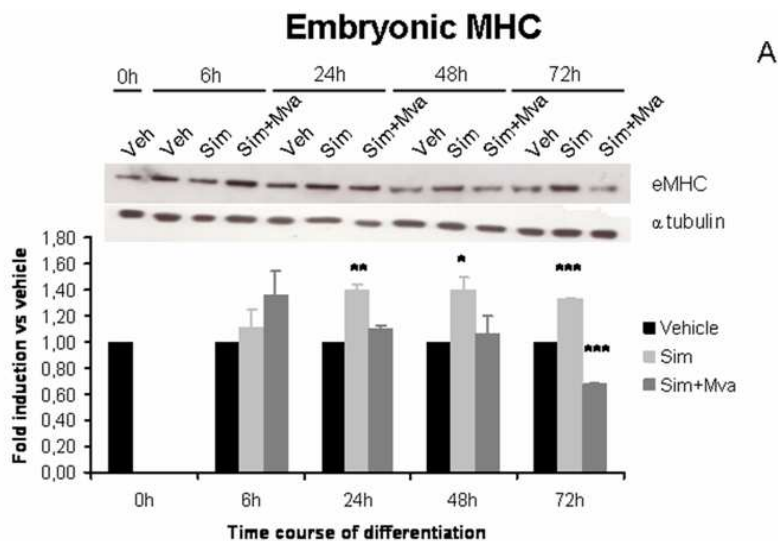
Mevalonate supplemented to Simvastatin completely prevented the Simvastatin effect (Fig. 2B dark grey columns) sustaining the pivotal role of HMGR product in skeletal muscle differentiation. No significant differences were detected either in total nuclei number (Fig. 2C) or apoptotic index (Fig. 2D) among the samples, indicating that the reduced fusion index detected in Simvastatin treated cells was not due to a different cell number.

The degree of SCDM differentiation and myotube maturation was determined by assaying the expression of eMHC, fMHC and sMHC. As expected from fusion index results, Simvastatin treated SCDM maintained eMHC levels higher than in Veh samples (Fig. 3A) and showed a general decrease in the amount of both the adult contractile proteins fMHC and sMHC in comparison with Veh at 24h, 48h and 72h (Fig. 3B and C). Rescue experiments abolished Simvastatin effect both on eMHC, fMHC and sMHC protein expression; nevertheless, after 72h, eMHC levels were lower compared with controls when SCDM were co-treated with Simvastatin and Mevalonate (Fig. 3A dark grey columns).

Since the results obtained *in vitro* suggested a delaying effect of Simvastatin on SCDM differentiation, *in vivo* experiments were performed in order to confirm whether Simvastatin could impair muscle regeneration.

The morphological features of *tibialis anterior* muscles from animals injured with CTX and chronically treated with Veh or Simvastatin or Simvastatin plus Mevalonate were analyzed. Muscles injected with CTX displayed a profoundly altered cytoarchitecture, at both day 3 and 10 after injury, compared to controls (Fig. 4A-C). In hematoxylin-eosin (H&E) stained sections from mice at 3 days after the toxic insult (Fig. 4B), a prominent inflammatory infiltrate was observed, and muscle fiber integrity was compromised. At 10 days (Fig. 4C), muscle regeneration ensues, as indicated by the presence of central nuclei in most muscle fibers. At 21 days after tissue injury (Fig. 4D), *tibialis anterior* muscles appeared completely recovered, as a regular cytoarchitecture was recognized in H&E stained sections. The large majority of muscle fibers showed a peripherally located nucleus, suggesting full cell differentiation. Histological analysis of Simvastatin treated mice demonstrated a delayed regeneration of CTX injured muscles. In fact, 21 days after the toxic insult, muscles were still in the process of regenerating their fibers, as assessed by the presence of numerous centrally located nuclei (Fig. 4E). Importantly, the effect exerted by Simvastatin was totally abolished by administration of Mevalonate (Fig. 4F). Quantitative analysis is provided in Table 1.

Lastly, to evaluate the degree of myotube maturation *in vivo*, fMHC and sMHC protein expression was checked in *tibialis anterior* muscles from animals injured with CTX and treated as described above. Three weeks (21 days) after the CTX injection, the levels of both the adult contractile proteins in injured muscles from animals treated with vehicle (I), were similar to those detected in non injured ones (NI); on the contrary, in injured muscles from treated animals (I+Sim) the content of MHCs was significantly reduced when compared to the muscles of injured Veh and Simvastatin+Mevalonate (I+Sim+Mva) treated animals (Fig. 5A, B)



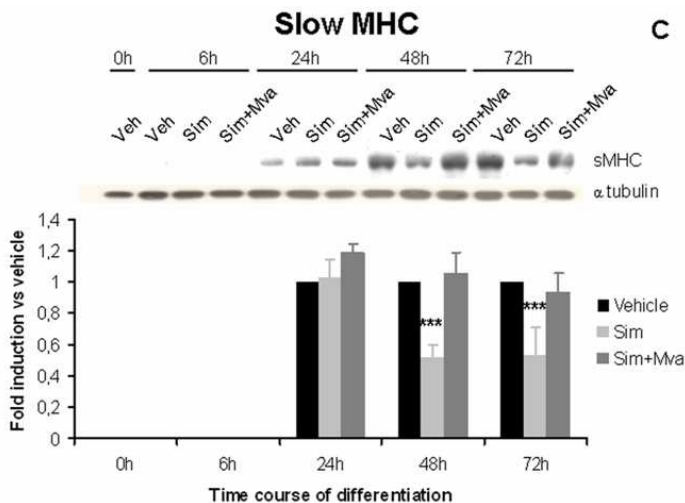


**Figure 3. Time course of differentiation of eMHC, fMHC and sMHC protein expression in Veh, Sim, and Sim+Mva treated SCDM.** A) Typical Western Blot and densitometric analysis of eMHC detected in Veh, Sim, and Sim+Mva treated SCDM 0, 6, 24, 48, 72h after the induction of differentiation. Data are expressed as the ratio between Sim or Sim+Mva versus Veh samples of each time considered. Each column represents the mean $\pm$ SD of at least three different experiments. B) Typical Western Blot and densitometric analysis of fMHC detected in Veh, Sim, and Sim+Mva treated SCDM 0, 6, 24, 48, 72h after the induction of differentiation. Data are expressed as the ratio between Sim or Sim+Mva versus Veh samples of each time considered. Each column represents the mean $\pm$ SD of at least three different experiments. C) Typical Western Blot and densitometric analysis of sMHC detected in Veh, Sim, and Sim+Mva treated SCDM 0, 6, 24, 48, 72h after the induction of differentiation. Data are expressed as the ratio between Sim or Sim+Mva versus Veh samples of each time considered. Each column represents the mean $\pm$ SD of at least three different experiments. \* $P < 0.05$ , \*\* $P < 0.01$ , \*\*\* $P < 0.001$  as from ANOVA followed by Dunnett post-test versus Veh sample of each time.



	<b>PNF</b>	<b>CNF</b>	<b>TN</b>
<b>Control</b>	87±5	0	87±5
<b>Injured Veh 21 days</b>	73±8	9±4	79±13
<b>Injured Sim 21 days</b>	15±3	77±6	92±6
<b>Injured Sim+Mva 21 days</b>	95±8	2±1	97±8

**Table 1: Quantitative analysis of muscle regeneration.** Data are the mean  $\pm$  SD of fibers displaying peripherally located nuclei (PNF), of fibers displaying centrally located nuclei (CNF), and of total fibers (TF) in ten different fields for each experimental condition.

### **Discussion**

In damaged muscle, the necrosis of the fibers stimulates an inflammatory response with the invasion of macrophages, followed by activation of satellite cells, which undergo proliferation, differentiation, and fusion to one another or to undamaged portions of the fiber (Charge and Rudnicki, 2004). Since the inhibition and down-regulation of HMGR, was demonstrated to be crucial for the myogenic process to occur (Martini et al., 2009), we hypothesized an involvement of the enzyme in the differentiation of adult SCDM, responsible for muscle repair, and in the regenerative program of muscle tissue. Once ascertained that the initial increase and the subsequent decrease of HMGR drew a similar trend of that previously observed in rat fetal L6 myoblasts (Martini et al., 2009), we analysed, in a time course ranging from 6 up to 72h, eMHC, fMHC and sMHC protein expression.

The time dependent pattern of MHC isoform expression in agreement to that already reported for regenerating muscles indicated that the activation, proliferation and fusion of adult satellite cells implied an initial expression of MHCs typical of developing muscle, such as eMHC, whose subsequent decline was partially overlapped and followed by the increase of the adult contractile proteins fMHC and sMHC respectively (as reviewed in Ciciliot and Schiaffino, 2011). The lack of any decrease of eMHC observed in Simvastatin-treated SCDM together with the inhibition of fMHC and sMHC expression demonstrated a delay in myotube maturation and in fiber formation.

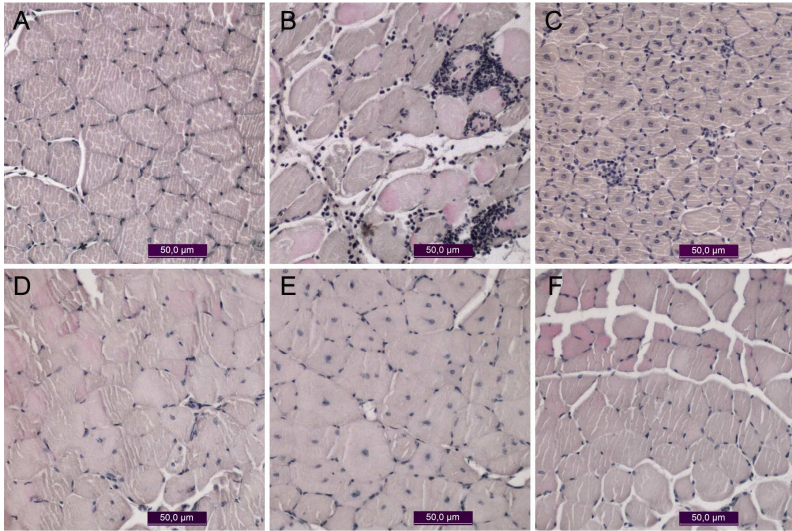


**Figure 4. Morphology of tibial muscles from mice of the different treatment groups. H&E stained paraffin sections.** *A*, Non injured muscle, showing regular histological features, including peripherally located cell nuclei. *B*, CTX-injected muscle, 3 days after injury. Damaged muscle fibers and large areas of inflammatory infiltrate are observed. *C*, CTX-injected muscle, 10 days after injury. Most muscle fibers show central nuclei, suggesting ongoing regeneration, while few areas of inflammatory infiltrate are still present. *D*, CTX-injected muscle, 21 days after injury. The tissue shows normal histological features. Most muscle fibers show peripheral nuclei, suggesting full differentiation. *E*, CTX-injected muscle from a Sim treated mouse, 21 days after injury. While the overall cytoarchitecture appears normal, several muscle fibers displaying a centrally located nucleus are still present, suggesting incomplete differentiation and/or delayed regeneration. *F*, CTX-injected muscle from a Sim and Mva treated mouse, 21 days after injury. The tissue shows normal histological features, similar to those shown in (*A*) and (*D*).

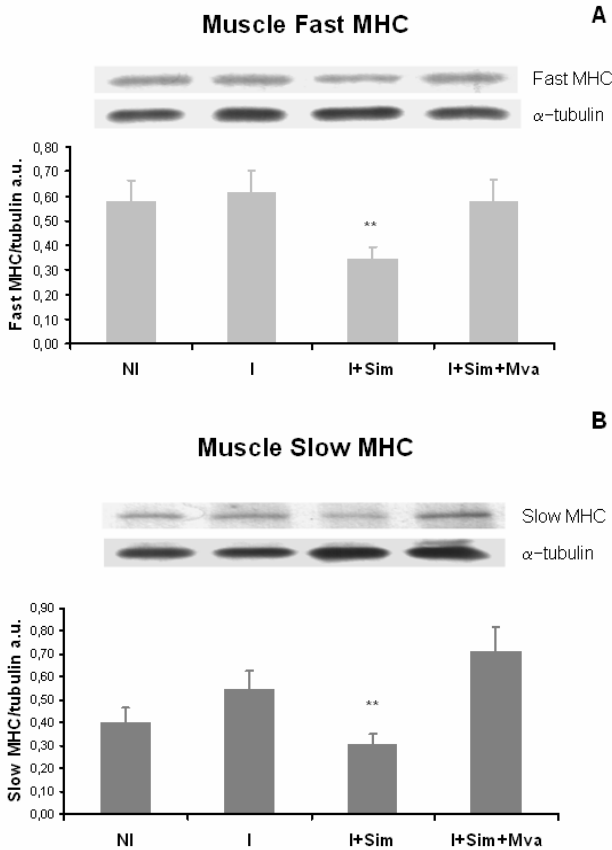


**Figure 5. fMHC and sMHC expression in injured tibialis anterior muscles of mice treated with Veh, or Sim or both with Sim+Mva for 21 days.** **A)** Typical Western Blot and densitometric analysis of fMHC detected in non injured (NI) and injured (I) tibialis anterior muscles of mice treated with Veh, or Sim (I+Sim) or both with Sim and Mva (I+Sim+Mva) for 21 days. **\*\*** $P < 0.01$ , as from ANOVA followed by Dunnett post-test versus NI samples. Data are expressed as the mean  $\pm$  SD of three different animals performed in duplicate. **B)** Typical Western Blot and densitometric analysis of sMHC detected in non injured (NI) and injured (I) tibialis anterior muscles of mice treated with Veh or Sim (I+Sim) or both with Sim and Mva (I+Sim+Mva) for 21 days. **\*\*** $P < 0.001$ , as from ANOVA followed by Dunnett post-test versus NI samples. Data are expressed the mean  $\pm$  SD of three different animals performed in duplicate.

This observation was further supported by morphological analysis which highlighted a reduced SCDM fusion index. In addition, myotubes derived from Simvastatin-treated showed a very immature phenotype as that reported in myotubes derived from satellite cells extracted from human fetuses affected by congenital myotonic dystrophy, an autosomal dominant disease characterized by myotonia and progressive muscle weakness (Furling et al., 2001). Interestingly, a range of cases have now been reported in which statin use has “uncovered” previously clinically silent or clinically tolerated conditions, among others myotonic dystrophy (Tsivgoulis et al., 2006).

The results obtained *in vitro*, led us to ascertain whether HMGR inhibition could impair muscle regeneration *in vivo*. Thus, we investigated the response to CTX-induced muscle damage in female mice treated with Veh, or Simvastatin, or with both Simvastatin plus Mevalonate, since CTX is a highly reproducible way to induce muscle regeneration (d'Albis et al., 1988). CTX, a peptide isolated from snake venoms, is known to induce the depolarization and contraction of muscular cells, to disrupt membrane organization, and to lyse muscle cells. Injected in adult mouse *tibialis anterior* muscle, CTX induces muscle degeneration leading to a wound coagulum with mononuclear cell infiltration within 1 day of injection. Inflammatory response and mononuclear cell proliferation is most active within 1-4 days of injection. By 10 days post injection, the architecture of the muscle is restored, although most regenerated myofibers are smaller and display central myonuclei. The return to a morphologically and histochemically normal mature muscle is observable 3 weeks after being damaged (Nakamura et al., 2010). Under normal conditions 21 days after CTX injection the regenerated muscle was morphologically and functionally indistinguishable from undamaged muscle. Remarkably, under simvastatin treatment the muscle was still regenerating. The rescue experiments assessed a completely restored cytoarchitecture of a fully repaired muscle and fast and slow MHC isoform amount very similar to that one of non injured animals.

The prevention of the harmful effect of Simvastatin by means of Mevalonate addition *in vitro* and *in vivo*, strongly demonstrated that the delayed myogenic process was due to the inhibition of HMGR activity rather than to an effect exerted by the drug *per se* and highlighted the pivotal role played by HMGR in muscle regeneration and, in turn, in muscle homeostasis maintenance. Notably, Mammen and co-workers showed that in muscle biopsy, fibers undergone regeneration process express high levels of HMGR (Mammen et al., 2011).

To explain the mechanisms underlying the observed effects we can speculate that they are likely ascribable to the impairment of prenylated protein activation (Rho protein family) and dolichol synthesis (Martini et al., 2009).

Thus, the data obtained strongly suggest that HMGR plays an essential role in physiological muscle regeneration. Therefore, patients for whom statins are prescribed in clinical practice, might not only eventually complain of myopathy but also might not be able to repair any muscle damage because of the impairment in SCDM differentiation and fusion.

### **Acknowledgment**

The financial support from the University of Roma Tre (CLAR) to VP and MM are gratefully acknowledged.

### **References**

- Belo RS, Jamieson JC, Wright JA. 1993. Studies on the effect of mevinolin (lovastatin) and mevastatin (compactin) on the fusion of L6 myoblasts. *Mol Cell Biochem* 126(2):159-167.
- Boldrin L, Muntoni F, Morgan JE. 2010. Are human and mouse satellite cells really the same? *J Histochem Cytochem* 58(11):941-955.
- Charge SB, Rudnicki MA. 2004. Cellular and molecular regulation of muscle regeneration. *Physiol Rev* 84(1):209-238.
- Cheng CW, Woo KS, Chan JC, Tomlinson B, You JH. 2005. Assessing adherence to statin therapy using patient report, pill count, and an electronic monitoring device. *Am J Health Syst Pharm* 62(4):411-415.
- Ciciliot S, Schiaffino S. 2011. Regeneration of mammalian skeletal muscle. Basic mechanisms and clinical implications. *Curr Pharm Des* 16(8):906-914.
- d'Albis A, Couteaux R, Janmot C, Roulet A, Mira JC. 1988. Regeneration after cardiotoxin injury of innervated and denervated slow and fast muscles of mammals. Myosin isoform analysis. *Eur J Biochem* 174(1):103-110.
- Delaunay A, Bromberg KD, Hayashi Y, Mirabella M, Burch D, Kirkwood B, Serra C, Malicdan MC, Mizisin AP, Morosetti R, Broccolini A, Guo LT, Jones SN, Lira SA, Puri PL, Shelton GD, Ronai Z. 2008. The ER-bound RING finger protein 5 (RNF5/RMA1) causes degenerative myopathy in transgenic mice and is deregulated in inclusion body myositis. *PLoS One* 3(2):e1609.

- Draeger A, Monastyrskaya K, Mohaupt M, Hoppeler H, Savolainen H, Allemann C, Babiychuk EB. 2006. Statin therapy induces ultrastructural damage in skeletal muscle in patients without myalgia. *J Pathol* 210(1):94-102.
- Fortier M, Comunale F, Kucharczak J, Blangy A, Charrasse S, Gauthier-Rouviere C. 2008. RhoE controls myoblast alignment prior fusion through RhoA and ROCK. *Cell Death Differ* 15(8):1221-1231.
- Furling D, Coiffier L, Mouly V, Barbet JP, St Guily JL, Taneja K, Gourdon G, Junien C, Butler-Browne GS. 2001. Defective satellite cells in congenital myotonic dystrophy. *Hum Mol Genet* 10(19):2079-2087.
- Iani C, Stalberg E, Falck B, Bishoff C. 1994. New approaches to motor unit potential analysis. *Ital J Neurol Sci* 15(9):447-459.
- Jarvinen TA, Jarvinen TL, Kaariainen M, Kalimo H, Jarvinen M. 2005. Muscle injuries: biology and treatment. *Am J Sports Med* 33(5):745-764.
- Lowry OH, Rosebrough NJ, Farr AL, Randall RJ. 1951. Protein measurement with the Folin phenol reagent. *J Biol Chem* 193(1):265-275.
- Mammen AL, Chung T, Christopher-Stine L, Rosen P, Rosen A, Doering KR, Casciola-Rosen LA. 2011. Autoantibodies against 3-hydroxy-3-methylglutaryl-coenzyme A reductase in patients with statin-associated autoimmune myopathy. *Arthritis Rheum* 63(3):713-721.
- Martini C, Pallottini V, Cavallini G, Donati A, Bergamini E, Trentalance A. 2007. Caloric restrictions affect some factors involved in age-related hypercholesterolemia. *J Cell Biochem* 101(1):235-243.
- Martini C, Trapani L, Narciso L, Marino M, Trentalance A, Pallottini V. 2009. 3-hydroxy 3-methylglutaryl coenzyme A reductase increase is essential for rat muscle differentiation. *J Cell Physiol* 220(2):524-530.
- Mauro A. 1961. Satellite cell of skeletal muscle fibers. *J Biophys Biochem Cytol* 9:493-495.
- Nakamura K, Tsukamoto Y, Hijiya N, Higuchi Y, Yano S, Yokoyama S, Kumamoto T, Moriyama M. 2010. Induction of GNE in myofibers after muscle injury. *Pathobiology* 77(4):191-199.
- Tsivgoulis G, Spengos K, Karandreas N, Panas M, Kladi A, Manta P. 2006. Presymptomatic neuromuscular disorders disclosed following statin treatment. *Arch Intern Med* 166(14):1519-1524.
- Turner NJ, Badylak SF. 2011. Regeneration of skeletal muscle. *Cell Tissue Res*.

- Zammit PS, Partridge TA, Yablonka-Reuveni Z. 2006. The skeletal muscle satellite cell: the stem cell that came in from the cold. *J Histochem Cytochem* 54(11):1177-1191.
- Zhao P, Hoffman EP. 2004. Embryonic myogenesis pathways in muscle regeneration. *Dev Dyn* 229(2):380-392.

## Effects of myosin heavy chain (MHC) plasticity induced by HMGCoA-reductase inhibition on skeletal muscle functions

Laura Trapani,<sup>\*1</sup> Luca Melli,<sup>†,1</sup> Marco Segatto,<sup>\*1</sup> Viviana Trezza,<sup>\*</sup> Patrizia Campolongo,<sup>†</sup> Adam Jozwiak,<sup>§</sup> Ewa Swiezewska,<sup>§</sup> Leopoldo Paolo Pucillo,<sup>#</sup> Sandra Moreno,<sup>\*</sup> Francesca Fanelli,<sup>\*</sup> Marco Linari,<sup>†</sup> and Valentina Pallotini<sup>\*2</sup>

<sup>\*</sup>Department of Biology, University of Roma Tre, Rome, Italy; <sup>†</sup>Department of Evolutionary Biology, University of Florence, Florence, Italy; <sup>‡</sup>Department of Physiology and Pharmacology, University of Rome La Sapienza, Rome, Italy; <sup>§</sup>Institute of Biochemistry and Biophysics, Polish Academy of Sciences, Warsaw, Poland; and <sup>#</sup>National Institute for Infectious Diseases, Rome, Italy

**ABSTRACT** The rate-limiting step of cholesterol biosynthetic pathway is catalyzed by 3-hydroxy-3-methylglutaryl coenzyme reductase (HMGCR), whose inhibitors, the statins, widely used in clinical practice to treat hypercholesterolemia, often cause myopathy, and rarely rhabdomyolysis. All studies to date are limited to the definition of statin-induced myotoxicity omitting to investigate whether and how HMGCR inhibition influences muscle functions. To this end, 3-mo-old male rats (*Rattus norvegicus*) were treated for 3 wk with a daily intraperitoneal injection of simvastatin (1.5 mg/kg/d), and biochemical, morphological, mechanical, and functional analysis were performed on extensor digitorum longus (EDL) muscle. Our results show that EDL muscles from simvastatin-treated rats exhibited reduced HMGCR activity; a 15% shift from the fastest myosin heavy-chain (MHC) isoform IIb to the slower IIa/x; and reduced power output and unloaded shortening velocity, by 41 and 23%, respectively, without any change in isometric force and endurance. Moreover, simvastatin-treated rats showed a decrease of maximum speed reached and the latency to fall off the rotaroad (~30%). These results indicate that the molecular mechanism of the impaired muscle function following statin treatment could be related to the plasticity of fast MHC isoform expression.—Trapani, L., Melli, L., Segatto, M., Trezza, V., Campolongo, P., Jozwiak, A., Swiezewska, E., Pucillo, L.P., Moreno, S., Fanelli, F., Linari, M., Pallotini, V. Effects of myosin heavy chain (MHC) plasticity induced by HMGCoA-reductase inhibition on skeletal muscle functions. *FASEB J.* 25, 000–000 (2011). www.fasebj.org

**Key Words:** cholesterol • HMGCoA-reductase • statins

THE MAIN PRODUCTS OF THE mevalonate (MVA) pathway—cholesterol, ubiquinone (CoQ), prenyl diphosphate, and dolichol—are essential compounds for survival, proliferation, and differentiation of all mammal tissues (1, 2). In skeletal muscle, cholesterol is essential

for the propagation of action potentials along the cell (3). CoQ participates in electron transport during oxidative phosphorylation in mammalian mitochondria, ensuring the production of ATP needed for muscle contraction (4). Oligoprenyl groups are necessary for post-translational modification of proteins crucial for cell proliferation and differentiation; among others, the small Rho GTPases, able to activate Rho-associated serin/threonine kinase (Rho-kinase) (5). Lastly, dolichol is needed for *N*-linked glycoprotein biosynthesis (6).

The rate-limiting step of the MVA pathway, the 4-electron reduction of 3-hydroxy-3-methylglutaryl coenzyme A (HMG CoA) to MVA, is catalyzed by HMGCoA reductase (HMGCR). Thus, as the central regulator of cholesterol homeostasis, HMGCR became the target for drugs that control plasma cholesterol levels. The enzyme is highly regulated; short-term regulation is achieved by phosphorylation/dephosphorylation reactions exerted by AMP-activated kinase (AMPK) and protein phosphatase 2A (PP2A), respectively. Long-term regulation concerns the modulation of HMGCR protein levels by several factors, among others sterol regulatory element binding protein (SREBP) and insulin-induced genes (Insigs), which can affect enzyme transcription and degradation as a function of an intracellular sterol amount and of cholesterol uptake by low-density lipoprotein receptor (LDLR) (7).

Statins, strong HMGCR competitive inhibitors widely used to treat hypercholesterolemia, besides the beneficial effects on plasma lipid profile, can cause myopathy characterized by weakness, pain, elevated serum creatine phosphokinase (CK) (2), and to a lesser extent (0.05%), rhabdomyolysis, a life-threatening condition (8). Moreover, previous data demonstrate that HMGCR

<sup>1</sup> These authors contributed equally to this work.

<sup>2</sup> Correspondence: Department of Biology, University of Roma Tre, Viale Marconi 446, 00146, Rome, Italy. E-mail: vpallotini@uniroma3.it

doi: 10.1096/fj.11-184218



is crucial for myoblast differentiation to occur (9); indeed, HMGR inhibition or down-regulation lead to both the reduction of muscle differentiation markers [myogenin and fetal myosin heavy chain (f-MHC)] and of myoblast fusion into multinucleated syncytia (9).

Although these combined findings bring out the importance of HMGR activity in skeletal muscle physiology, all the studies so far are limited to the definition of statin-induced myotoxicity, omitting to investigate whether and how the inhibition of HMGR activity influences muscle functions. Moreover, epidemiological studies show that some patients treated with statins complain of muscle pain without any increase in plasma content of muscle damage markers, such as serum CK (4), which suggests that HMGR inhibition could impair muscle function without exerting any muscle toxicity.

Here we studied *in vivo* the role of HMGR inhibition by simvastatin on skeletal muscle physiology through biochemical, morphological, mechanical, and functional approaches.

## MATERIALS AND METHODS

### Reagents

All chemicals were obtained from commercial sources and of the highest quality available. Sources not specified were obtained from Sigma-Aldrich (Milan, Italy).

### Animals

Wistar *Rattus norvegicus*, 3-mo-old male (Harlan Nossan, S. Pietro al Natisone, Italy), were housed under controlled temperature ( $20 \pm 1^\circ\text{C}$ ), humidity ( $55 \pm 10\%$ ), and illumination (lights on for 12 h daily, from 7 AM to 7 PM). Food and water were provided *ad libitum*. The experiments were performed according to the ethical guidelines for the conduct of animal research (Ministero della Salute, Official Italian Regulation No. 116/92, Communication to Ministero della Salute no. 391/121). Rats were divided into 2 groups of 28 animals each. The first group was treated daily with intraperitoneal injection of 1.5 mg/kg simvastatin in vehicle [dimethyl sulfoxide (DMSO), 1 ml/kg] for 3 wk, a dose comparable to the highest one used in therapies against human hypercholesterolemia. Control animals received daily an equal volume of vehicle. At the end of the treatment, rats were anesthetized with ether in a fume cupboard, and plasma was obtained from blood collected into EDTA (1 mg/ml blood). Extensor digitorum longus (EDL) and gastrocnemius muscles of 7 animals/group were dissected and immediately frozen in liquid nitrogen for subsequent biochemical assays. Eight animals from each group were used for mechanical analyses; in particular, after dissection, EDL muscles were mounted in an experimental trough to analyze the contractile properties. For immunolocalization studies, EDL muscles from both sides of 3 animals/group were isolated and fixed by immersion in phosphate-buffered saline (PBS; pH 7.4) containing 4% freshly depolymerized paraformaldehyde, overnight at  $4^\circ\text{C}$ . For rotarod motor coordination test and open-field locomotor activity, 10 animals/group were used.

### Biochemical analysis

#### Plasma cholesterol analysis

Plasma cholesterol content of rats was assessed through the colorimetric CHOD-POD kit (Assel, Rome, Italy) according to manufacturer's instructions. Briefly, by the catalysis of cholesterol esterase and cholesterol oxidase, cholesterol ester was catalyzed to yield  $\text{H}_2\text{O}_2$ , which oxidates 4-aminoantipyrine with phenol to form a colored dye of quinoneimine. The absorbancy increase is directly proportional to the concentration of cholesterol.

#### Triglyceride and creatin kinase assays

Plasma triglyceride levels and creatin kinase activity were measured by standardized commercial methods on a fully automated system (Modular; Roche, Basel, Switzerland). Triglycerides are hydrolyzed to glycerol by lipoprotein lipase and oxidized to dihydroxyacetone phosphate and hydrogen peroxide, which reacts with Trinder reagent to form a red dye. The color intensity is directly proportional to triglyceride concentration. This method is linear between 4 and 1000 mg/dl. Activity of creatin kinase measurement is in accordance with the method recommended by the International Federation of Clinical Chemistry at  $37^\circ\text{C}$ .

#### HMGR activity

The assay was carried out with the radioisotopic method, following the production of [ $^{14}\text{C}$ ]-MVA from 3-[ $^{14}\text{C}$ ]-hydroxymethylglutaryl coenzyme A (3-[ $^{14}\text{C}$ ]-HMGCoA; specific activity 57.0 mCi/mmol; GE Healthcare, Little Chalfont, UK). Microsomes were prepared as described previously (10) from gastrocnemius. Microsomes were incubated in presence of cofactors (20 mM glucose-6 phosphate, 20 mM  $\text{NADP}^+$  sodium salt, 1 IU glucose-6 phosphate dehydrogenase, and 5 mM dithiothreitol). The assay, in a final volume of 200  $\mu\text{l}$ , was started by the addition of 10  $\mu\text{l}$  (0.088  $\mu\text{Ci}/11.7$  nmol) of 3-[ $^{14}\text{C}$ ]-HMG CoA. The [ $^{14}\text{C}$ ]-MVA produced was isolated by chromatography on AG-X8 ion-exchange resin (Bio-Rad Laboratories, Milan, Italy), and the radioactivity was counted by a liquid scintillation analyzer (Tri-Carb 2100 TR; Canberra Packard, Schwadorf, Austria[b]). An internal standard (3-[ $^3\text{H}$ ]-MVA, specific activity 24.0 mCi/mmol; GE Healthcare) was added to calculate the recovery.

#### Membrane and lysate preparation

Total membrane and total lysate were obtained as follows: 100 mg skeletal muscle tissue was homogenized in 0.01 M Tris-HCl, 0.001 M  $\text{CaCl}_2$ , 0.15 M NaCl, and 0.001 M PMSF (pH 7.5). An aliquot of homogenate was collected and used for lysate preparation. The remaining homogenate was centrifuged for 20 min at 10,000 *g*. The supernatant was centrifuged at 100,000 *g* for 45 min, and the pellet was resuspended and centrifuged again at 100,000 *g* for 45 min. The pellet was solubilized in 0.125 M Tris-HCl (pH 6.8) containing 10% SDS and protease inhibitor cocktail (sample buffer) and transferred into microtubes. The aliquot of homogenate was solubilized by sonication in sample buffer and centrifuged for 5 min at 15,600 *g*, and the supernatant was transferred into microtubes. Protein concentration was determined by the method of Lowry *et al.* (11). All samples were boiled for 3 min before loading for Western blotting.

### Protein analysis

Protein profiles were analyzed by Western blotting. Western blot analysis of LDLr and RhoA were performed on total gastrocnemius and EDL plasma membranes, respectively, while the analysis of MHC isoforms, poly(ADP-ribose) polymerase-1 (PARP-1), AMPK $\alpha$ , and Akt were performed on total EDL lysates. Protein (20  $\mu$ g) from solubilized membranes was resolved by 12% (for RhoA), 10% (for P-Akt, total Akt, P-AMPK $\alpha$ , and total AMPK $\alpha$ ), and 7% (for LDLr, MHC isoforms, and PARP-1) SDS-PAGE at 100 V for 60 min. SDS-PAGE for MHC isoforms was performed at 140 V for 6 h at 4°C. The proteins were subsequently transferred electrophoretically onto nitrocellulose for 90 min at 100 V. The nitrocellulose membrane was blocked at room temperature with 5% fat-free milk in Tris-buffered saline (138 mM NaCl, 27 mM KCl, 25 mM Tris-HCl, and 0.05% Tween-20, pH 6.8), and probed at 4°C overnight with primary antibodies (RhoA 26C4 and PARP-1 F-2, Santa Cruz Biotechnology, Santa Cruz, CA, USA; LDLr ab30532, Abcam, Cambridge, UK; fast MHC MY-32, slow MHC NOQ7.5.4D, Sigma; P-AMPK $\alpha$ , total AMPK $\alpha$ , P-Akt, and Akt, Cell Signaling, Danvers, MA, USA) followed by incubation for 1 h with secondary IgG antibodies coupled to horseradish peroxidase (Bio-Rad Laboratories, Milan, Italy). The nitrocellulose membrane was then stripped with Restore Western blot stripping buffer (Pierce Chemical, Rockford, IL, USA) for 10 min at room temperature and reprobed with anti-tubulin ( $\alpha$ -tubulin DM-1A; Sigma) or anti-caveolin (caveolin-1 N-20; Santa Cruz Biotechnology) antibodies. Bound antibodies were visualized using enhanced chemoluminescence detection (GE Healthcare). All images derived from Western blotting were analyzed with ImageJ (National Institutes of Health, Bethesda, MD, USA) software for Windows. Each reported value was derived from the ratio between arbitrary units obtained by the protein band and the respective tubulin or caveolin band (chosen as housekeeping proteins).

### Lipid extraction

EDL muscle (~100 mg) was homogenized in NaCl (150 mM; 1:9, v/v); 6 nmol coenzyme Q6 (CoQ6), 600  $\mu$ l water, 4 ml methanol, and 4 ml chloroform were added to homogenate. CoQ6 was added as internal standard to calculate the recovery. The samples were incubated for 30 min at 37°C. Then, 800  $\mu$ l NaCl 150mM and 2 ml chloroform were added, and 2 phases were obtained. The lower phase was evaporated with a stream of nitrogen. Samples were dissolved in 0.5 ml chloroform and then divided into halves. The samples used to measure CoQ9 amount were dissolved in 50  $\mu$ l isopropanol:ethanol (1:1, v/v); the samples employed to estimate cholesterol and dolichol levels were hydrolyzed in 0.5 ml 15% KOH in ethanol:water (95:5, v/v) for 60 min at 95°C. Then the organic phase was extracted with 0.5 ml of water and 1 ml of hexane. The upper phase was collected and evaporated with a stream of nitrogen, then dissolved in 50  $\mu$ l isopropanol:ethanol (1:1, v/v).

### HPLC-UV analysis of polyisoprenoids

Lipids were analyzed according to previously described protocol (12) with modifications. Briefly, two parallel runs, one for CoQ9 and another for cholesterol, were performed on a 4.6-  $\times$  75-mm Zorbax XDB-C18 (3.5  $\mu$ m) reversed-phase column (Agilent, Santa Clara, CA, USA) using a Waters dual-pump apparatus, a Waters gradient programmer, and a Waters photodiode array detector (spectrum range: 210–400 nm; Waters Corp., Milford, MA, USA). For elution, a combination of convex gradients (Waters No. 5, from 0 to 75% B for the initial 20 min and linear, from 75 to 100% B during the following 10 min) was used; in the last 5 min, reequilibration

back to 0% B was performed, where solvent A was methanol: water (9:1, v/v), and solvent B was methanol:propan-2-ol/hexane (2:1:1, v/v/v). The solvent flow rate was 1.5 ml/min. HPLC solvents were obtained from POCh (Gliwice, Poland). The chain length and identity of lipids were confirmed by applying following standards: CoQ<sub>6</sub>, CoQ<sub>10</sub>, and cholesterol. CoQ<sub>10</sub> and cholesterol were purchased from Sigma-Aldrich; CoQ<sub>6</sub> was from the Collection of Polyisoprenols (Institute of Biochemistry and Biophysics, PAS, Warsaw, Poland).

### Morphological analysis

Fixed EDL muscles were dehydrated in graded ethanol, transferred to Bioclear (BioOptica, Milan, Italy) and then to a 1:1 mixture of Bioclear and paraffin, and finally embedded in paraffin. Transverse, 7- $\mu$ m-thick sections were cut by a microtome and collected on Vectabond precoated slides (Vector, Burlingame, CA, USA). Sections were deparaffinized, rehydrated, and submitted to antigen retrieval, using antigen unmasking solution (Vector). After cooling, slides were transferred to PBS containing 3% hydrogen peroxide, for 5 min, in the dark, then to PBS with 0.2% Triton X-100 and 3% bovine serum albumin (BSA), for 1 h at room temperature. Sections were incubated overnight at 4°C with either of the following mouse polyclonal antibodies, diluted in PBS containing 0.1% Triton X-100 and 1.5% BSA: fast MHC MY-32 1:1000, slow MHC NOQ7.5.4D 1:5000 (Sigma). In control sections, the primary antibody was omitted. Slides were then incubated for 1 h at room temperature with biotinylated goat anti-rabbit IgG (Vector), diluted 1:200 in PBS containing 1% normal goat serum (Vector). Immuno-complexes were revealed by means of an avidin biotin system (Vectastain Elite ABC kit, Vector), using 3,3'-diamino-benzidine (DAB Substrate kit for peroxidase; Vector), as the chromogen. Sections were counterstained with hematoxylin, then dehydrated and mounted with Eukitt (Kindler GmbH & Co., Freiburg, Germany). Slides were observed under an Olympus BX 51 microscope (Olympus, Tokyo, Japan) equipped with a Leica DFC 420 camera (Leica Microsystems, Wetzlar, Germany); electronic images were captured by a Leica Application Suite system, and composed in an Adobe Photoshop CS2 format (Adobe Systems, San Jose, CA, USA).

### Mechanical analysis

EDL muscle was dissected by using scissors and forceps under a stereomicroscope (Stemi SV11; Carl Zeiss MicroImaging, Oberkochen, Germany) and mounted horizontally, between the lever of a motor/force transducer system (305C, Aurora Scientific Inc., Aurora, ON, Canada) and a lever carried by a micromanipulator, in a trough, containing physiological solution (Krebs-Henseleit solution, composition, in mM: 119 NaCl, 4.7 KCl, 2.5 CaCl<sub>2</sub>, 1.0 MgSO<sub>4</sub>, 25 NaHCO<sub>3</sub>, 1.2 KH<sub>2</sub>PO<sub>4</sub>, and 1.1 glucose) gassed with carbogen (95% O<sub>2</sub> and 5% CO<sub>2</sub>, pH7.4). The muscle was straightened just above its slack length by means of the micromanipulator. The trough was sealed with a Perspex cover and mounted vertically on the stage with the motor/force transducer system on top. The solution was continuously saturated with carbogen during the experiment. Room temperature was in the range 20–22°C.

Trains of stimuli of alternate polarity to elicit fused tetani (frequency 70–80 Hz) were delivered by means of two platinum wire electrodes running parallel to the muscle, 1 cm apart. The intensity of the stimuli was increased until the isometric plateau force reached a maximum constant value  $T_0$  (indicating that all the cells in the muscle were activated). The muscle length was finely adjusted further by means of the micromanipulator to obtain the maximum isometric force,

corresponding to the plateau of the force-length relation. To compare isometric force among muscles, the isometric plateau force was normalized by the wet weight of the muscle, measured at the end of each experiment with an electrobalance (CP124S; Sartorius, Goettingen, Germany). The force-velocity relation was determined by measuring the velocity of steady shortening  $V$  after a drop in force from the isometric value  $T_0$  to a preset value  $T < T_0$ . The force-velocity points were fitted to the Hill hyperbolic equation (Eq. 1):

$$(T + a) \cdot (V + b) = (V_0 + b) \cdot a \tag{1}$$

where  $a$ ,  $b$ , and  $V_0$  (the unloaded shortening velocity) are the regression parameters.

To investigate the effects of simvastatin on muscle endurance, a fatiguing protocol was used. EDL muscle was given a 400-ms fused tetanus every 3 s over a period of 150 s. The muscle was then allowed to recover for a period of 40 min, during which force recovery was monitored with a tetanus every 5 min. Force, length change, and stimulus were recorded with a multifunction I/O board (PCI-6110E; National Instruments, Austin, TX, USA) at 0.5-ms sampling rate. A program written in LabVIEW (National Instruments) was used for signal recording and analysis.

Functional analysis

Rotarod motor coordination test

To assess any effect of simvastatin on motor coordination and balance, rats were tested in an automated accelerating rotarod apparatus (Biological Research Apparatus; Ugo Basile, Varese, Italy; ref. 13). The apparatus consisted of 7-cm-diameter plastic drums machined with grooves to improve grip, that could be set on accelerating speed (4, 10, 12, 15, 19, 22, 26, 29 34 and 40 rpm, 30 s at each speed).

Before testing, the rats were trained for 2 d, applying the following schedule (14): the first day, the rats were trained for 3 min with an unlimited number of trials on the rotarod, followed by 4 trials of maximum 60 s with a 30 s intertrial interval; the second day, the rats were placed on the rotarod at accelerating speed for a maximum of 300 s. Testing was performed after 21 d of treatment with simvastatin; each rat was individually placed on the rotarod at accelerating speed for a maximum of 300 s, and the latency to fall off the rotarod and the maximum speed reached within this time period were recorded. Immediately after each session, the apparatus was thoroughly cleaned with cotton pads wetted with 70% ethanol;water solution and dried. Rats were allowed to habituate to the experimental room for 60 min before both training and testing. Training and testing were performed between 10:00 AM and 1:00 PM.

Open-field locomotor activity

The day after rotarod testing, the rats were tested for horizontal locomotor activity. The animals were transferred from the holding room to the experimental room, where they were allowed to habituate for 60 min. Testing was conducted under dim light between 10:00 AM and 1:00 PM. The test started by

placing each animal in the center of an open-field arena (80×80 cm) made of gray Plexiglas. Behavior was videorecorded for 10 min using a digital video camera for subsequent analysis. All scores were assigned by the same observer, who was unaware of animal treatment. Immediately after each session, the apparatus was thoroughly cleaned with cotton pads wetted with 70% ethanol;water solution and dried. The following behavioral parameters were scored: number of crossings (crossing with both forepaws the lines in which the floor of the arena was subdivided on the monitor), time spent near the walls (periphery), time spent in the central part of the arena, and frequency and duration of rearing (standing with the body inclined vertically, forequarters raised), wall-rearing (standing on the hind-limbs and touching the walls of the apparatus with the forelimbs), and grooming (rubbing the body with paws or mouth and rubbing the head with paws).

Statistical analysis

Data are expressed as means ± sd. The difference of parameters was statistically tested for significance with unpaired Student's  $t$  test. Values of  $P < 0.05$  were considered to indicate a significant difference. Statistical analysis was performed using GraphPad In-stat3 (GraphPad, Inc., La Jolla, CA, USA) and SigmaPlot (Systat Software Inc., San Jose, CA, USA) for Windows.

RESULTS

Simvastatin efficacy and tolerance

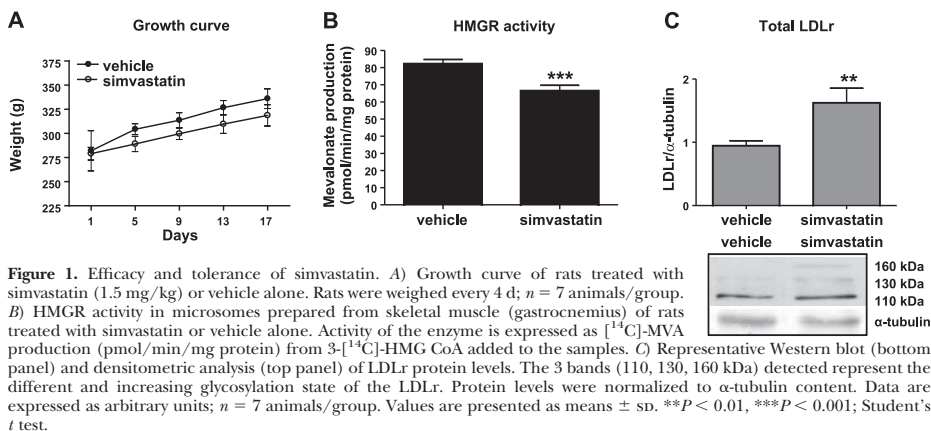
Simvastatin efficacy in lowering plasma LDL-cholesterol (15) and triglycerides (16) by hepatic LDLr up-regulation (17) was verified by checking rat plasma cholesterol and triglyceride content (Table 1). As expected, both the metabolic parameters decreased significantly with the following treatment, by 30% and 53%, respectively. Nevertheless, simvastatin treatment did not modify animal weight, even though the weight of treated animals was slightly lower than that of rats receiving vehicle (Fig. 1A). Moreover, simvastatin treatment lowered HMGR activity in the gastrocnemius muscle by 20% (Fig. 1B). Evidence for drug efficacy on skeletal muscle was also given by the increased levels of LDLr protein in the gastrocnemius muscle of treated rats (Fig. 1C), in good agreement with the rise of LDLr mRNA observed previously (18).

Once simvastatin efficacy on skeletal muscle was ascertained, our attention focused on the effects exerted by HMGR inhibition on EDL muscle, which consists mainly of fast and glycolytic fibers, given that the glycolytic fibers appear to be the most susceptible to statin side effects (19). Thus, the levels of HMGR end products involved in skeletal muscle contraction, such as CoQ9 (4), cholesterol (3), and a prelynnated protein

TABLE 1. Effect of simvastatin on metabolism of treated and control rats

Component	Vehicle	Simvastatin, 1.5 mg/kg	P
Cholesterol (mg/dl plasma)	82.35 ± 9.45	57.52 ± 9.22	<0.01
Triglycerides (mg/dl plasma)	189.6 ± 37.71	88.86 ± 30.48	<0.001

Seven rats contributed to each value. Statistical analysis was done by unpaired  $t$  test.



(RhoA) (5, 20), were assessed. As shown in **Table 2**, no significant differences were detected in EDL muscles of simvastatin-treated rats either in cholesterol or in CoQ9 content. In addition, as shown in **Fig. 2A**, the translocation of RhoA on EDL plasma membrane and its consequent activation (21) did not differ in simvastatin-treated animals when compared to controls.

### Effects of simvastatin treatment on muscular damage

To ascertain whether the pharmacological treatment could have caused possible muscle damage, as described previously (2, 8), plasma CKs (22), and muscle cleaved PARP-1 protein levels, markers for muscle fiber necrosis and apoptosis, respectively, were checked (**Fig. 2B, C**). Both CK and PARP-1 protein levels were not increased in simvastatin treated rats with respect to the control showing the absence of muscle fiber necrosis and/or apoptosis.

### MHC isoform determination

Previous data demonstrated that HMGR inhibition by mevinolin (3  $\mu$ M) can modulate fetal MHC expression in L6 myoblasts (9). This finding prompted us to assess whether a putative modification of MHC isoform expression could occur in EDL muscle after simvastatin treatment. Morphological observation of sections from simvastatin-treated EDL muscles indicated unaltered cytoarchitecture, compared to controls. The immuno-

histochemical localization of fast and slow MHC isoforms on EDL muscles from simvastatin-treated and control rats showed similar, though not identical, distribution of positive fibers in either conditions (**Fig. 3**). Muscle cells immunoreactive to anti-fast MHC isoform represented the large majority of fibers in sections from both treated and untreated muscles (**Fig. 3A, B**). However, the occurrence of negative fibers, most probably corresponding to slow MHC isoform-expressing cells, appeared to be increased after treatment. Accordingly, simvastatin seemed to produce an increased frequency of slow MHC immunoreactive fibers, as shown in **Fig. 3C, D**, but the data are not statistically significant. Moreover, an enhanced immunodensity of the positive cells was detected after the pharmacological treatment, suggesting that the expression of slow MHC isoform could be higher under this condition.

Immunohistochemical analysis suggests that a change in fiber structure could occur. To better ascertain putative differences in MHC isoform expression, Western blot analysis was performed. As observed in **Fig. 4A**, no differences were detected in the slow MHC isoform expression. The apparent discrepancy between the data obtained by immunohistochemistry and those obtained by Western blot can be explained if the low percentage of EDL fibers expressing the slow MHC isoform is considered. Thus, Western blot analysis is not sensitive enough to detect the difference highlighted through morphological observation. Electrophoresis separation shows a shift of the fast MHC isoforms, from the fastest

TABLE 2. Effect of simvastatin treatment on HMGR end products of the mevalonate pathway

End product	Vehicle	Simvastatin, 1.5 mg/kg	P
Cholesterol ( $\mu$ g/g tissue)	92.10 $\pm$ 10.94	106.56 $\pm$ 10.87	0.22
CoQ9 ( $\mu$ g/g tissue)	19.09 $\pm$ 8.04	17.43 $\pm$ 5.63	0.84

Seven muscles contributed to each value. Statistical analysis was done by unpaired *t* test.

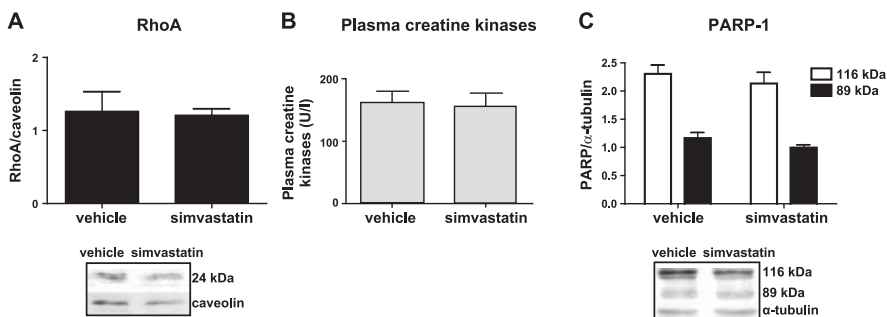


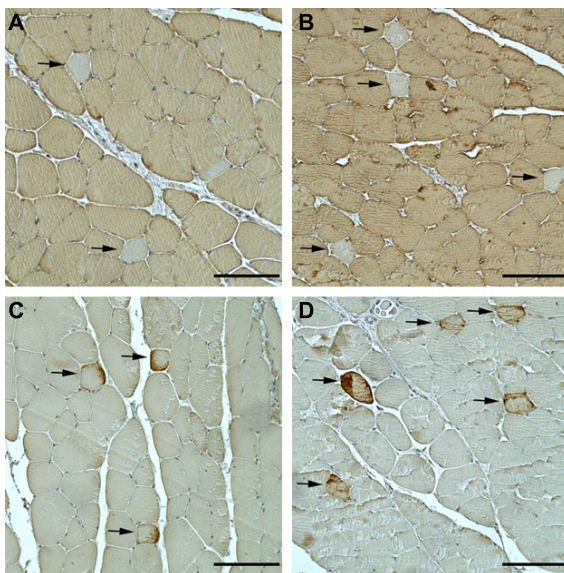
**Figure 2.** Biochemical measurements on simvastatin-treated and control rats. *A*) RhoA levels in EDL membranes of simvastatin-treated and control rats. Representative Western blot (bottom panel) and densitometric analysis (top panel) of RhoA detected in total membranes prepared from EDL muscle of rats treated with simvastatin or vehicle alone. Protein levels were normalized to caveolin content. Data are expressed as arbitrary units;  $n = 7$  animals/group. *B*) Creatine kinase levels (U/L) detected from plasma of rats treated with simvastatin or vehicle alone. *C*) Representative Western blot (bottom panel) and densitometric analysis (top panel) of full-length (116 kDa) and cleaved (89 kDa) PARP-1 detected in total lysates obtained from EDL muscle of rats treated with simvastatin or vehicle alone. Protein levels were normalized to  $\alpha$ -tubulin content. Data are expressed as arbitrary units;  $n = 7$  animals/group. Values are presented as means  $\pm$  SD.

MHC IIb to the slower MHC IIa/x (Fig. 4*B*) in the simvastatin-treated rats with respect to control. In the control group, EDL muscle contained  $\sim 85\%$  of MHC IIb isoform, with a small (15%) amount of MHC IIa/x isoforms, while EDL muscle of simvastatin-treated rats contained  $\sim 70\%$  of MHC IIb isoform, and 30% of MHC IIa/x isoforms.

Statin treatment can interfere with the intracellular pathways responsible for MHC isoform switch; thus, the

activity of Akt and of AMPK, whose phosphorylation states were demonstrated to be modified by statins (23, 24), was analyzed. In particular, Akt and AMPK are negative and positive regulators, respectively, of peroxisome proliferator-activated receptor- $\gamma$  coactivator 1- $\alpha$  (PGC-1 $\alpha$ ), which plays a central role in muscle plasticity (25). **Figure 5** shows that no changes in the phosphorylation levels of these two kinases are observable after simvastatin treatment.

**Figure 3.** Immunohistochemical localization of fast and slow MHC isoforms in EDL muscle sections from simvastatin-treated and control rats. *A, B*) Fast MHC isoform immunohistochemistry in control (*A*) and simvastatin-treated (*B*) EDL muscle sections. Positive fibers are widely distributed in the tissue, under both conditions. However, immunonegative cells (arrows) are more numerous in simvastatin-treated muscle, compared to control. *C, D*) Slow MHC isoform immunohistochemistry in control (*C*) and simvastatin-treated (*D*) EDL muscle sections. Scattered, positive fibers are observed in the tissue, under both conditions. However, higher numbers of positive cells (arrows), showing intense immunoreactivity, are present in treated muscle, compared to control. Scale bars = 100  $\mu$ m.





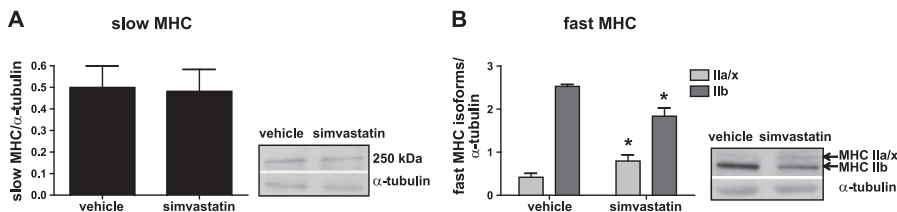


**Figure 4.** Slow and fast MHC protein levels in EDL muscle of simvastatin-treated and control rats. *A*) Typical Western blot (right panel) and densitometric analysis (left panel) of slow MHC detected in total lysates prepared from EDL muscle of rats treated with simvastatin or vehicle alone. *B*) Representative Western blot (right panel) and densitometric analysis (left panel) of fast MHC detected in total lysates prepared from EDL muscle of rats treated with simvastatin or vehicle alone. Protein levels were normalized to  $\alpha$ -tubulin content. Data are expressed as arbitrary units;  $n = 7$  animals/group. Values are presented as means  $\pm$  SD. \* $P < 0.05$ ; Student's  $t$  test.

### Effect of simvastatin treatment on muscle function

To understand whether the observed shift from the fastest MHC IIb isoform to the slower MHC IIa/x isoforms could affect the mechanical properties of EDL muscle, the effects of simvastatin treatment on the contractile properties of fast skeletal muscle were evaluated. In particular, the maximum steady force elicited by the isometric tetanus  $T_0$ , twitch-to-tetanus ratio  $t/T_0$ , time to attain half of the isometric tetanic plateau force  $t_{1/2}$ , and force-velocity relation (Table 3 and Fig. 6) were recorded.  $T_0$  was normalized by the different mass of muscles by mean of the procedure described in Materials and Methods. Simvastatin treatment, with respect to control, reduced  $T_0$  and  $t/T_0$  by 23 and 22%, respectively (but the difference is not statistically significant; Table 3); significantly increased  $t_{1/2}$  by 25% (Table 3); and reduced the shortening velocity at any load below  $T_0$  (Fig. 6C and Table 3). Consequently, the power, calculated as the product  $T \cdot V$ , was significantly reduced in simvastatin-treated rats (Fig. 6D). At the load for the maximum power,  $\sim 0.3 T_0$ , the power ( $W_{\max}$ ) was 41% lower in simvastatin-treated than in control rats (Table 3). The unloaded shortening velocity  $V_0$ , estimated as parameter of the Hill hyperbolic equation (Eq. 1), was 23% lower in simvastatin-treated than in control rats (Table 3). To investigate whether simvastatin treatment affects not

only power but also endurance, EDL muscles were subjected to a fatigue protocol (see Materials and Methods). Results showed no difference in the time course of isometric force reduction to get 40% of the prefatigue value (Fig. 7), indicating that endurance performance is not affected by simvastatin treatment. Also, the time course of force recovery from fatigue, over 40 min from the end of the fatigue protocol, which allows isometric force to recover  $\sim 30\%$  of force decay in control, showed no effect of simvastatin treatment (ascending part of the curves in Fig. 7).

### Rotarod motor coordination and open-field locomotor activity tests

To assess further whether the effects of simvastatin on skeletal muscle could result in functional impairments, we tested the effect of this treatment regimen on motor coordination and locomotor activity in rats. Treatment with simvastatin impaired performance in the rotarod test. Indeed, simvastatin-treated rats showed reduced latency to fall off the rotarod and reduced maximum speed reached during test compared to vehicle-treated animals (Fig. 8). Simvastatin-treated rats did not differ from vehicle-treated rats for any parameter measured in the open-field test (number of crossings, Fig. 9A;

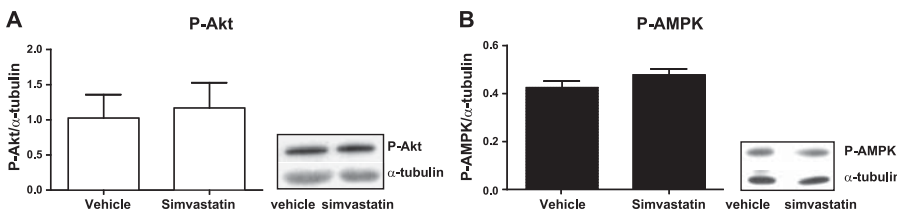


**Figure 5.** P-Akt and P-AMPK protein levels of simvastatin-treated and control rats. *A*) Typical Western blot (right panel) and densitometric analysis (left panel) of P-Akt detected in total lysates prepared from EDL muscle of rats treated with simvastatin or vehicle alone. *B*) Typical Western blot (right panel) and densitometric analysis (left panel) of P-AMPK detected in total lysates prepared from EDL muscle of rats treated with simvastatin or vehicle alone. Protein levels were normalized to  $\alpha$ -tubulin content. Data are expressed as arbitrary units;  $n = 7$  animals/group. Values are presented as means  $\pm$  SD.

TABLE 3. Effect of simvastatin treatment on mechanical parameters during isometric contraction and isotonic shortening of EDL muscle

Parameter	Vehicle	Simvastatin, 1.5 mg/kg	P
Isometric contraction			
$L_0$ (cm)	$2.96 \pm 0.06$	$2.90 \pm 0.17$	0.56
$w$ (g)	$0.157 \pm 0.020$	$0.164 \pm 0.015$	0.85
CSA (cm <sup>2</sup> )	$0.110 \pm 0.013$	$0.134 \pm 0.021$	0.88
$T_0$ (N/g)	$13.49 \pm 1.25$	$10.33 \pm 5.26$	0.21
$t/T_0$	$0.325 \pm 0.043$	$0.254 \pm 0.019$	0.06
$t_{1/2}$ (ms)	$22.9 \pm 3.5$	$28.7 \pm 6.7$	<0.01
Isotonic shortening			
$V_0$ (L <sub>0</sub> /s)	$3.87 \pm 0.13$	$2.98 \pm 0.14$	<0.01
$a/T_0$	$2.78 \pm 0.31$	$2.42 \pm 0.40$	0.47
$b$ (L <sub>0</sub> /s)	$2.14 \pm 0.29$	$2.00 \pm 0.37$	0.77
$W_{\max}$ (mW/g)	$134.7 \pm 11.3$	$79.7 \pm 3.4$	<0.01

Four muscles contributed to each value. Statistical analysis was done by unpaired *t* test. Isometric contraction parameters:  $L_0$ , muscle length at the plateau of the force-length relation;  $w$ , muscle wet weight; CSA, cross-sectional area of muscle, calculated using the relation  $CSA = w/(L_0 * k * \delta)$  (cm<sup>2</sup>), where  $\delta$  is the density of the muscle (1.056 g/cm<sup>3</sup>) and  $k$  is a constant (0.40 for EDL muscle; ref. 39);  $T_0$ , isometric force;  $t/T_0$ , twitch-to-tetanus ratio;  $t_{1/2}$ , time to attain half of the tetanic isometric force. Isotonic shortening parameters:  $V_0$ ,  $a/T_0$ , and  $b$  are regression parameters of the Hill hyperbolic equation (Eq. 1) fitted to the pooled data for simvastatin-treated rats and control, with statistical analysis by Student's *t* test of difference of means;  $W_{\max}$ , maximum power, obtained with a load  $\sim 1/3$  the isometric force.

time in periphery, Fig. 9B; time in center, Fig. 8C; data not shown for frequency and duration of wall-rearing, rearing, and grooming).

## DISCUSSION

In the current study, we investigated the role of HMGR inhibition by simvastatin on skeletal muscle physiology. This lipophilic HMGR inhibitor was chosen because the lipophilic statins are generally taken up much more widely into a broad range of tissues and cells by diffusion compared with hydrophilic statins (26). Chronic treat-

ment with simvastatin (1.5 mg/kg) inhibits HMGR activity in skeletal muscle to a similar extent as in the liver, where the effect of statins is well documented (19); induces a shift of MHC isoforms toward a slower phenotype; reduces the power output and the unloaded shortening velocity of EDL muscle without a significant reduction in isometric force and resistance to fatigue; and induces functional impairment, *i.e.*, reduction in the latency to fall off the rotarod.

Because power involves not just force production but also the speed at which the force is produced, deficits in muscle power can be related to impairment in movement

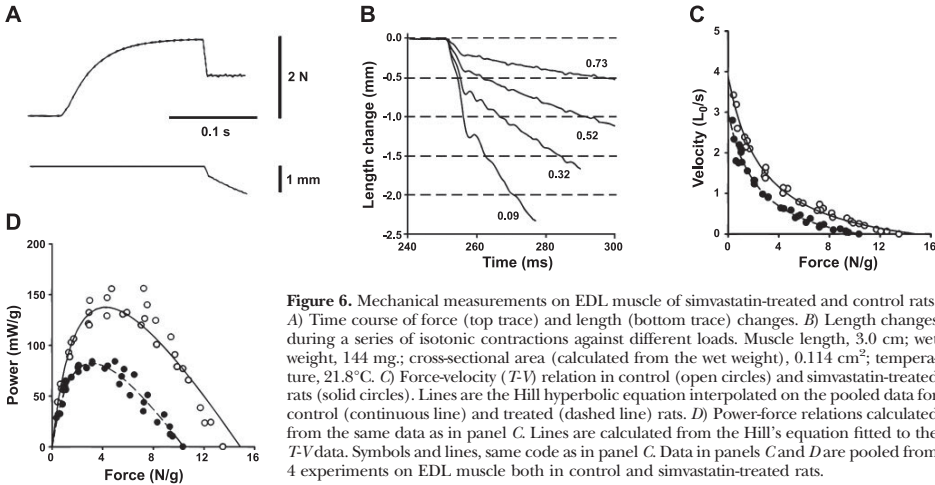
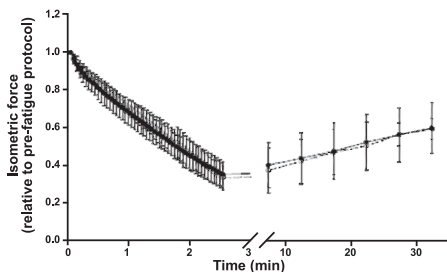


Figure 6. Mechanical measurements on EDL muscle of simvastatin-treated and control rats. A) Time course of force (top trace) and length (bottom trace) changes. B) Length changes during a series of isotonic contractions against different loads. Muscle length, 3.0 cm; wet weight, 144 mg.; cross-sectional area (calculated from the wet weight), 0.114 cm<sup>2</sup>; temperature, 21.8°C. C) Force-velocity (*T-V*) relation in control (open circles) and simvastatin-treated rats (solid circles). Lines are the Hill hyperbolic equation interpolated on the pooled data for control (continuous line) and treated (dashed line) rats. D) Power-force relations calculated from the same data as in panel C. Lines are calculated from the Hill's equation fitted to the *T-V* data. Symbols and lines, same code as in panel C. Data in panels C and D are pooled from 4 experiments on EDL muscle both in control and simvastatin-treated rats.



**Figure 7.** Effects of simvastatin on muscle endurance. Changes in isometric force on EDL muscle in simvastatin-treated (solid circles) and control rats (open circles) during fatigue and recovery. EDL muscles were subjected to a fatigue protocol consisting of a 400-ms, 100-Hz tetanus every 3 s for 150 s. Descending part of the curve shows the decline in isometric force. Ascending part of the curve shows the partial recovery of isometric force up to 40 min from the end of the fatigue protocol.  $n = 4/\text{group}$ . Data are means  $\pm$  sd.

and locomotion (27, 28). Biochemical analysis shows that simvastatin treatment, by means of the shift toward a slower MHC isoform phenotype, reduces EDL muscle functions without exerting any muscle damage, in agreement with the lack of evidence for reduction in isometric force.

The drug efficacy on skeletal muscle tissue was ascertained by determining HMGR activity and LDLr protein levels. In agreement with previous studies in hepatocytes, simvastatin inhibits HMGR activity and increases the expression of LDLr (19). The putative myotoxic effects of the drug, whose underlying mechanisms are still debated, were excluded by the analysis of muscle damage markers. It is known that statin administration can induce muscle fiber necrosis, with release of cellular constituents such as CK into the bloodstream (2), and a caspase-dependent apoptotic cascade leading to the PARP-1 cleavage (29). Any significant increase of plasma CK and cleaved PARP-1 protein levels in simvastatin-treated rats was found, indicating that, in agreement with the lack of evidence for reduction in isometric force, the reduced muscle function is not related to muscle fiber loss due to apoptosis or necrosis. The absence of muscle damage could be explained by the lower dose of simvastatin used in our study, 1.5 mg/kg (comparable to the highest dose used to treat hypercholesterolemia in the clinical practice), with respect to the doses used in previous studies where muscle damages were described (30). In fact, the maximum simvastatin dose administered in clinical practice is 80 mg/d, corresponding, on average, to 1.14 mg/kg/d; since the metabolism rate of rats is higher than that of humans, the dose administered to the animals was slightly increased. We also excluded that the impairment of EDL muscle function was due to modified levels of HMGR end products directly involved in muscle contraction; neither cholesterol nor CoQ9 changed significantly in treated ani-

mals. However, this result cannot rule out a modulation of HMGR main end products by simvastatin, since only 50% of the body CoQ9 is derived from endogenous synthesis through the MVA pathway, and the remaining 50% is thought to be obtained through fat ingestion (4) and carried mainly by LDL in the circulation (12). Thus, like cholesterol, putative CoQ9 depletion due to enzyme inhibition by simvastatin could have been restored within the cells and, in turn, within the tissues by an enhanced LDLr-mediated uptake, as suggested by the increased LDLr protein expression. Furthermore, the levels of RhoA were evaluated both because the post-translational modification with a prenyl group (an HMGR product) is necessary for its membrane association and consequent activation, and because RhoA can activate Rho-kinase, responsible for MLC phosphorylation and, in turn, involved in the regulation of muscle contraction. Nevertheless, RhoA activation state did not change in either animal group.

Morphological but overall biochemical analysis show a change of sarcomeric proteins belonging to the contractile machinery of the muscle toward a slower phenotype, especially in the MHC composition of the fibers within the muscle, which leads to the reduced muscle function (31, 32). Specifically, simvastatin treatment induces a shift from the fastest MHC IIb isoform to the slower MHC IIa/x isoforms. The amount of reduction of  $V_0$  (23%),  $W_{\text{max}}$  (41%), and  $t_{1/2}$  (25%), as well as the lack of significant change in  $T_0$ , are in qualitatively good agreement with the changes of these parameters described in muscles and in fully  $\text{Ca}^{2+}$ -activated skinned fibers from fast skeletal muscles of mammals containing different MHC isoforms (31–35). In particular, fast fibers from rats containing pure MHC IIa isoform have  $V_0 \sim 30\%$  lower than those containing MHC IIx isoform, and the latter have  $V_0 \sim 20\%$  lower than fibers containing MHC IIb isoform, while the maximum power in fibers containing MHC IIa/x isoforms is 30–60% lower than in fibers containing MHC IIb isoform (33). Moreover, the endurance of EDL muscle, determined by a fatigue protocol, is not affected by simvastatin.

The simvastatin-induced impairment of muscle performance was also supported by an *in vivo* functional test. These changes resulted in reduced maximum speed reached and reduced latency to fall off the accelerating rotarod in the absence of general impair-

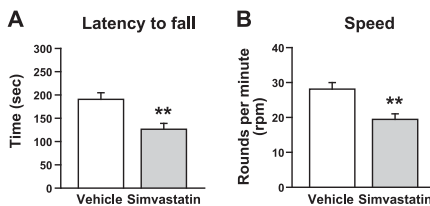


**Figure 8.** Effects of simvastatin in the rotarod test. Simvastatin-treated rats showed reduced latency to fall off the rotarod ( $t=3.35$ ,  $df=17$ ,  $P<0.01$ ; A) and reduced maximum speed reached during the test ( $t=3.48$ ,  $df=17$ ,  $P<0.01$ ; B).  $n = 10/\text{group}$ . \*\* $P < 0.01$ ; Student's *t* test.



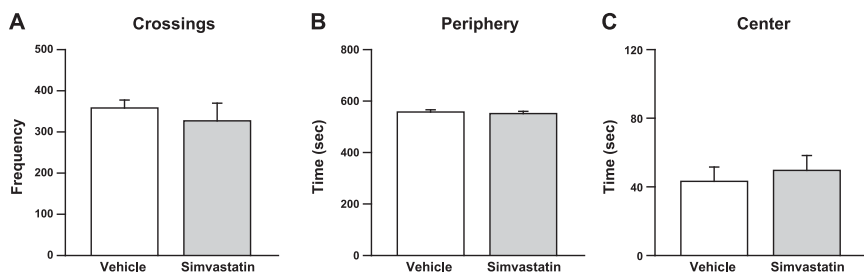


**Figure 9.** Effects of simvastatin in the open-field test. Simvastatin-treated rats did not differ from vehicle-treated rats in the number of crossings ( $t=0.67$ ,  $df=17$ , n.s.; *A*) and in the time spent both in periphery ( $t=0.51$ ,  $df=17$ , n.s.; *B*) and in center ( $t=-0.53$ ,  $df=17$ , n.s.; *C*). Moreover, simvastatin- and vehicle-treated rats did not differ in frequency and duration of wall-rearing, rearing, and grooming (data not shown);  $n = 10/\text{group}$ .

ments in basal locomotor activity, as measured in the open-field test. Thus, simvastatin-treated rats showed normal coordination and were still able to run on the rotarod at low speeds but, compared to vehicle-treated animals, could not run the rod at high speeds.


Our results indicate that the simvastatin-induced impairment of muscle function is not related either to changes in Akt and AMPK phosphorylation or to changes in HMGR end products directly involved in muscle contraction, suggesting that a putative modification of other MVA pathway downstream compounds,

such as prenylated proteins (*i.e.*, Cdc42, Ras, Rac) not evaluated in this work could be at the root of the observed phenomena (**Fig. 10**).

Further investigations must define the molecular mechanisms responsible for the fast MHC isoform plasticity. This work establishes that a shift in the fast MHC isoforms is involved in muscle contraction impairment following statin treatment. The observed fast MHC isoform shift could be responsible for the reduced muscle activity, at least in fast muscle, and functional impairment described in statin-treated pa-

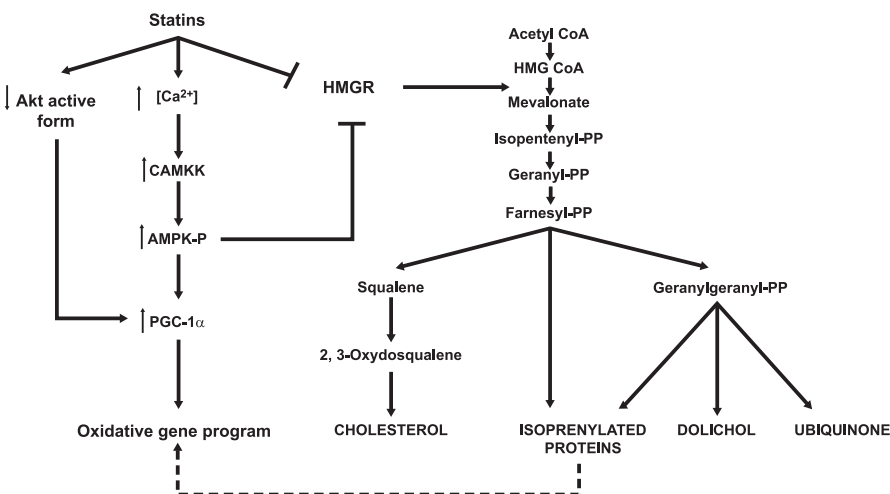


**Figure 10.** Possible mechanisms responsible for the shift of the fast MHC isoforms in EDL muscle fibers. Simvastatin competitively inhibits the enzyme HMGR (37); can increase the intracellular  $\text{Ca}^{2+}$  concentration (38), which, in turn, causes an increase of AMPK activity (23); and can suppress Akt phosphorylation. Both the activation of AMPK and the suppression of Akt phosphorylation positively modulate PGC-1 $\alpha$ , which drives a coordinated conversion to fibers having characteristics of oxidative type I, IIa, and IIx fibers (25). The lack of any modification in both Akt and AMPK phosphorylation and the absence of changes in HMGR main end products (cholesterol, CoQ9, RhoA) found here, exclude their involvement in MHC shift to slower phenotype in our experimental model. The shift could be ascribable to other prenylated proteins involved in intracellular signal transduction pathway (dotted line in the scheme).

tients (4, 36). This finding suggests that alternative pharmacological approaches should be considered in the management of hypercholesterolemia. 

The authors thank Prof. Maria Marino and Anna Trentalance (Department of Biology University Roma Tre) and Prof. Vincenzo Lombardi (Department of Evolutionary Biology, University of Florence) for the helpful discussion. The authors also thank Dr. Maria Morena (Department of Physiology and Pharmacology V. Erspamer, University of Rome La Sapienza, Rome, Italy) for helping with behavioral experiments and Mr. Mario Dolfi (Department of Evolutionary Biology, University of Florence) for skilled technical assistance in mechanical experiments.

## REFERENCES

- Viccia, G., Vignali, E., and Marocchi, C. (2007) Role of the cholesterol biosynthetic pathway in osteoblastic differentiation. *J. Endocrinol. Invest.* **30**, 8–12
- Ogura, T., Tanaka, Y., Nakata, T., Namikawa, T., Kataoka, H., and Ohtsubo, Y. (2007) Simvastatin reduces insulin-like growth factor-I signaling in differentiating C2C12 mouse myoblast cells in an HMG-CoA reductase inhibition-independent manner. *J. Toxicol. Sci.* **32**, 57–67
- Draeger, A., Monastyrskaya, K., Mohaupt, M., Hoppeler, H., Savolainen, H., Allemann, C., and Babychuk, E. B. (2006) Statin therapy induces ultrastructural damage in skeletal muscle in patients without myalgia. *J. Pathol.* **210**, 94–102
- Thompson, P. D., Clarkson, P., and Karas, R. H. (2003) Statin-associated myopathy. *JAMA* **289**, 1681–1690
- Van Aelst, L., and D'Souza-Schorey, C. (1997) Rho GTPases and signalling network. *Genes Dev.* **11**, 2295–2322
- Burda, P., and Aebi, M. (1999) The dolichol pathway of N-linked glycosylation. *Biochim. Biophys. Acta* **1426**, 239–257
- Espenshade, P. J., and Hughes, A. L. (2007) Regulation of sterol synthesis in eukaryotes. *Annu. Rev. Genet.* **41**, 401–427
- Dirks, A. J., and Jones, K. M. (2006) Statin-induced apoptosis and skeletal myopathy. *Am. J. Physiol. Cell Physiol.* **291**, C1208–C1212
- Minini, C., Trapani, L., Narciso, L., Marino, M., Trentalance, A., and Pallottini, V. (2009) 3-hydroxy 3-methylglutaryl coenzyme A reductase is essential for rat muscle differentiation. *J. Cell. Physiol.* **220**, 524–530
- Bruscalupi, G., Leoni, S., Mangiantini, M. T., Minieri, M., Spagnuolo, S., and Trentalance, A. (1985) True uncoupling between cholesterol synthesis and 3-hydroxy-3-methylglutaryl coenzyme A reductase in an early stage of liver regeneration. *Cell. Mol. Biol.* **31**, 365–368
- Lowry, O. H., Rosebrough, N. J., Farr, A. L., and Randall, R. J. (1951) Protein measurement with the Folin phenol reagent. *J. Biol. Chem.* **193**, 265–275
- Tang, P. H., Miles, M. V., DeGrauw, A., Hershey, A., and Pesce, A. (2001) HPLC analysis of reduced and oxidized coenzyme Q(10) in human plasma. *Clin. Chem.* **47**, 256–265
- Carter, R. J., Morton, J., and Dummett, S. B. (2001) Motor coordination and balance in rodents. *Curr. Protoc. Neurosci.* Chap. 8, Unit 8.12
- Voss, J., Sanchez, C., Michelsen, S., and Ebert, B. (2003) Rotarod studies in the rat of the GABAA receptor agonist gaboxadol: lack of ethanol potentiation and benzodiazepine cross-tolerance. *Eur. J. Pharmacol.* **482**, 215–222
- Chao, Y., Chen, J. S., Hunt, V. M., Kuron, G. W., Karkas, J. D., Liou, R., and Alberts, A. W. (1991) Lowering of plasma cholesterol levels in animals by lovastatin and simvastatin. *Eur. J. Clin. Pharmacol.* **40**(Suppl. 1), S11–S14
- Ginsberg, H. N. (1998) Effects of statins on triglyceride metabolism. *Am. J. Cardiol.* **81**, 32B–35B
- Brown, M. S., and Goldstein, J. L. (2004) Lowering plasma cholesterol by raising LDL receptors. 1981. *Atheroscler. Suppl.* **5**, 57–59
- Yokoyama, M., Seo, T., Park, T., Yagyu, H., Hu, Y., Son, N. H., Augustus, A. S., Vikramadithyan, R. K., Ramakrishnan, R., Pulawa, L. K., Eckel, R. H., and Goldberg, I. J. (2007) Effects of lipoprotein lipase and statins on cholesterol uptake into heart and skeletal muscle. *J. Lipid Res.* **48**, 646–655
- Westwood, F. R., Bigley, A., Randall, K., Marsden, A. M., and Scott, R. C. (2005) Statin-induced muscle necrosis in the rat: distribution, development, and fibre selectivity. *Toxicol. Pathol.* **33**, 246–257
- Bozzo, C., Stevens, L., Toniolo, L., Mounier, Y., and Reggiani, C. (2003) Increased phosphorylation of myosin light chain associated with slow-to-fast transition in rat soleus. *Am. J. Physiol. Cell Physiol.* **285**, C575–C583
- Dubroca, C., Loyer, X., Retailliau, K., Loirand, G., Pacaud, P., Feron, O., Balligand, J. L., Levy, B. I., Heymes, C., and Henrion, D. (2007) RhoA activation and interaction with Caveolin-1 are critical for pressure-induced myogenic tone in rat mesenteric resistance arteries. *Cardiovasc. Res.* **73**, 190–197
- Schreiber, D. H., and Anderson, T. R. (2006) Statin-induced rhabdomyolysis. *J. Emerg. Med.* **31**, 177–180
- Kou, R., Sartoretto, J., and Michel, T. (2009) Regulation of Rac1 by simvastatin in endothelial cells: differential roles of AMP-activated protein kinase and calmodulin-dependent kinase kinase-beta. *J. Biol. Chem.* **284**, 14734–14743
- Wang, W., and Wong, C. W. (2010) Statins enhance peroxisome proliferator-activated receptor gamma coactivator-alpha activity to regulate energy metabolism. *J. Mol. Med.* **88**, 309–317
- Arany, Z., Lebrasseur, N., Morris, C., Smith, E., Yang, W., Ma, Y., Chin, S., and Spiegelman, B. M. (2007) The transcriptional coactivator PGC-1beta drives the formation of oxidative type IIX fibers in skeletal muscle. *Cell Metab.* **5**, 35–46
- Izumo, N., Fujita, T., Nakamura, H., and Koida, M. (2001) Lipophilic statins can be osteogenic by promoting osteoblastic calcification in a Cbfa1- and BMP-2-independent manner. *Methods Find. Exp. Clin. Pharmacol.* **23**, 389–394
- Rome, L. C., Sosnicki, A. A., and Goble, D. O. (1990) Maximum velocity of shortening of three fibre types from horse soleus muscle: implications for scaling with body size. *J. Physiol.* **431**, 173–185
- Puthoff, M. L., and Nielsen, D. H. (2007) Relationships among impairments in lower-extremity strength and power, functional limitations, and disability in older adults. *Phys. Ther.* **87**, 1334–1347
- Von Tresckow, B., von Strandmann, E. P., Sasse, S., Tawadros, S., Engert, A., and Hansen, H. P. (2007) Simvastatin-dependent apoptosis in Hodgkin's lymphoma cells and growth impairment of human Hodgkin's tumors in vivo. *Haematologica* **92**, 682–685
- Cohen, G. M. (1997) Caspases: the executioners of apoptosis. *Biochem. J.* **326**(Pt. 1), 1–16
- Schiaffino, S., and Reggiani, C. (1996) Molecular diversity of myofibrillar proteins: gene regulation and functional significance. *Physiol. Rev.* **76**, 371–423
- Bottinelli, R., and Reggiani, C. (2000) Human skeletal muscle fibres: molecular and functional diversity. *Prog. Biophys. Mol. Biol.* **73**, 195–262
- Pellegrino, M. A., Canepari, M., Rossi, R., D'Antona, G., Reggiani, C., and Bottinelli, R. (2003) Orthologous myosin isoforms and scaling of shortening velocity with body size in mouse, rat, rabbit and human muscles. *J. Physiol.* **546**, 677–689
- Pette, D., and Staron, R. S. (1990) Cellular and molecular diversities of mammalian skeletal muscle fibers. *Rev. Physiol. Biochem. Pharmacol.* **116**, 1–76
- Bottinelli, R., Betto, R., Schiaffino, S., and Reggiani, C. (1994) Unloaded shortening velocity and myosin heavy chain and alkali light chain isoform composition in rat skeletal muscle fibres. *J. Physiol.* **478**(Pt. 2), 341–349
- Scott, D., Blizzeard, L., Fell, J., and Jones, G. (2009) Statin therapy, muscle function and falls risk in community-dwelling older adults. *QJM* **102**, 625–633
- Istvan, E. S., and Deisenhofer, J. (2000) The structure of the catalytic portion of human HMG-CoA reductase. *Biochim. Biophys. Acta* **1529**, 9–18
- Sirvent, P., Bordenave, S., Vermaelen, M., Roels, B., Vassort, G., Mercier, J., Raynaud, E., and Lacampagne, A. (2005) Simvastatin induces impairment in skeletal muscle while heart is protected. *Biochem. Biophys. Res. Commun.* **338**, 1426–1434
- Payne, A. M., Dodd, S. L., and Leeuwenburgh, C. (2003) Life-long caloric restriction in Fischer 344 rats attenuates age-related loss in skeletal muscle-specific force and reduces extracellular space. *J. Appl. Physiol.* **95**, 2554–2562

Received for publication March 14, 2011.

Accepted for publication July 21, 2011.

# **HMG CoA reductase inhibition gets rat $\beta$ -Myosin Heavy Chain disappeared: a statin paradox**

*(Submitted to Journal of Cellular Biochemistry)*

Laura Trapani<sup>¶1</sup>, Marco Segatto<sup>1</sup>, Adam Jozwiak<sup>2</sup>, Ewa Swiezewska<sup>2</sup>,  
Valentina Pallottini<sup>1</sup>

<sup>1</sup> Department of Biology, University of Rome, Roma Tre, Viale Marconi 446, 00146, Rome, Italy.

<sup>2</sup> Institute of Biochemistry and Biophysics, Polish Academy of Sciences, Pawinskiego 5a, 02-106 Warsaw, Poland.

<sup>¶</sup>Corresponding author: Laura Trapani, Department of Biology, University of Rome, Roma Tre, Viale Marconi 446, 00146, Rome, Italy

Tel. +39.06.57336344

Fax: +39.06.57336321

e-mail: ltrapani@uniroma3.it

### **Abstract**

3-hydroxy-3methylglutaryl Coenzyme A reductase, the rate limiting enzyme of mevalonate pathway, generates a range of products, in addition to cholesterol, such as oligoprenyl groups, dolichol and ubiquinone, involved in several biological functions. In particular, the latter participates in electron transport chain and, in turn, in tissue energy supply. The enzyme is inhibited by statins that, besides lowering cholesterolemia, seem to impair human energy-dependent myocardial functions (e.g. stroke volume, cardiac output, and contractile index). The modulation of heart contractile properties could be explained by the decrease of ventricle ubiquinone content and/or by putative changes in proportion of the different myosin heavy chain isoforms. Since we previously demonstrated that chronic statin treatment modifies myosin heavy chain isoform pattern in skeletal muscle impairing its functional properties, aim of this work was to investigate the effects of statin chronic treatment on both ventricle ubiquinone content and myosin heavy chain isoforms. Our results showed that simvastatin treatment leads to a reduced amount of rat ventricle ubiquinone and to  $\beta$  myosin heavy chain disappearance. Thus, statins which are prescribed to prevent cardiovascular disease, might induce cardiac metabolic and structural modifications whose functional implications on contractility are still to be established and carefully considered.

**Key words:** Heart, Myosin Heavy Chains, Statins, Ubiquinone.

## **Introduction**

The well established link between plasma cholesterol levels and coronary artery disease and the contribution of elevated plasma cholesterol, specifically Low Density Lipoprotein (LDL)-cholesterol, to other diseases including cancer, obesity and diabetes, have made control of plasma cholesterol a major health aim [Heynekamp et al., 2008].

The decrease of cellular cholesterol synthesis leads to a homeostatic response involving up-regulation of cell-surface receptors that bind atherogenic LDL and Very Low Density Lipoproteins (VLDL). These lipoproteins are taken up by the cell and degraded [Brown and Goldstein, 2009]. The reduction of plasma LDL-cholesterol accounts for the clinical utility of statins [Trapani and Pallottini, 2010] which block an early step of cholesterol biosynthetic pathway by inhibiting 3-hydroxy-3-methylglutaryl Coenzyme A (HMGR) [Buhaescu and Izzedine, 2007]. This enzyme generates a range of other products, in addition to cholesterol, such as ubiquinone (CoQ), heme-A, oligoprenyl groups and dolichol which play pivotal roles in cell biology and human physiology [Goldstein and Brown, 1990]; [Mach, 2004]; [Keyhani and Keyhani, 1978].

Besides the beneficial effects exerted on plasma lipid profile, statin treatment can lead to severe adverse effects on muscle tissues going from fatigue, weakness, and pain to symptoms associated with rhabdomyolysis, which is a life-threatening condition [Golomb and Evans, 2008].

Although less investigated statin side effects were detected also on cardiac muscle. Pisarenko and co-workers demonstrated that 1-month lovastatin therapy impairs human energy-dependent myocardial functions by decreasing stroke volume, cardiac output, and contractile index. The authors ascribed the impairment of myocardium energy supply to the suppression of CoQ synthesis caused by statin treatment [Pisarenko et al., 2001]. Although studies have repeatedly demonstrated a reduction of circulating CoQ concentrations with statin therapy, it is unclear whether tissue level of CoQ are significantly affected [Nawarskas, 2005].

The modulation of the contractile properties of the heart could also be explained by putative changes in proportion of the different Myosin Heavy Chain (MHC) isoforms that seems to be related to the level of mechanical performance of the heart [Morkin, 2000]. Indeed, our previous work demonstrates that simvastatin chronic treatment (1.5 mg/kg/die) induces in rats functional impairment and reduces muscle power output and unloaded shortening velocity because of a shift of MHC isoforms from the fastest IIB to the slower IIA/x in fast skeletal muscle (*Extensor digitorum longus*) [Trapani et al., 2011]. Myosin is a major protein component of

heart and skeletal muscles and is the element responsible for energy transduction and force development in these tissues [Eisenberg and Greene, 1980]; [Harrington and Rodgers, 1984]. Each myosin molecule contains four light chains (MLC) and two heavy chains with ATPase activity. Ventricular muscle has three myosin isoforms that are designated, V1–3, in order of decreasing electrophoretic mobility and ATPase activity [Hoh et al., 1978]. These isoforms differ only in their MHC composition. The V1 form is comprised of two  $\alpha$ -MHCs, V3 has two  $\beta$ -MHCs, and V2 has one MHC of each type [Morkin, 2000].

Differences in speed of contraction are well documented for the ventricles and are correlated with variations in the ratio of  $\alpha$  to  $\beta$ -MHCs (reviewed in Swynghedauw, 1986 [Swynghedauw, 1986]). Fast-contracting ventricles (e.g., mice and rats) contain predominately the V1 form ( $\alpha\alpha$ ); ventricles with intermediate speed (rabbit and guinea pig) are predominately V3 ( $\beta\beta$ ) but possess small amounts of the V1 and V2 ( $\alpha\beta$ ) forms; slow ventricles (human and bovine) contain less than 10% V1 [Morkin, 2000].

Thus, owing to the ability of statins to impair skeletal muscle performance through a MHC isoform shift and to the inadequate knowledge about their capacity to reduce ventricular CoQ content, the aim of our research was to evaluate whether HMGR inhibition by simvastatin could modify ventricular CoQ9 (the predominant ubiquinone form in rats) content and could affect cardiac fiber phenotype.

## **Material and methods**

### **Reagents**

All chemicals were obtained from commercial sources and were of the highest quality available; when the source is not specified they were obtained from Sigma-Aldrich (Milan, Italy).

### **Animals**

3-months-old male Wistar *Rattus norvegicus* (Harlan Nossan, S. Pietro al Natisone, Italy) were housed under controlled temperature ( $20 \pm 1^\circ\text{C}$ ), humidity ( $55 \pm 10\%$ ), and illumination (lights on for 12 hours daily, from 7 A.M. to 7 P.M.). Food and water were provided *ad libitum*. The experiments were performed according to the ethical guidelines for the conduct of animal research (Ministero della Salute, Official Italian Regulation No. 116/92, Communication to Ministero della Salute no. 391/121). Rats were divided in two groups of 7 animals each. The first group was treated daily with intraperitoneal injection of 1.5 mg/kg simvastatin in vehicle (dimethyl sulfoxide – DMSO – 1 ml/kg) for 3 weeks,

a dose comparable to the highest one used in therapies for human hypercholesterolemia. Control animals received daily an equal volume of vehicle. At the end of the treatment rats were anaesthetized with ether in a fume cupboard and plasma was obtained from blood collected into EDTA (1 mg/ml blood).

The cardiac ventricles of the animals from each group were dissected and immediately frozen in liquid nitrogen for subsequent biochemical assays.

### **Biochemical Analysis**

*Plasma cholesterol analysis.* Plasma cholesterol content of rats was assessed through the colorimetric CHOD-POD kit according to manufacturer's instructions (Assel, Rome, Italy). Briefly, by the catalysis of cholesterol esterase and cholesterol oxidase, cholesterol ester was catalyzed to yield  $H_2O_2$ , which oxidates 4-aminoantipyrine with phenol to form a colored dye of quinoneimine. The absorbancy increase is directly proportional to the concentration of cholesterol.

*Triglyceride and Creatin Kinase assays.* Plasma Triglycerides amount and Creatin Kinase activity were measured by standardized commercial methods on a fully automated system (Modular, Roche, Basel Switzerland). Triglycerides are hydrolyzed to glycerol by lipoprotein lipase and oxidized to dihydroxyacetone phosphate and hydrogen peroxide which reacts with Trinder reagent to form a red dyestuff. The colour intensity is directly proportional to triglyceride concentration. This method is linear between 4-1000 mg/dL. Activity of Creatin Kinase measurement is in accordance with the method recommended by the International Federation of Clinical Chemistry (IFCC) at 37 °C .

*Lysate preparation.* Total lysates were obtained as follows: 100 mg cardiac ventricle were homogenized in 0.01 M Tris-HCl, 0.001 M  $CaCl_2$ , 0.15 M NaCl, 0.001 M PMSF, pH 7.5. The homogenate was solubilized by sonication in Sample Buffer, centrifuged for 5 min at 15,600 g and the supernatant was transferred in microtubes. Protein concentration was determined by the method of Lowry et al. [Lowry et al., 1951]. All samples were boiled for 3 min before loading for Western blotting.

*Protein analysis.* Protein profiles were analysed by Western blotting. Western blot analysis of  $\alpha$  and  $\beta$ -MHC isoforms were performed on cardiac ventricle lysates. Twenty  $\mu$ g of protein were resolved by 7% SDS-PAGE at 140V for 6 hours at 4°C. The proteins were subsequently transferred electrophoretically onto nitrocellulose for 90 min at 100V. The nitrocellulose membrane was blocked at room temperature with 5% fat-free milk in Tris-buffered saline (138 mM NaCl, 27 mM KCl, 25 mM Tris-HCl,

0.05% Tween-20, pH 6.8), and probed at 4°C overnight with primary antibodies ( $\beta$ -MHC NOQ7.5.4D, Sigma-Aldrich;  $\alpha$ -MHC BA-G5, Abcam, Cambridge, UK). The nitrocellulose membrane was then stripped with Restore Western Blot Stripping Buffer (Pierce Chemical, Rockford, IL, USA) for 10 min at room temperature and re-probed with anti-vinculin (vinculin, Sigma-Aldrich) antibody. Bound antibodies were visualized using enhanced chemoluminescence detection (GE Healthcare). All images derived from Western blotting were analyzed with ImageJ (NIH, Bethesda, MD, USA) software for Windows. Each reported value was derived from the ratio between arbitrary units obtained by the protein band and the respective vinculin band (chosen as housekeeping protein).

*Lipid extraction.* Cardiac ventricle (approx. 100 mg) was homogenized in NaCl 150mM 1:9 w/v.; 6 nmoles Coenzyme Q6 (CoQ6), 600  $\mu$ l water, 4 ml methanol, and 4 ml chloroform were added to the homogenate. CoQ6 was added as internal standard to calculate the recovery. The samples were incubated for 30 min at 37 °C. Then, 800  $\mu$ l NaCl 150mM and 2 ml chloroform were added and two phases were obtained. The lower phase was evaporated with a stream of nitrogen. Samples were dissolved in 0.5 ml chloroform and then divided in 2 halves. The samples used to measure CoQ9 amount were dissolved in 50  $\mu$ l isopropanol:ethanol 1:1 v/v; the samples employed to estimate cholesterol levels were hydrolyzed in 0.5 ml 15% KOH in ethanol:water 95:5 v/v for 60 min at 95°C. Then the organic phase was extracted with 0.5 ml of water and 1 ml of hexane. The upper phase was collected and evaporated with a stream of nitrogen, then dissolved in 50  $\mu$ l isopropanol:ethanol 1:1 v/v.

*HPLC-UV analysis of polyisoprenoids.* Lipids were analyzed according to previously described protocol [Tang et al., 2001] with modifications. Briefly, two parallel runs, one for CoQ9 and another for cholesterol were performed on a 4.6  $\times$  75 mm ZORBAX XDB-C18 (3,5  $\mu$ m) reversed-phase column (Agilent, USA) using a Waters dual-pump apparatus, a Waters gradient programmer, and a Waters Photodiode Array Detector (spectrum range: 210-400 nm). For elution, a combination of convex gradients (Waters No. 5, from 0 to 75% B for the initial 20 min and linear, from 75 to 100% B during the following 10 min) was used; in the last 5 min, re-equilibration back to 0% B was performed, where solvent A was methanol/water, 9:1, vol/vol, and solvent B was methanol/propan-2-ol/hexane, 2:1:1, by vol). The solvent flow rate was 1.5 ml/min. HPLC solvents were obtained from POCh, Gliwice. The chain length and identity of lipids were confirmed by applying following standards: CoQ6, CoQ10, cholesterol. CoQ10 and cholesterol were purchased from Sigma-Aldrich,



CoQ6, was from the Collection of Polyprenols, Institute of Biochemistry and Biophysics, PAS, Warsaw.

## **Results**

Simvastatin efficacy in lowering plasma LDL-cholesterol [Chao et al., 1991] and triglycerides [Ginsberg, 1998] by hepatic LDLr up-regulation [Brown and Goldstein, 2004], was verified by checking rat plasma cholesterol and triglyceride content (Fig. 1). As expected, both the metabolic parameters were significantly decreased following the statin treatment, by 30% and 50% respectively. Nevertheless, simvastatin treatment did not statistically modify animal weight (at the end of treatment all animals weighted g  $335 \pm 43$ ).

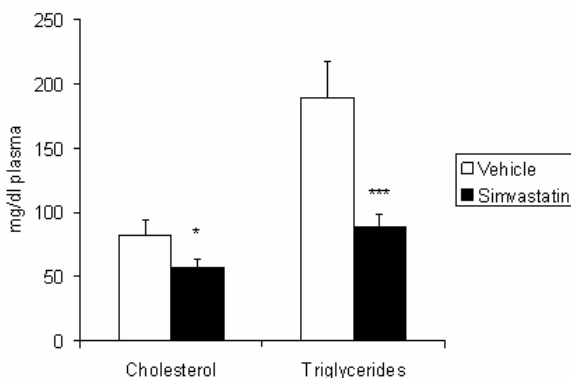


***Figure 1 Plasma cholesterol and triglyceride content in rats treated with vehicle (DMSO) or simvastatin for 21 days. Data are expressed as mean  $\pm$  SD of 7 different animals. \* $P < 0.05$ , \*\*\* $P < 0.001$  as determined by Student's  $t$  test.***

Once proved the systemic efficacy of simvastatin, our attention was focused on the effects exerted by HMGR inhibition in rat cardiac ventricle. Thus, the levels of HMGR main end-products were assessed. Cholesterol was analyzed in order to ascertain whether simvastatin was effective even in

the heart; CoQ9 was checked due to its implication in cardiomyocyte energy supply. As shown in Table 1, tissue content of cholesterol was increased in the cardiac ventricles of simvastatin-treated animals when compared to control (vehicle) rats whereas the amount of ventricular CoQ9 was significantly reduced.

	<b>Vehicle (7)</b>	<b>Simvastatin (7)</b> (1.5 mg/kg)	<b>P-value</b> (unpaired <i>t</i> -test)
<b>Cholesterol</b> ( $\mu\text{g/g}$ tissue)	106.56 $\pm$ 10.87	172.76 $\pm$ 6.88**	0.0037
<b>CoQ9</b> ( $\mu\text{g/g}$ tissue)	97.48 $\pm$ 5.45	58.12 $\pm$ 9.21**	0.0081

**Table 1. Effect of simvastatin treatment on HMGR end-products of the mevalonate pathway.** Number of ventricles contributing to each value are shown in brackets. \*\*=  $P < 0.01$ .

Moreover, as we previously described that simvastatin was able to induce a shift of MHC isoforms in skeletal muscle [Trapani et al., 2011] ventricular content of  $\beta$ -MHC was evaluated in order to investigate if simvastatin treatment could cause modification of MHC protein profile even in cardiac muscle. Intriguingly, as shown in Fig 2, tissue amount of  $\beta$ -MHC was strikingly reduced, on the contrary non-statistically significant differences were detected in ventricular  $\alpha$ -MHC content of simvastatin-treated animals when compared to controls.

### **Discussion**

Our work highlights the strict connection between HMGR main end-products and cardiac physiology showing that the inhibition of the enzyme, which catalyzes the key and rate limiting step of cholesterol biosynthetic pathway, was able to reduce the amount of CoQ9 and  $\beta$ -MHC in rat ventricle. The enzyme activity was chronically inhibited by means of simvastatin, among the lipophilic statins generally taken up much more

widely into a broad range of tissues compared with hydrophilic ones [Izumo et al., 2001].

The hypocholesterolemic property of simvastatin was displayed by the reduction of plasma cholesterol content. The efficacy of simvastatin on cardiac muscle was supported by the reduced amount of ventricular CoQ9 which guarantees the energy supply to the heart being involved in mitochondrial electron transport chain. On the contrary, tissue cholesterol levels increased. This result is not surprising if it is considered that statin treatment induces a compensatory upregulation of genes involved in cholesterol uptake [Horton et al., 2002].

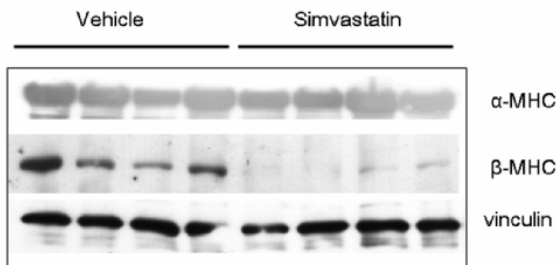


**Figure 2** Western blot analysis of ventricular  $\beta$ -MHC of rats treated with vehicle (DMSO) or simvastatin for 21 days. Typical Western blot of  $\alpha$ -MHC and  $\beta$ -MHC detected in total lysates prepared from cardiac ventricles of rats under simvastatin treatment and of rats receiving vehicle. 4 different animals for each experimental group were used. For details see the main text.

Given that fibers having distinct MHC isoforms exhibit different metabolisms and since an alteration in the energy metabolic system can affect cardiac gene expression [Kakinuma et al., 2002], we investigated whether the observed reduction of ventricular CoQ9 content, following statin treatment, could cause putative modifications in the phenotype of ventricular myocytes. Very interestingly, our hypothesis was confirmed by the strong reduction of  $\beta$ -MHC protein expression. Thus, the partial lack of one among the components of electron transport chain could cause a

disproportion in fiber phenotype, inducing a shift towards a glycolytic metabolism.

The immunologic method (Western blot) we used did not allow as to detect any statistically significant difference in ventricular  $\alpha$ -MHC content probably due to the elevated amount of  $\alpha$ -MHC compared to  $\beta$ -MHC. Nevertheless, we cannot exclude that a putative compensative increase of  $\alpha$ -MHC protein levels occurred parallel to  $\beta$ -MHC disappearance. These results seem apparently to contradict our previous data obtained from *Extensor Digitorum Longus* muscle of simvastatin treated rats, where the statin induced a shift of MHC isoforms towards a slower phenotype [Trapani et al., 2011]. Actually, this discrepancy might be ascribed to the reduction of CoQ9 (among the effectors of fiber oxidative metabolism) content which occurs in rat heart but was not observed in rat skeletal muscle [Trapani et al., 2011].

Since the different cardiac MHC isoforms exhibit distinct functional characteristics and are distributed regionally within the heart to match the mechanical and functional demands of the different areas, Krenz and co-workers assess that relatively minor changes in overall MHC isoform content could have significant functional consequences [Krenz et al., 2007].

Whether the statin-induced decrease of both  $\beta$ -MHC and CoQ could positively or negatively affect cardiac physiology is still debated. Indeed, if on one hand the statin treatment was associated to an improvement of cardiac function in models of heart failure [Bauersachs et al., 2001]; [Patel et al., 2001]; [Ichihara et al., 2006]; [Senthil et al., 2005], on the other the statin-induced reduction of CoQ was associated to an impairment in human energy-dependent myocardial functions (Pisarenko et al., 2001). Thus, a shift toward a faster phenotype could be a good compensatory response on a hypertrophic heart, but, what could happen if statins are administrated to a hypercholesterolemic patient with healthy heart?

Thus, our results seem to highlight a paradox; drugs such as statins, prescribed to prevent cardiovascular diseases, should not cause cardiac metabolic and structural modifications whose functional implications are still to be established. In the light of our observations and of the conflicting data present in literature, to what extent preventing cardiovascular diseases but at the same time causing myocardial function changes under statin treatment is worthwhile to be investigated.

### **Acknowledgment**

The financial support from the University of Roma Tre (CLAR) to VP is gratefully acknowledged.

## **References**

- Bauersachs J, Galuppo P, Fraccarollo D, Christ M, Ertl G. 2001. Improvement of left ventricular remodeling and function by hydroxymethylglutaryl coenzyme a reductase inhibition with cerivastatin in rats with heart failure after myocardial infarction. *Circulation* 104:982-5.
- Brown MS, Goldstein JL. 2004. Lowering plasma cholesterol by raising ldl receptors. 1981. *Atheroscler Suppl* 5:57-9.
- Brown MS, Goldstein JL. 2009. Cholesterol feedback: from Schoenheimer's bottle to Scap's MELADL. *J Lipid Res* 50 Suppl:S15-27.
- Buhaescu I, Izzedine H. 2007. Mevalonate pathway: a review of clinical and therapeutical implications. *Clin Biochem* 40:575-84.
- Chao Y, Chen JS, Hunt VM, Kuron GW, Karkas JD, Liou R, Alberts AW. 1991. Lowering of plasma cholesterol levels in animals by lovastatin and simvastatin. *Eur J Clin Pharmacol* 40 Suppl 1:S11-4.
- Eisenberg E, Greene LE. 1980. The relation of muscle biochemistry to muscle physiology. *Annu Rev Physiol* 42:293-309.
- Ginsberg HN. 1998. Effects of statins on triglyceride metabolism. *Am J Cardiol* 81:32B-35B.
- Goldstein JL, Brown MS. 1990. Regulation of the mevalonate pathway. *Nature* 343:425-30.
- Golomb BA, Evans MA. 2008. Statin adverse effects : a review of the literature and evidence for a mitochondrial mechanism. *Am J Cardiovasc Drugs* 8:373-418.
- Harrington WF, Rodgers ME. 1984. Myosin. *Annu Rev Biochem* 53:35-73.
- Heynekamp JJ, Hunsaker LA, Vander Jagt TA, Royer RE, Deck LM, Vander Jagt DL. 2008. Isocoumarin-based inhibitors of pancreatic cholesterol esterase. *Bioorg Med Chem* 16:5285-94.
- Hoh JF, McGrath PA, Hale PT. 1978. Electrophoretic analysis of multiple forms of rat cardiac myosin: effects of hypophysectomy and thyroxine replacement. *J Mol Cell Cardiol* 10:1053-76.
- Horton JD, Goldstein JL, Brown MS. 2002. SREBPs: activators of the complete program of cholesterol and fatty acid synthesis in the liver. *J Clin Invest* 109:1125-31.
- Ichihara S, Noda A, Nagata K, Obata K, Xu J, Ichihara G, Oikawa S, Kawanishi S, Yamada Y, Yokota M. 2006. Pravastatin increases survival and suppresses an increase in myocardial matrix metalloproteinase activity in a rat model of heart failure. *Cardiovasc Res* 69:726-35.

- Izumo N, Fujita T, Nakamuta H, Koida M. 2001. Lipophilic statins can be osteogenic by promoting osteoblastic calcification in a Cbfa1- and BMP-2-independent manner. *Methods Find Exp Clin Pharmacol* 23:389-94.
- Kakinuma Y, Miyauchi T, Suzuki T, Yuki K, Murakoshi N, Goto K, Yamaguchi I. 2002. Enhancement of glycolysis in cardiomyocytes elevates endothelin-1 expression through the transcriptional factor hypoxia-inducible factor-1 alpha. *Clin Sci (Lond)* 103 Suppl 48:210S-214S.
- Keyhani J, Keyhani E. 1978. Mevalonic acid as a precursor of the alkyl sidechain of heme a of cytochrome c oxidase in yeast *Saccharomyces cerevisiae*. *FEBS Lett* 93:271-4.
- Krenz M, Sadayappan S, Osinska HE, Henry JA, Beck S, Warshaw DM, Robbins J. 2007. Distribution and structure-function relationship of myosin heavy chain isoforms in the adult mouse heart. *J Biol Chem* 282:24057-64.
- Lowry OH, Rosebrough NJ, Farr AL, Randall RJ. 1951. Protein measurement with the Folin phenol reagent. *J Biol Chem* 193:265-75.
- Mach F. 2004. Statins as immunomodulatory agents. *Circulation* 109:II15-7.
- Morkin E. 2000. Control of cardiac myosin heavy chain gene expression. *Microsc Res Tech* 50:522-31.
- Nawarskas JJ. 2005. HMG-CoA reductase inhibitors and coenzyme Q10. *Cardiol Rev* 13:76-9.
- Patel R, Nagueh SF, Tsybouleva N, Abdellatif M, Lutucuta S, Kopelen HA, Quinones MA, Zoghbi WA, Entman ML, Roberts R, Marian AJ. 2001. Simvastatin induces regression of cardiac hypertrophy and fibrosis and improves cardiac function in a transgenic rabbit model of human hypertrophic cardiomyopathy. *Circulation* 104:317-24.
- Pisarenko OI, Studneva IM, Lankin VZ, Konovalova GG, Tikhaze AK, Kaminnaya VI, Belenkov YN. 2001. Inhibitor of beta-hydroxy-beta-methylglutaryl coenzyme A reductase decreases energy supply to the myocardium in rats. *Bull Exp Biol Med* 132:956-8.
- Senthil V, Chen SN, Tsybouleva N, Halder T, Nagueh SF, Willerson JT, Roberts R, Marian AJ. 2005. Prevention of cardiac hypertrophy by atorvastatin in a transgenic rabbit model of human hypertrophic cardiomyopathy. *Circ Res* 97:285-92.
- Swynghedauw B. 1986. Developmental and functional adaptation of contractile proteins in cardiac and skeletal muscles. *Physiol Rev* 66:710-71.

- Tang PH, Miles MV, DeGrauw A, Hershey A, Pesce A. 2001. HPLC analysis of reduced and oxidized coenzyme Q(10) in human plasma. *Clin Chem* 47:256-65.
- Trapani L, Melli L, Segatto M, Trezza V, Campolongo P, Jozwiak A, Swiezewska E, Pucillo LP, Moreno S, Fanelli F, Linari M, Pallottini V. 2011. Effects of myosin heavy chain (MHC) plasticity induced by HMGCoA-reductase inhibition on skeletal muscle functions. *FASEB J*. [Epub ahead of print]
- Trapani L, Pallottini V. 2010. Age-Related Hypercholesterolemia and HMG-CoA Reductase Dysregulation: Sex Does Matter (A Gender Perspective). *Curr Gerontol Geriatr Res*:420139.

## GENERAL CONCLUSIONS

In most mammals, skeletal muscle comprises about 55% of individual body mass and plays vital roles in locomotion, heat production and overall metabolism, whereas cardiac muscle imparts energy to blood in order to generate and sustain an arterial blood pressure necessary to provide adequate perfusion of organs.

Mva pathway displays a pivotal role both in skeletal and cardiac muscles due to the production of compounds such as cholesterol, CoQ, dolichol and prenyls involved in membrane structure maintenance, in mitochondrial electron transportation, in protein glycosylation and prenylation respectively. The statin-induced inhibition of HMGR, the key and rate limiting enzyme of Mva pathway, in addition to plasma hypolipidemic property, also leads to muscle adverse effects with symptoms ranging from weakness and pain to rhabdomyolysis, a life threatening condition. Owing to the structural similarity between skeletal and cardiac muscles if compared to other tissues, possible side effects exerted by HMGR inhibitors on heart were hypothesized: few papers in literature highlighted the impairment of human energy-dependent myocardial functions following statin treatment (Pisarenko et al., 2001). Although the molecular mechanisms of statin-induced myotoxicity are still debated, it is likely that the partial deficiency of HMGR main end products could be at the root of muscle distress and cardiac function impairment.

Due to the increasing incidence of cardiovascular disease, for which the rise of lipid levels into the bloodstream represents a primary risk factor, the control of plasma cholesterol has become one of the major health aims. To what extent the risk/benefit ratio suggests the administration of drugs which are supposed to decrease the risk of cardiovascular disease but, at the same time, might affect skeletal and cardiac muscle physiology, has still to be established.

In the light of the above reported considerations, the PhD project was aimed at providing a comprehensive analysis of the role played by the enzymes and the main end-products of Mva pathway in rat skeletal and cardiac muscle physiology in terms of functions, metabolism, differentiation and regeneration.

Supported by data present in literature (Belo et al., 1993) (Castellani et al., 2006) assessing the pivotal role of some of HMGR main end-products in muscle differentiation, it was demonstrated that the inhibition of HMGR activity and transcription or the induction of the enzyme degradation lead



not only to decreased levels of both the early and late markers of myoblast differentiation, but also to an impairment of myoblast fusion into multinucleated syncytia (Martini et al., 2009). Moreover the elucidation of HMGR long term regulation during myogenesis (Trapani et al., 2010) assessed that different mechanisms are involved in the modulation of the enzyme and added new insights in the understanding of myogenesis, the failure of which might impair the proper muscle formation.

The results obtained on myoblasts suggested that the inhibition of Mva pathway could also affect muscle regeneration, a process that in many but not all respects recapitulates the sequence of events observed during embryonic myogenesis and guarantees the maintenance of a working skeletal musculature.

Indeed, simvastatin impaired *in vitro* the differentiation and fusion of murine myoblasts derived from satellite cells, responsible for muscle repair, and delayed *in vivo* the regeneration of mouse muscles. Although the effect of HMGR inhibition on the myogenic process started to be investigated, none of the studies was carried out on those cells directly involved in muscle repair and on animal model of muscle damage. Most importantly, rescue experiments clearly showed that the delayed regeneration was due to the inhibition of HMGR activity rather than to an effect exerted by simvastatin itself. It underlined the pivotal role played by HMGR in skeletal muscle differentiation and the strict relationship between the Mva pathway and muscle repair.

Due to the occurrence of myopathy in patients under statin treatment, the effects of HMGR inhibition on glycolytic adult muscles (EDL) among the most susceptible to statin administration (Westwood et al., 2005), were investigated. Rat chronic treatment with simvastatin induced a shift of MHC isoforms toward a slower phenotype, reduced power output and unloaded shortening velocity of EDL muscles, and induced functional impairment. The novelty of the study was the investigation of mechanical and functional parameters, never examined in this research field. Surprisingly, even in the absence of muscle damage, simvastatin treatment reduced EDL functions proving that HMGR inhibition could affect muscle performance without leading to muscle mass loss in terms of necrosis or apoptosis but affecting the MHC isoform pattern. Furthermore a deep connection between muscle metabolism and plasticity was established highlighting the dependence of MHC isoform shift on Mva pathway inhibition. Although further investigations are needed, the results assessed the involvement of modification of muscle fiber phenotype in statin-induced muscle performance reduction (Trapani et al., 2011).

The statin side effects spread well beyond the impairment of skeletal muscle function and regeneration, also affecting the organ they are supposed to protect: the heart. As previously reported, lovastatin treatment impaired human stroke volume, cardiac output, and contractile index. The results obtained in the current research showed that chronic HMGR inhibition reduces rat ventricular content of CoQ9 and  $\beta$ MHC. Although  $\beta$ MHC accounts for a small percentage of ventricular MHC isoform content in rodents, even relatively minor changes in overall amount of MHC isoforms might lead significant functional consequences, according to Krenz and co-workers (Krenz et al., 2007).

When considered as a whole, the obtained data highlight the pivotal role exerted by HMGR activity and main end products both in skeletal and cardiac muscle. The thesis provides evidence that besides the well known lipid lowering properties, the inhibition of HMGR might also affect the mechanical and functional features of glycolytic fibers, the development and regeneration of skeletal muscle and the fiber phenotype of cardiac ventricles.

Thus, statin users might not only suffer from myopathy but also might not be able to repair any muscle damage because of the impairment of both differentiation and fusion of the cells responsible for muscle regeneration. Furthermore, even though statins are supposed to reduce the risk of cardiovascular disease, they can also modify cardiac fiber phenotype.

Due to the essential role of HMGR main end-products in cell structure, proliferation, growth, survival and differentiation, and owing to the necessity to maintain plasma cholesterol content at low levels in the attempt to reduce the risk of cardiovascular diseases, more efforts should be spent to find alternative pharmacological approach to statin treatment, able to block cholesterol biosynthetic pathway downstream to HMGR, the inhibition of which can affect body health at multiple levels.

## References

- Belo RS, Jamieson JC, Wright JA. 1993. Studies on the effect of mevinolin (lovastatin) and mevastatin (compactin) on the fusion of L6 myoblasts. *Mol Cell Biochem* 126(2):159-167.
- Castellani L, Salvati E, Alema S, Falcone G. 2006. Fine regulation of RhoA and Rock is required for skeletal muscle differentiation. *J Biol Chem* 281(22):15249-15257.

- Krenz M, Sadayappan S, Osinska HE, Henry JA, Beck S, Warshaw DM, Robbins J. 2007. Distribution and structure-function relationship of myosin heavy chain isoforms in the adult mouse heart. *J Biol Chem* 282(33):24057-24064.
- Martini C, Trapani L, Narciso L, Marino M, Trentalance A, Pallottini V. 2009. 3-hydroxy 3-methylglutaryl coenzyme A reductase increase is essential for rat muscle differentiation. *J Cell Physiol* 220(2):524-530.
- Pisarenko OI, Studneva IM, Lankin VZ, Konovalova GG, Tikhaze AK, Kaminnaya VI, Belenkov YN. 2001. Inhibitor of beta-hydroxy-beta-methylglutaryl coenzyme A reductase decreases energy supply to the myocardium in rats. *Bull Exp Biol Med* 132(4):956-958.
- Trapani L, Martini C, Trentalance A, Pallottini V. 2010. Mechanism underlying long-term regulation of 3-hydroxy-3-methylglutaryl coenzyme A reductase during L6 myoblast differentiation. *J Cell Biochem* 110(2):392-398.
- Trapani L, Melli L, Segatto M, Trezza V, Campolongo P, Jozwiak A, Swiezewska E, Pucillo LP, Moreno S, Fanelli F, Linari M, Pallottini V. 2011. Effects of myosin heavy chain (MHC) plasticity induced by HMGCoA-reductase inhibition on skeletal muscle functions. *FASEB J*.
- Westwood FR, Bigley A, Randall K, Marsden AM, Scott RC. 2005. Statin-induced muscle necrosis in the rat: distribution, development, and fibre selectivity. *Toxicol Pathol* 33(2):246-257.

## ACKNOWLEDGEMENTS

Many people contributed to this dissertation in innumerable ways, and I am grateful to all of them.

First and foremost I want to thank my supervisor, Prof. Valentina Pallottini. It has been a pleasure to be her first master degree and Ph.D. student. Besides the obvious financial support, her encouragement to develop my own ideas and directions for this thesis were invaluable. I appreciate all her contributions of time and ideas to make my Ph.D. experience productive and stimulating. Her agreement or disagreement with my wanting to go the extra mile taught me to think more rigorously and to face experimental topics with a scientific mindset.

Special thanks go to my “buddy”, Dr Marco Segatto: a better adjective with which to express my gratitude for his support does not exist. Whatever we did, wherever we went he made the time we spent together, unrepeatable and full of fun despite the fatigue! I’ll never forget our taking care of Obamina, the nights spent in Florence working on our experiments and desperately looking for Linari’s house, the uncountable “travels” in my or in his car comfortably speaking of all subjects...

Thank you for being there for me from the very beginning!

I could not have wished for a better collaborator and “coach”: with you I worked and laughed a lot!

Thanks to Prof. Maria Marino and Dr Filippo Acconcia for their precious advice and helpful contribution to my work.

Thanks to Prof. Anna Trentalance who has always encouraged me and spurred me to keep on working at the bench even before I started my PhD project.

Thanks to Prof. Linari and Dr. Luca Melli of University of Florence , to Prof. Ewa Swiezewska and Dr. Adam Jozwiak of the Polish Academy of Sciences: the periods I spent in Florence and in Warsaw gave me the opportunity to learn new methods and scientific approaches and, most importantly, to meet marvellous and generous people.

Thanks to Dr. Sandra Moreno, Dr. Francesca Fanelli, Dr. Viviana Trezza, Dr. Antonia Manduca for the scientific support and encouragement.

Thanks to Prof. Pucillo of Istituto Lazzaro Spallanzani for the biochemical analysis on rat and mouse plasma.

Thanks to Dr. Marco Crescenzi of Istituto Superiore di Sanità for the generous gift of the satellite cells.

I would like to thank present and past members of lab 3.4: Dr. Paola Galluzzo, Dr. Pamela Bulzomi and Dr. Elisabetta De Marinis...with whom I shared almost all my lab period, and with whom I overcame the “entropy” of our male counterparts in the lab! Thanks to Dr. Alessandro Bolli, Dr. Marco Pellegrini, Dr. Piergiorgio La Rosa, Dr. Marco Fiocchetti who made daily lab duties fun with their jokes...and who made the lab a convivial place to work. Who will now assign me with “chef score” and who will take notes of all my complaints?

The group has been a source of friendship as well as good advice and collaboration.

Lastly, I would like to thank my family for all their love and encouragement and in particular my parents who supported me in all my pursuits.

And most of all I wish to thank my supportive, encouraging, and patient husband Eugenio whose faithful support during the final stages of this Ph.D. is so appreciated.

Thank you!